Oceanographical Magazine
(2)
N.I.D.
11(2)
LIBRARY
JUL 12 1960
FISH & WILDLIFE SERVICE

# 気象庁欧文海洋報告

第11巻 第2号

# THE OCEANOGRAPHICAL MAGAZINE

Vol. 11 No. 2

## CONTENTS

T. ICHIYE: On the hydrography near Mississippi Delta ..... 65
J. SUGIURA: On the currents south off Hokkaidō in the Western North Pacific (II) ... 79
T. ICHIYE: On the deep water in the Western North Pacific ..... 99
T. ICHIYE: On water budget in a two-layered ocean ..... 111
J. FUKUOKA: An analysis on the mechanism of the cold water mass appearance in the Enshū-nada ..... 127

**Preliminary Report of the Japanese Expedition of Deep Sea**

K. TERADA and H. FUTI: Introductory remarks of Japanese Expedition of Deep Sea ... 145
J. MASUZAWA, M. YASUI and H. AKAMATSU: A hydrographic section across the Kurile Trench ..... 165
Y. TAKENOUTI and M. YASUI: A note on the ball breaker and the ball ..... 173
Y. MIYAKE and others: Chemistry in the Japanese Expedition of Deep Sea (JEDS-2) ..... 181
Y. SUYEHIRO and others: Notes on the sampling gears and the animals collected on the second cruise of the Japanese Expedition of Deep Seas (JEDS-2) ..... 187
N. NASU, A. IIJIMA and H. KAGAMI: Geological results in the Japanese Deep Sea Expedition in 1959 ..... 201
K. KOBAYASHI, K. OINUMA and T. SUDO: Clay mineralogical study on Recent marine sediments (I), (II) ..... 215
A. IIJIMA: The bottom sediments of the Japan and Kurile Trenches collected by the Ryofu Maru during the Japanese Deep Sea Expeditions in 1959 ..... 225
H. KAGAMI and A. IIJIMA: On the bottom sediments off Onagawa and Kushiro, the adjacent continental slope of Japan Trench ..... 233

*Published by the Japan Meteorological Agency*

March 1960

The Oceanographical Magazine
Vol. 11. No. 2, March 1960

# On the Hydrography near Mississippi Delta*

By

Takashi ICHIYE

*Oceanographic Institute, Florida State University*

**Abstract:** The behaviors of fresh water discharge of the Mississippi flowing into the northern Gulf of Mexico are described by use of data obtained recently including two synoptic surveys in 1954 to 1955. The discharge is found to spread not so far from the coast as in the China Sea, owing to the effects of the permanent current, bottom topography, wind and morphology of the river mouth. An example of vertical mixing of fresh water with sea water is discussed and a simple mathematical model of mixing of a discharge with sea water is proposed, in connection with the observed conditions off river mouths.

## *1. Introduction*

The sea off the Mississippi Delta gives a good example for the mixing of fresh water with sea water. Since mixing and diffusion in the ocean are not understood so well as similar processes in the atmosphere and river waters, hydrography of the area should have been given more attention for understanding of these processes. There were a few oceanographic works about the area, which discussed the shallow water close to the Delta in relation to sedimentation (BATES, 1953; SCRUTTON, 1956).

This preliminary work is aimed to study the mixing over the continental shelf. The data used were collected by the Jakkula of the A & M College of Texas (1952–1957) and the Alaska of U. S. Fish and Wildlife Service since 1951. The conditions in the northern Gulf are compared with those of the Eastern China Sea where the Yangtze and the Hwang Ho drainage mix with sea water.

* Contribution No. 132. Oceanographic Institute, Florida State University.

*2. Synoptic data near the Mississippi Delta*

Two cruises of the Jakkula, Cruise 54-9 in July, 1954 and Cruise 55-4 in April, 1955, give synoptic data near the Mississippi Delta. Spread of the fresh water is most clearly recognized in salinity distributions. Surface and 5 m-depth salinity distributions of the Cruise 54-9 are shown in Fig. 1 and 2. Average salinities at the surface and 5 m-depth in summer of the offshore water in the western Gulf are 36.6 to 36.8 ‰ and those in the eastern Gulf are 34.8 to 35.2 ‰ (ICHIYE, 1959). The area considered is located on the boundary of these two water masses and thus the isohalines of 35 and 35.5 ‰ are considered as the boundaries of the offshore water in surface and 5 m-layer, respectively. Then mixing of drainage can be recognized as far about 60 sm from the coast. The lowest surface salinity east of the Delta is due to the surface flow caused by hydraulic head along the coast (SCRUTTON, 1956). An isolated higher salinity domain west of the Delta seems to be due to a vortex associated with bottom topography. In 5 m-layer isolated low salinity is found at the tip of the fresh water east of the Delta.

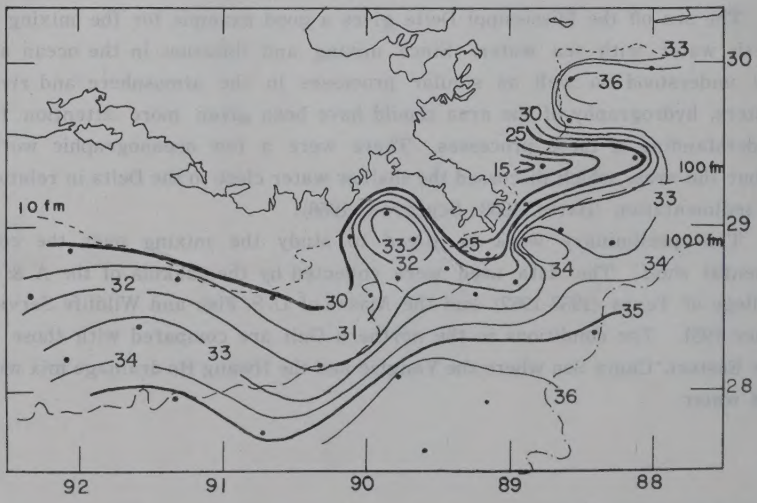


Fig. 1. Surface salinity (‰) of the Cruise 54-9 in July, 1954.

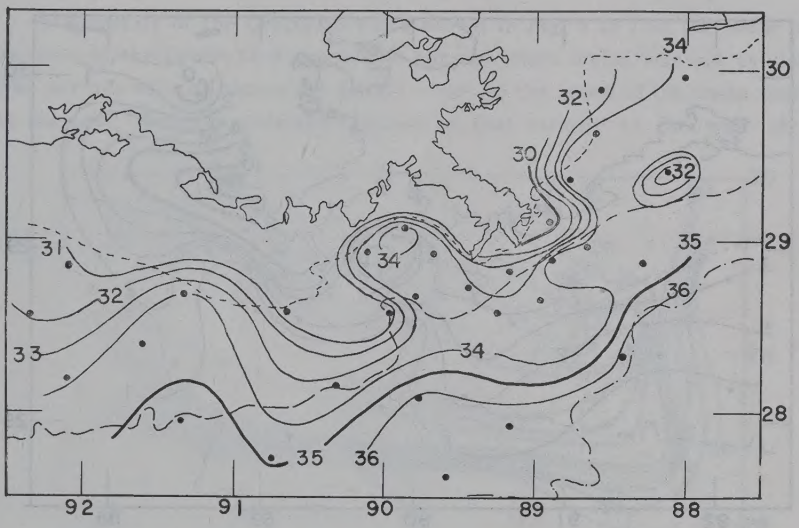


Fig. 2. Salinity (‰) at 5 m-depth of the Cruise 54-9. (Fine-dot lines indicate 10 fathom contour, fine broken lines 100 fathom and fine chain lines 1000 fathom.)

In Fig. 3 is shown the difference of sigma-T between the surface and 10 m-depth as an indication of vertical stability. It is noted that large stability is found to the east of the Delta and small stability in the isolated high salinity west of the Delta. General small stability in the offshore water represents the condition of the western Gulf water proper which has almost uniform temperature and salinity in upper 30 m depths even in summer (ICHIYE, 1959).

In open seas the temperature in the intermediate depths coincides with streamlines obtained by dynamic computation. In Fig. 4 are shown the surface dynamic topography based on 1000 dbar level as a reference level and temperatures at 200 m (ICHIYE, 1959). These two distributions indicate that the current south of the Delta is towards ENE and is almost parallel to the bottom contours as usually is the case in the continental slope. This current seems to be a part of the permanent vortex in the northeastern Gulf forming at the end of loop of the Florida Current (AUSTIN, 1954; ICHIYE, 1959). The velocity is apparently intensified by the wind, because the estimated wind drift of the season has the same direction as the geostrophic current (ICHIYE, 1959).

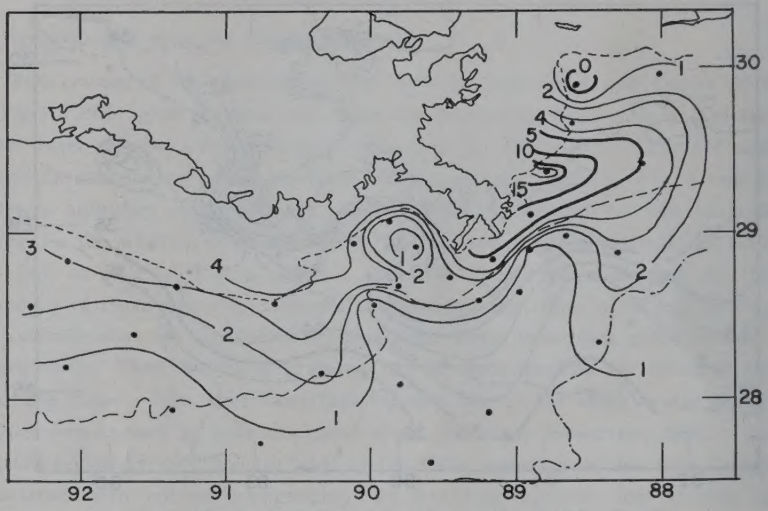


Fig. 3. Difference of sigma-T at the surface and 10 m-depth of the Cruise 54-9.

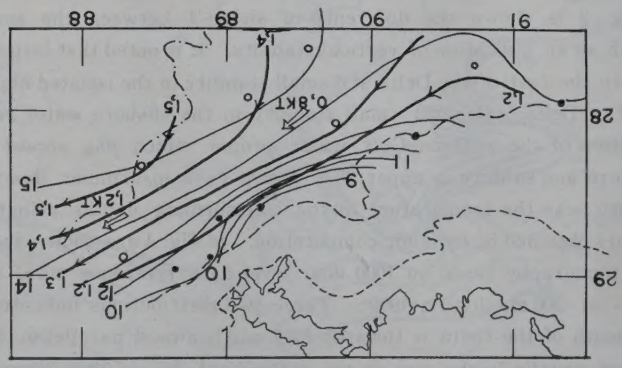


Fig. 4. Temperature (°C) at 200 m-depth (fine lines) and dynamic depth anomalies (in dbar) of the surface referred to 1000 dbar level (heavy lines) of the Cruise 54-9. (White circles indicate the stations for dynamic computation. Arrows with numbers indicate surface velocities (kts) determined by dynamic computation.)

The results of the Cruise 55-4 are shown in Fig. 5 to 7 in the same way as those of the Cruise 54-9 except the current chart which was not available. The surface salinity shows the lowest value to the south of the Delta instead to the east. General tendency suggests us that salinity to the west of the

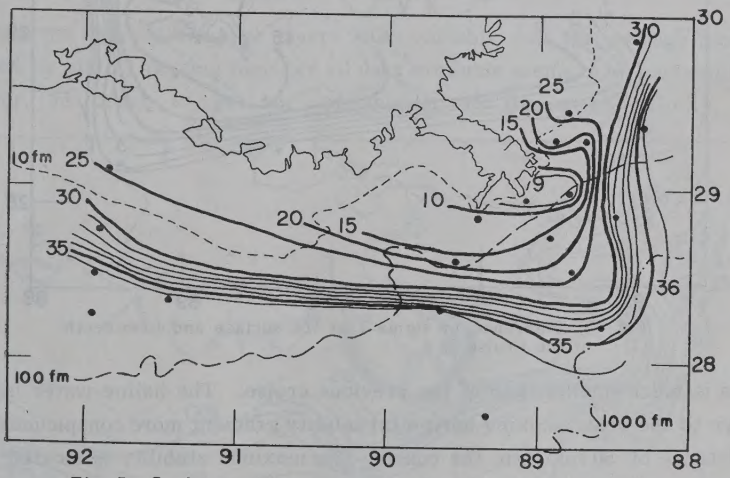


Fig. 5. Surface salinity (‰) of the Cruise 55-4 in April, 1955.

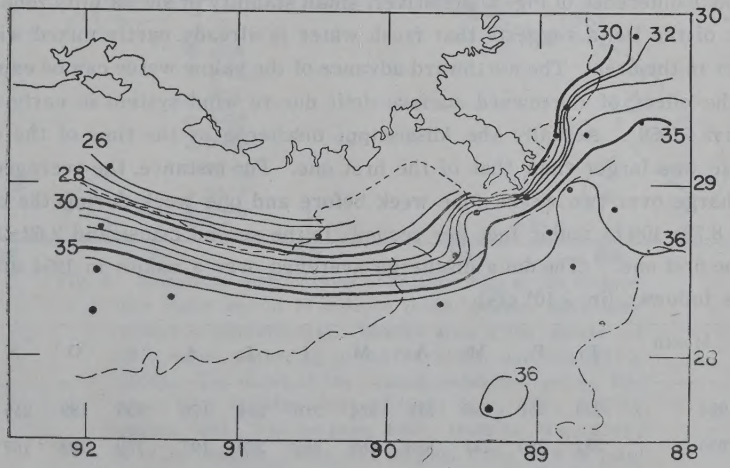


Fig. 6. Salinity (‰) at 5 m-depth of the Cruise 55-4.

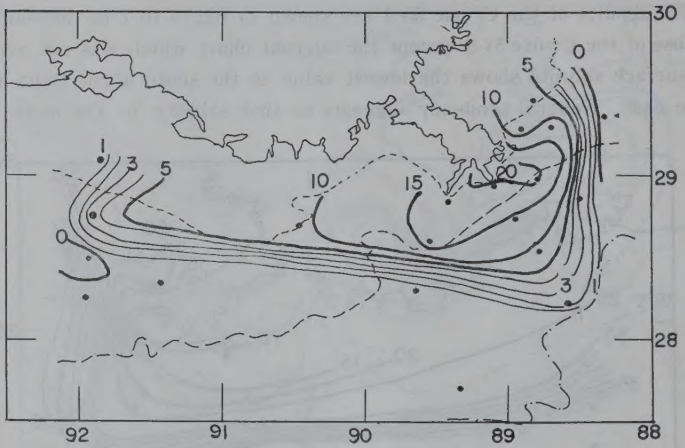


Fig. 7. Difference of sigma-T at the surface and 10 m-depth of the Cruise 55-4.

Delta is much smaller than in the previous cruise. The haline water is found closer to the coast, making horizontal salinity gradient more conspicuous along a distance of 50 sm from the coast. The maximal stability is located in the region of minimal salinity to the south of the Delta in the distribution of sigma-T difference of Fig. 7. Relatively small stability in low salinity zone to the west of the Delta suggests that fresh water is already partly mixed with sea water in the area. The northward advance of the haline water can be explained as the effect of northward surface drift due to wind system in early spring (ICHIYE, 1959). Actually the Mississippi discharge at the time of the second cruise was larger than that of the first one. For instance, the averaged daily discharge over two weeks (one week before and one week during the cruise) was $8.72\times10^5$cfs (cubic feet per second) in the second cruise and $2.62\times10^5$ cfs in the first one. (The daily discharge averaged over a month in 1954 and 1955 is as follows: (in $\times10^3$ cfs)

| Year \ Month | J | F | M | A | M | J | J | A | S | O | N | D |
|---|---|---|---|---|---|---|---|---|---|---|---|---|
| 1954 | 224 | 331 | 293 | 316 | 524 | 316 | 234 | 170 | 155 | 189 | 215 | 179 |
| 1955 | 387 | 380 | 741 | 866 | 468 | 352 | 270 | 197 | 139 | 198 | 167 | 199 |

The data of discharges are based on daily gage heights at Red River Landing, Louisiana, through the courtesy of Corps of Engineers, U. S. Army New Orleans District Office.)

### 3. *Composite distributions of salinity*

Since the salinity in upper layers is so variable that the average picture obtained by simply putting together all data available seems to be meaningless. However, in order to get an information of the mean salinity, the

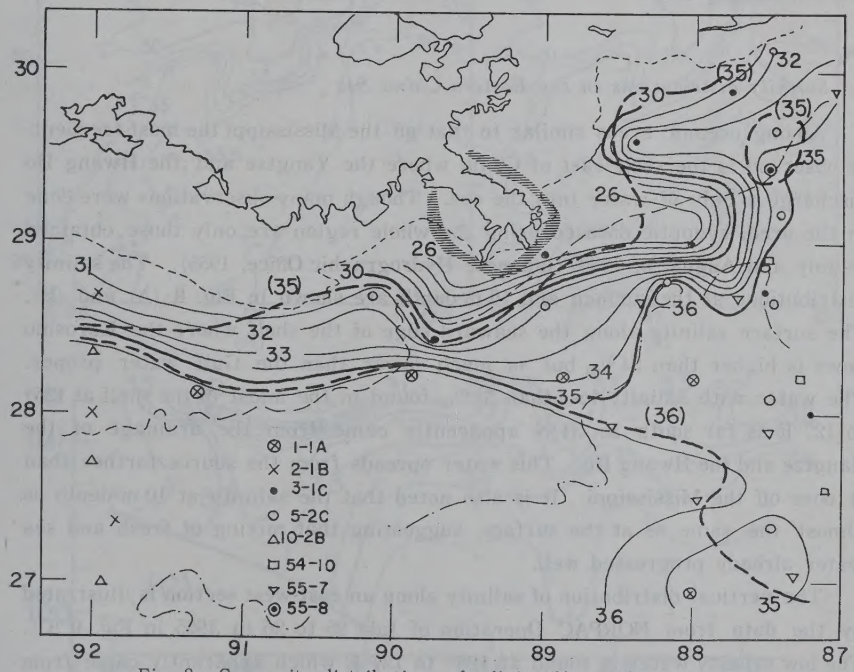


Fig. 8. Composite distributions of salinity ($^0/_{00}$) at the surface (fine lines) and at 10 m-depth (heavy broken lines with salinity in parentheses). Shaded area is the source of fresh water, according to BATES (1953) and SCRUTTON (1956). The dates of the cruises numbered are as follows: 1-1A in May, 1951; 2-1B in June, 1951; 3-1C in August, 1951; 5-2C in June, 1952; 10-2B in May, 1953; 54-10 in August, 1953; 55-7 in July, 1955; 55-8 in July, 1955.

scarceness of the data forces us to use this kind of averaging process. Yet the result obtained seems to be more consistent than expected. In Fig. 8 is shown the composite salinity distribution at the surface and 10 m-depth of all data in summer from 1951 to 1955, except the Cruise 54-9. In the surface the water with salinity less than 35 ‰ is found neither beyond 1000 fathom contour nor farther than 70 sm from the coast. In 10 m-layer this water is limited within the distance of 30 sm from the coast even near the Delta. This chart confirms the fact that the Mississippi drainage does not spread beyond the continental shelf.

*4. Salinity distributions in the Eastern China Sea*

Among oceanic areas similar to that off the Mississippi the most frequently observed is the shelf east of China where the Yangtze and the Hwang Ho discharge a bulk of water into the sea. Though many observations were done in the area, synoptic data covering the whole region are only those obtained in July and August of 1939 (Japanese Hydrographic Office, 1955). The salinity distributions at the surface and 10 m-depth are shown in Fig. 9 (A) and (B). The surface salinity along the seaward edge of the shelf where the Kuroshio flows is higher than 34 ‰ but is much lower than the Gulf water proper. The water with salinity less than 31 ‰ found in the midst of the shelf at 125° to 127°E as far south as 34°N apparently came from the drainage of the Yangtze and the Hwang Ho. This water spreads from the source farther than it does off the Mississippi. It is also noted that the salinity at 10 m-depth is almost the same as at the surface, suggesting that mixing of fresh and sea water already progressed well.

The vertical distribution of salinity along an east-west section is illustrated by the data from NORPAC Operation of July 25 to 26 in 1955 in Fig. 9 (C). The low salinity water is found at 126° to 127°E which apparently came from the drainage of the continental rivers. The low salinity water between 128° and 129°E seems to be separated from the main spread of the drainage. The decrease of salinity from the normal values is found down to the depth of 20 m, in contrast to the condition off the Mississippi Delta where mixing of fresh and sea water is limited in upper 10 m.

The comparison of the salinity distributions off the China coast with those

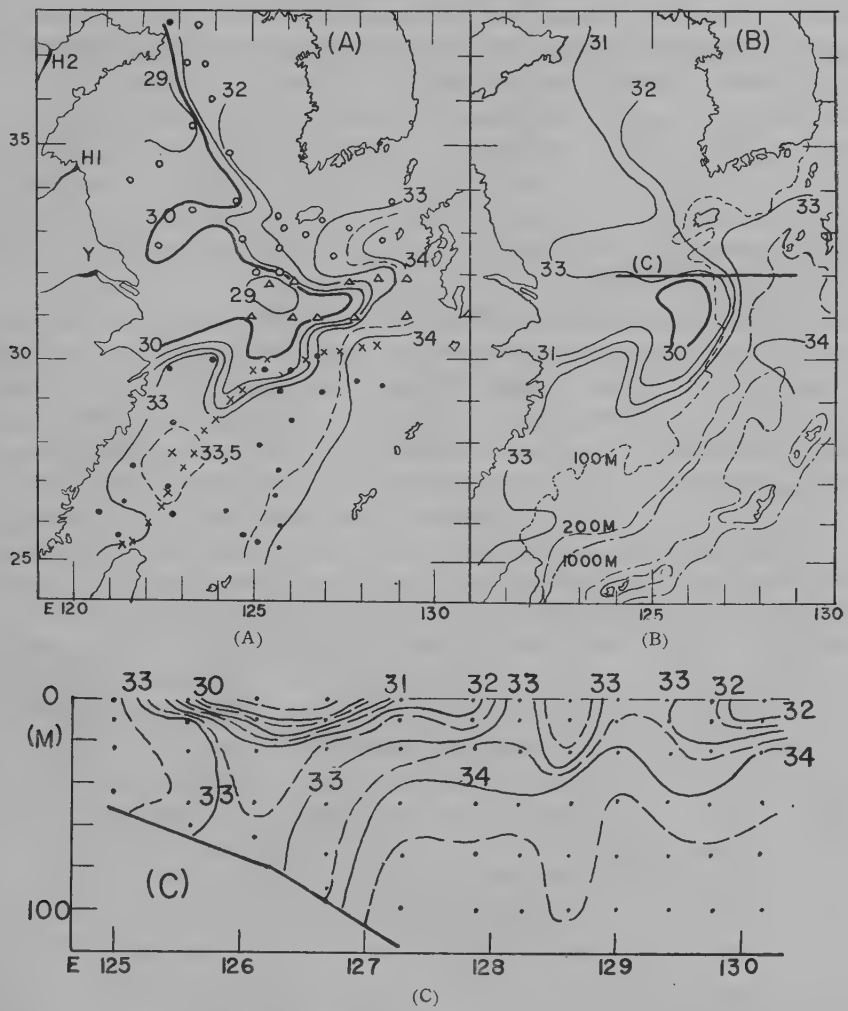


Fig. 9. Salinity (‰) at the surface (A) and at 10 m-depth (B) of the survey in July to August, 1939, by Japanese Hydrographic Office. The Yangtze is indicated by "Y", the Hwang Ho during 1938-1947 by "H1" and the latter after then by "H2". (C): Vertical section of salinity along 31°N of the survey on 25 to 26 of July, 1955.

in the northern Gulf indicates that the influence of the discharge on surface salinity is much larger in the former than in the latter. The average discharge of the Yangtze is about $7.7\times10^5$ cfs (Britanica) and that of the Hwang Ho is less than half of it. (Since 1947, the Hwang Ho has changed its course to the north as shown in Fig. 9 (A).) The average discharge of the Mississippi in 1954-55 is about $3.1\times10^5$ cfs, according to the data shown in Section 2. Thus total discharge is higher in the China Sea than in the northern Gulf. However, other oceanographic characteristics as well as the discharge contribute to produce different conditions.

First, the bottom topography indicates that the shelf with the depth less than 200 m is very narrow in the northern Gulf. Since vertical mixing due to scale effect of increasing depth is much intensified in the slope, a narrow shelf means a small area of spread of the drainage. Secondly, the prevailing wind in the northern Gulf which is easterly in summer and southeasterly in winter makes the offshore water drift toward the coast (Ichiye, 1959), while in the China Sea westerly or northwesterly wind throughout the year except in summer pushes the fresh water toward the sea. Thirdly, the semi-permanent longshore current flows eastward closely to the coast off the Mississippi, while the Kuroshio flows far from the coast in the China Sea. Fourthly, morphology of a river mouth is quite different in the Mississippi and the Yangtze. The former has several tributaries which form orifices at the mouth, sending the drainage to all directions except to the northwest. The Yangtze has, on the other hand, one orifice opening eastwards. The decrease of maximal (or characteristic) velocity in multiple jets like the Mississippi Delta may be proportional to $x^{-1}$ ($x$ is the distance from the source) from the momentum consideration (Goldstein, 586-588). This quantity decreases as $x^{-\frac{1}{2}}$ in a single two-dimensional jet (ibid, 592-594). Thus it is expected that the drainage in the China Sea can reach farther from the coast than in the northern Gulf.

### *5. Concluding remark*

The drainage from a river contributes very little to the water budget of the ocean even for a river as the Mississippi or the Yangtze, as pointed out by Scrutton (1956). However, various conditions off the mouth change the influence of the drainage illustrated by two examples.

*APPENDIX* *Mixing of fresh water with sea water.*

The mixing process of fresh water discharge with sea water is not fully understood yet. Particularly hydrodynamical problems about the process are difficult because the current existing is influenced by the discharge and eddy diffusivity also changes owing to the changes in stability and mean current as mixing proceeds. However, the general behaviors of the discharge flowing into the sea are as follows: The fresh water spreads first like a jet from an orifice (SCRUTTON, 1956), and tidal currents carry the water to and fro, producing intense horizontal mixing, while vertical mixing proceeds relatively slowly. Eventually some parts of the mixed water are caught by a permanent current and carried away. In some occasions such traces of drainage were found as far as 400 to 500 sm from the source in the upper layer of the Kuroshio (ICHIYE, 1956 and 1957).

As an example of mixing of fresh water with sea water, the change of salinity since two days after the heavy precipitation caused by a typhoon is shown in Fig. 10. The salinity data are averaged values of seven station in

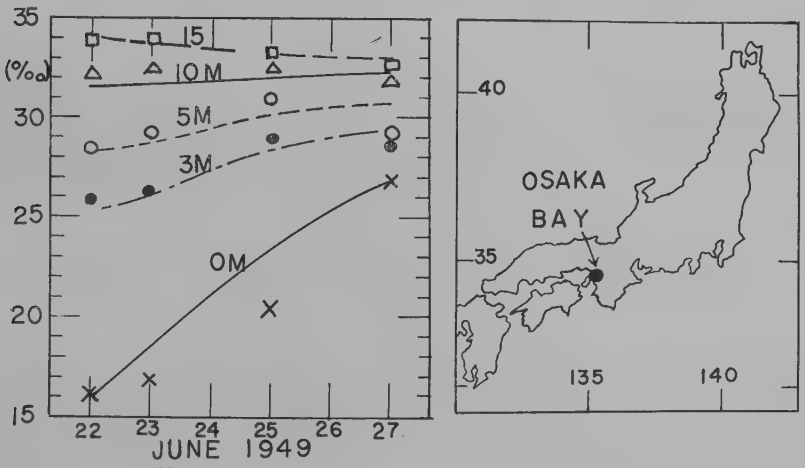


Fig. 10. Change of salinity in Osaka Bay after a heavy precipitation. Curves indicate theoretical values.

the northern part of a small estuary, Osaka Bay, the mean depth of which is about 18 m. In mathematical formulation of the problem the variation of

salinity $S$ is assumed to be due to vertical mixing only. Such an assumption is not far from truth, because horizontally averaged values are discussed and there was no noticeable runoff during the time of the survey. Thus the equation becomes

$$\partial S/\partial t = k\partial^2 S/\partial z^2. \qquad (1)$$

The plausible boundary conditions are

at the surface ($z=0$), $\partial S/\partial z=0$ and at the bottom ($z=\infty$), $S=S_0=$const. (2)

The depth is actually finite but the effect of finite depth does not change the result, since the eddy diffusivity is small enough. When the initial distribution of $S$ is given by

$$S=S_0-S_1\exp(-\alpha z) \qquad (3)$$

corresponding to the observed salinity distribution on the first day, the solution of (1) under the conditions (2) is

$$S=S_0-\frac{1}{2}S_1\exp(\alpha^2 kt)\left[\exp(-\alpha z)\left\{1-\mathrm{Erf}\left(\alpha n-\frac{1}{2}zn^{-1}\right)\right\}\right.$$
$$\left.+\exp(\alpha z)\left\{1-\mathrm{Erf}\left(\alpha n+\frac{1}{2}zn^{-1}\right)\right\}\right] \qquad (4)$$

where $n=(kt)^{\frac{1}{2}}$.

The constants $S_0$, $S_1$ and $\alpha$ are determined from the data such as

$$S_0=35\ (^0/_{00}),\quad S_1=24\ (^0/_{00})\quad \alpha=0.2\ (\mathrm{m}^{-1})$$

The computed curves with $k=1$ cm$^2$/sec are in good agreement with the data. This eddy diffusivity is small compared with other values estimated in water bodies of the same scale (for instance, vertical mixing of the drainage under a normal discharge, Ichiye, 1952). The extreme vertical stability seems to have reduced eddy diffusivity in this example.

In stationary diffusion as encountered off river mouths the diffusion equation is given by

$$u\partial S/\partial x=\partial(k\partial S/\partial z)/\partial z. \qquad (5)$$

Under an assumption that the velocity $u$ and eddy diffusivity $k$ are functions of $x$ only, the solution of (5) with boundary conditions (2) and the initial distribution (3) is also expressed by (4) in which $n^2(=kt)$ is replaced with $\tau$ defined by

$$\tau=\int_0^x\{k(x)/u(x)\}dx. \qquad (6)$$

The surface salinity of this solution becomes

$$S_s = S_0 - S_1 \exp(\tau\alpha^2)\{1 - \mathrm{Erf}(\alpha\tau^{\frac{1}{2}})\}. \qquad (7)$$

In the following table the coefficient of $S_1$ is shown as a function of $x$ the distance from the source for a velocity proportional to $x^{-\frac{1}{2}}$ which is simulated to that of turbulent jet. The vertical eddy difiusivity $k$ is assumed to be proportional to the depth, which is assumed to increase linearly with $x$ in the example I and to increase suddenly beyond 50 km from the source in II. It is seen that increasing depth (and also increasing $k$) produces intense mixing beyond this distance of 50 km. The velocity is taken so as to give 2 cm/sec at 200 km. In the example I which is simulated to the China Sea increase of salinity seems to be faster than observed, suggesting that the actual velocity is larger or eddy viscosity is smaller than in this model. The example II agrees well with the condition off the Mississippi.

Table

| $x$ (km) | | 10 | 20 | 50 | 100 | 150 | 200 |
|---|---|---|---|---|---|---|---|
| $u$ (cm/sec) | | 8.9 | 6.3 | 4.0 | 2.3 | 2.8 | 2.0 |
| $k$ (cm²/sec) | (I) | 0.1 | 0.2 | 0.5 | 1.0 | 1.5 | 2.0 |
| | (II) | 0.1 | 0.2 | 0.5 | 4.0 | 10.0 | 20.0 |
| $(S_0-S_s)/S_1$ | (I) | 0.865 | 0.773 | 0.427 | 0.217 | 0.139 | 0.098 |
| | (II) | 0.865 | 0.773 | 0.427 | 0.141 | 0.067 | 0.039 |

*Acknowledgement*: This work was aided by a contract between the Office of Naval Research, Department of the Navy and the Florida State University, N.R. 163-396. The author wishes to thank Dr. Sidney W. Fox and Dr. F.C.W. Olson who encouraged him throughout the work.

## *References*

A & M College of Texas, 1952-1957: *Oceanographic Data of the Gulf of Mexico.* No. 1 to No. 6.

Austin, G., 1955: Some recent oceanographic surveys of the Gulf of Mexico. *Trans. Am. Geophys. Union.* **36** (5), 885-892.

Bates, C. C., 1953: Rational theory of delta formation. *Bull. Am. Assoc. Petr. Geol.* **37** (9), 2119-2102.

Britanica, 1953 Ed.

Goldstein, S., 1938: Modern development in fluid dynamics. Oxford at the Clarendon Press.

Ichiye, T., 1949: On the hydrographic conditions in Osaka Bay after heavy precipitation caused by Typhoon "Della" (Mimeographed). *Papers and Reports in Oceanography.* No. 3, Kobe Marine Observatory.

ICHIYE, T., 1952: On the variation of oceanographical elements due to tidal currents. *Oceanog. Mag.* **4** (3).

ICHIYE, T., 1956: On the annual variation of chlorinities at the upper layer of the Kuroshio. *Oceanog. Mag.* **7** (2).

ICHIYE, T., 1957: On the relationship between the plankton distribution and hydrographic condition. *Rec. Oceanog. Works in Japan.* Spec. No.

ICHIYE, T., 1959: On the hydrography of the Gulf of Mexico (To be published).

Japanese Hydrographic Office, 1955: *Hydrog. Bull.* Spec. No. 16.

Japan Meteorological Agency, 1956: *The Results of Mar. Met. and Oceanog.* No. 17. NORPAC Data.

SCRUTTON, P. C., 1956: Oceanography of Mississippi Delta sedimentary environment. *Bull. Am. Assoc. Petr. Geol.* **40** (12), 2864-2952.

The Oceanographical Magazine
Vol. 11. No. 2, March 1960

# On the Currents South off Hokkaidō in the Western North Pacific (II)

By

Jiro Sugiura

*Hakodate Marine Observatory*

## 1. *Introduction*

In a previous paper (Sugiura 1959) a general survey was presented on the currents of three kinds in the sea south off Hokkaidō in the western North Pacific. Hereafter, details and further developments will be reported about some points which were mentioned rather roughly in the previous paper. In that paper, current velocity data obtained by the geomagnetic electro-kinetograph (GEK) were reported fragmentarily, but data on the general distribution of the current velocity over the whole sea area south off Hokkaidō were not available.

A set of current charts in that sea area was presented some years ago in "Coastwise passage pilot (Maritime Safety Agency 1951)" based upon the data obtained in the period from 1935 to 1942. The data may have been based on the drift of ships or on dynamic calculations, so the accuracy of the data may be lower than that of recent data obtained by GEK.

In this paper new current charts of the sea south off Hokkaidō are presented. They are based upon the results of recent GEK observations. Moreover, velocity distribution of each different water mass is presented based upon the bathythermograph (BT) observations which were made simultaneously with those of the GEK.

## 2. *The used data*

The GEK data are gathered from the sea area south off Hokkaidō north of the parallel of lat. 40°N and between the meridians of long. 141°E and 151°E. Previous to June 30, 1959, 435 GEK stations in that sea area were

occupied on 13 different cruises of the Yūshio-maru of the Hakodate Marine Observatory and 246 GEK stations were occupied on 11 cruises of the Ryōfū-

Table 1-1. List of the cruises on which GEK observations were made in the area 40-46°N, 141-151°E up to June 1959.

| Year | Period | Ship | Number of the GEK stations |
|---|---|---|---|
| 1955 | September 8-13 | Ryōfū-maru | 37 |
| 1956 | February 24 | 〃 | 8 |
| 〃 | May 21-22 | 〃 | 3 |
| 〃 | August 14-30 | Yūshio-maru | 40 |
| 〃 | September 29 | Ryōfū-maru | 7 |
| 〃 | October 27-November 4 | Yūshio-maru | 33 |
| 1957 | February 20-25 | 〃 | 22 |
| 〃 | May 2-8 | 〃 | 25 |
| 〃 | May 12-18 | Ryōfū-maru | 20 |
| 〃 | August 8-28 | Yūshio-maru | 47 |
| 〃 | August 29-September 3 | Ryōfū-maru | 31 |
| 〃 | September 16-17 | 〃 | 3 |
| 〃 | November 9-15 | Yūshio-maru | 9 |
| 1958 | February 19-25 | Ryōfū-maru | 33 |
| 〃 | February 28-March 9 | Yūshio-maru | 38 |
| 〃 | May 17-31 | 〃 | 45 |
| 〃 | July 19-28 | 〃 | 16 |
| 〃 | August 1-September 8 | Ryōfū-maru | 44 |
| 〃 | September 1-8 | Yūshio-maru | 28 |
| 〃 | November 8-19 | 〃 | 50 |
| 〃 | November 10-15 | Ryōfū-maru | 31 |
| 1959 | February 17-21 | 〃 | 29 |
| 〃 | February 24-March 1 | Yūshio-maru | 33 |
| 〃 | May 23-June 3 | 〃 | 49 |

Table 1-2. Numbers of the GEK stations in each year and each period in the area 40-46°N, 141-151°E.

| Year / Period | 1955 | 1956 | 1957 | 1958 | 1959 | Total |
|---|---|---|---|---|---|---|
| Feb.-Mar. | | 8 | 22 | 71 | 62 | 163 |
| May-Jun. | | 3 | 45 | 45 | 49 | 142 |
| Jul.-Sept. | 37 | 47 | 81 | 88 | | 253 |
| Oct.-Nov. | — | 33 | 9 | 81 | | 123 |
| Total | 37 | 91 | 157 | 285 | 111 | 681 |

Table 1-3. Numbers of the GEK stations in each area in the period from September 1955 through June 1959.

| Lat. (N) / Long. (E) | 40-41° | 41-42° | 42-43° | 43-46° | Total |
|---|---|---|---|---|---|
| 141-145° | 96 | 221 | 83 | — | 400 |
| 145-151° | 75 | 91 | 90 | 25 | 281 |
| Total | 171 | 312 | 173 | 25 | 681 |

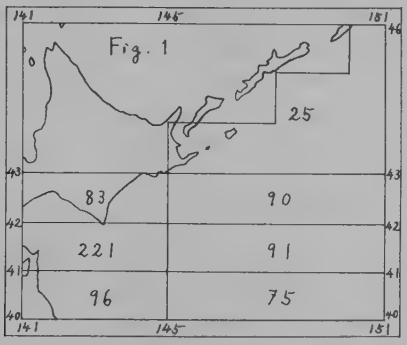


Fig. 1. Numbers of the GEK stations in each area in the period from September 1955 through June 1959. (the same with Table 1-3.)

maru of the Japan Meteorological Agency. The details are shown in Table 1-1 to 1-3.

On the cruises of both ships current velocity was measured with GEK at intervals of three hours; at the same time water temperature to the depth of 200 meters was measured with BT. The distance between adjoining GEK-BT stations was about 24 naut. miles for the Yūshio-maru and about 27 naut. miles for the Ryōfū-maru.

### 3. *Accuracy of the GEK data*

GEK on board both the Yūshio-maru and the Ryōfū-maru were made by the "Kagaku-Kenkyujo" Co., Tokyo. The interval between the two electrodes was 60 meters. A voltage of 1 mV between the electrodes corresponded to a current velocity of about 1 knot. Droop correction was calculated using a chart in an appendix of "Oceanographic Observation Manual (C.M.O. 1955)". The droop

correction is inversely proportional to the square root of the ship speed (Shoji 1955), so at the normal speed of the Yūshio-maru, 8.5 knots, the droop correction reaches to 0.4 knot in the maximum.

The error based upon the reading of an electronic recording potentiometer is estimated at 0.1 knot in a calm sea and 0.25 knot in a very rough sea. The error of the calculated droop correction due to uncertainty of ship speed is estimated at 0.05 knot in the maximum. In the investigated sea area, the depth is more than 200 meters at most stations, so in this paper k-factor (von Arx 1950) was taken always as 1.00. The error based upon the k-factor may be smaller than 0.1 knot in the sea deeper than 200 meters. Thus, the total error in the current velocity determined with GEK of the Yūshio-maru and the Ryōfū-maru in that sea area may be smaller than 0.25 knot in a calm sea and smaller than 0.4 knot in a very rough sea.

### *4. Current charts in each season without distinction of water masses*

The GEK data shown in Table 1-2 were sorted without distinction of years, (1) by the months of observation into four periods: February to March, May to June, July to September and October to November, and (2) by the localities of GEK stations in each field of one degree.

Throughout the four periods, the maximum number of GEK stations in each field of one degree is 22, and number of fields in which numbers of GEK stations N is more than 10 is 25 throughout the four periods as shown in Table 2.

Table 2. Numbers of the fields of one degree corresponding to N in each period in the area 40-46°N, 141-151°E.

| N \ Period | Feb.-Mar. | May-Jun. | Jul.-Sep. | Oct.-Nov. | Total |
|---|---|---|---|---|---|
| 1-9 | 19 | 19 | 28 | 22 | 88 |
| 10-22 | 7 | 5 | 10 | 3 | 25 |
| Total | 26 | 24 | 38 | 25 | 113 |

For the 25 fields in which N is more than 10, following three values are calculated: scalar mean velocity A, vector mean velocity (direction and magnitude) B and stability C. Here stability C was defined (Hidaka 1955) as

$$C\ (\%) = \frac{B}{A} \times 100.$$

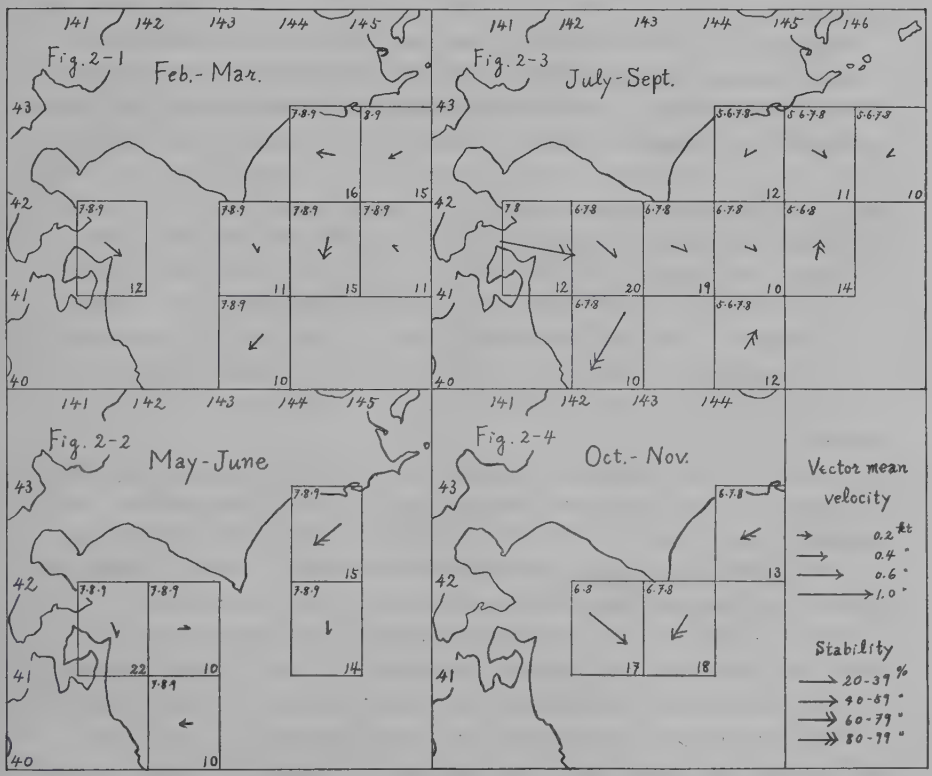


Fig. 2. Current charts in four periods: Fig. 2-1 February-March, Fig. 2-2 May-June, Fig. 2-3 July-September, Fig. 2-4 October-November.

Direction, length and feathers of an arrow show the direction, magnitude and the stability of the vector mean velocity in each field of one degree.

Number at lower right-hand corner means the number of the stations in each field (N) and numbers at top left mean the years of observation (5: 1955, 6: 1956, ..., 9: 1959).

In the current charts Figs. 2-1 to 2-4, direction and magnitude of vector mean velocity B are shown by direction and length of an arrow, and the stability C is shown by the number of feathers of the arrow. In these charts are also shown N and the years of observations. For most fields in the charts, GEK data of three years are gathered, so errors due to inter-annual variation are

insignificant.

From Figs. 2-1 to 2-4, throughout four periods, the scalar mean velocity A changes within the limits of 0.3～1.3 knot, the magnitude of the vector mean velocity B does within 0.1～1.0 knot and the stability C does within the limit of 24–94%. As the fields in which N is less than 9 are neglected in Figs. 2-1 to 2-4, these current charts can not cover the three kinds of currents in all seasons, but following points will be seen from these charts : The most distinct current in the investigated area is found in the period from July to September in the area 40–42°N, 141–143°E near Shiriya-zaki, with the scalar mean velocity A of 0.9–1.3 knot, the vector mean velocity B of 0.9–1.0 knot and the stability C of 76–94%. This current corresponds to the Tsugaru current. Also in the period from October to November in the same area, a current having A of 1.2 knot, B of 0.6 knot and C of 60% is found corresponding to the Tsugaru current.

The second most distinct current is found in May to June in the area 42–43°N, 144–145°E off Kushiro with the stability C of 70%. This current corresponds to the Oyashio current, but its scalar mean velocity A is 0.6 knot, its vector mean velocity B is 0.4 knot, each about half of the corresponding values of the Tsugaru current in the period from July to September.

In the period from July to September in the fields with their centers at 40.5°N, 144.5°E and at 41.5°N, 145.5°E a north-northeastward current is formed with the scalar mean velocity A of 0.4–0.5 knot, the vector mean velocity B of 0.2–0.3 knot and the stability C of 60%. This current may correspond to the Oyashio front (Kawai 1955) ; the values of A, B and C are comparable to those of the Oyashio current off Kushiro in the period February through June.

### *5. Current velocity of different water masses*

In the investigated sea area three kinds of water masses are found accompanying the three kinds of currents mentioned in the previous paper. They are (a) the Oyashio water, (b) the Kuroshio water (in most cases transmuted) and (c) the Tsugaru current water. In many fields of one degree shown in Table 2, two or three different water masses are found, so it is not satisfactory to sort GEK data only by the locality of stations. For this reason the current data is sorted in regard to each water mass as distinguished by the BT data. In this paper, from the BT data only the temperature in the

100 meter layer ($T_{100}$) is used for brevity.

For instance, in the period from July to November the field of one degree with its center at 41.5°N, 143.5°E off Erimo-misaki is crossed by a front between the Tsugaru current and the Oyashio current. Therefore as seen in Table 3, the warm water mass with $T_{100}$ above 6.0°C (Tsugaru current water)

Table 3. Mean current velocities of the Tsugaru current water and the Oyashio water in the field of one degree with its center at 41.5°N, 143.5°E in the period from July through November.

| Period | $T_{100}$ (°C) | Scalar mean velocity (kt) | Vector mean velocity | | Stability (%) | N |
|---|---|---|---|---|---|---|
| | | | direction | kt | | |
| Jul.–Sept. | >6.0 | 0.74 | SE | 0.51 | 69 | 9 |
| | <5.9 | 0.65 | N | 0.15 | 27 | 10 |
| | Total | 0.64 | ESE | 0.21 | 33 | 19 |
| Oct.–Nov. | >6.0 | 0.79 | SSW | 0.57 | 72 | 9 |
| | <5.9 | 0.36 | SSW | 0.17 | 47 | 9 |
| | Total | 0.57 | SSW | 0.37 | 64 | 18 |

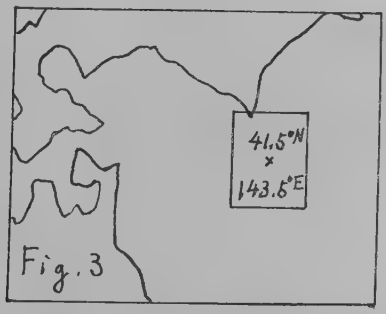


Fig. 3. The field of one degree which is referred in Table 3.

and the cold water mass with $T_{100}$ below 5.9°C (Oyashio water) in that field show different mean velocity and stability. That is, in the period July through November, in that field the Tsugaru current water has larger mean velocity and stability, while the Oyashio water has smaller mean velocity and stability.

In the following sections, GEK data are analysed in regard to the three water masses above mentioned.

*6. Current velocity of Oyashio water*

(1) The Oyashio base water and the transmuted Oyashio water

KAWAI (1955) gave the mean values of $T_{100}$ at the Oyashio front (a strong current zone between the Oyashio water and the transmuted Kuroshio water) as shown in Table 4.

On the other hand, according to the data from the hydrographic stations occupied by the Yūshio-maru and the Ryōfu-maru simultaneously with GEK, temperature and chlorinity in the 100 meter layer ($T_{100}$ and $Cl_{100}$) have a relation as shown in Table 5-1. Referring to Table 4 and Table 5-1, in this

Table 4. Mean temperature (°C) in the 100 m layer ($T_{100}$) at the axis as well as the edges of the Oyashio front in each period (after KAWAI).

| Period / the Oyashio front | Jan.-Mar. | Aug. | Nov. |
|---|---|---|---|
| Northern edge | 2.4 | 1.7 | 9.1 |
| Axis | 5.9 | 6.2 | 12.3 |
| Southern edge | 9.3 | 10.7 | 15.4 |

Table 5-1. Relation between the temperature and the chlorinity in the 100 m layer ($T_{100}$, $Cl_{100}$) of the Oyashio water in the area 40-46°N, 141-151°E in the period from September 1955 through June 1959.

| No. of stations | $T_{100}$ (°C) | $Cl_{100}$ (‰) |
|---|---|---|
| 101 | 0.3-2.9 | 18.14-18.48 |
| 68 | 3.0-5.9 | 18.38-18.75 |

Table 5-2. Frequency (%) of the Oyashio water among the GEK stations in the area 40-46°N, 141-151°E in the four periods.

| Period / $T_{100}$ Water mass | $T_{100}$<2.9°C The Oyashio base water | $T_{100}$=3.0-5.9°C The transmuted Oyashio water | $T_{100}$<5.9°C The Oyashio water in broad sense |
|---|---|---|---|
| Feb.-Mar. | 54 | 25 | 79 |
| May-Jun. | 32 | 24 | 56 |
| Jul.-Sept. | 34 | 21 | 55 |
| Oct.-Nov. | 19 | 25 | 44 |
| Total | 34 | 23 | 57 |

paper a water mass with $T_{100}$ less than 5.9°C is defined as the Oyashio water in broad sense. This water mass is divided in two, the one the Oyashio base water with $T_{100}$ less than 2.9°C and the other the transmuted Oyashio water with $T_{100}$ of 3.0–5.9°C. In Table 5–2, frequencies of the Oyashio base water and the transmuted Oyashio water in four periods in the investigated area are shown based upon the data of the GEK-BT stations in Table 1–2. Frequency of the Oyashio base water is maximum in the period from February to March (54%) and is minimum in the period from October to November (19%). But frequency of the transmuted Oyashio water is almost constant (21–25%) throughout the year.

All GEK data of the Oyashio base water and the transmuted Oyashio water throughout the year in the area 40–44°N, 141–150°E are tabulated in Table 5–3. The scalar mean velocities A of the two water messes are nearly equal (0.5 knot) but the stabilities C of the transmuted Oyashio water is smaller (1%) than that of the Oyashio base water (23%).

Table 5–3. Mean velocity of the Oyashio water throughout the year in the area 40–44°N, 141–150°E.

| Water mass | Oyashio base water | Transmuted Oyashio water |
|---|---|---|
| $T_{100}$ (°C) | <2.9 | 3.0–5.9 |
| Numbers of stations | 210 | 147 |
| Scalar mean velocity (kt) | 0.47 | 0.45 |
| Vector mean velocity (kt) | SSW 0.11 | ENE 0.01 |
| Stability (%) | 23 | 1 |
| Maximum velocity (kt) | 2.2 | 2.1 |
| Frequency (%) of the strong current above 1.0 kt | 6.7 | 5.2 |

Table 5–4. The maximum velocity and the frequency of the strong current above 1.0 kt of the Oyashio water in the area 40–44°N, 141–150°E.

| Water mass | Oyashio base water | | | Transmuted Oyashio water | | |
|---|---|---|---|---|---|---|
| Period | Numbers of stations | Maximum velocity (kt) | Frequency (%) above 1.0 kt | Numbers of stations | Maximum velocity (kt) | Frequency (%) above 1.0 kt |
| Feb.–Mar. | 81 | 2.1 | 2.5 | 40 | — | 0.0 |
| May–June | 45 | 2.2 | 15.5 | 34 | 2.0 | 8.8 |
| Jul.–Sept. | 64 | 1.1 | 6.3 | 50 | 2.1 | 8.0 |
| Oct.–Nov. | 20 | 1.2 | 5.0 | 30 | 1.0 | 3.3 |

The Oyashio base water flows to SSW at 0.1 knot in the mean throughout the year in the area 40–44°N, 141–150°E. On the other hand the transmuted Oyashio water is at a standstill on the average.

The maximum velocity as well as the frequency of the strong current above 1.0 knot of the Oyashio water mass in the area 40–44°N, 141–150°E has a seasonal variation as shown in Table 5–4.

(2) Frequency of current direction and current velocity of the Oyashio base water throughout the year

Frequency and mean velocity in each current direction of the Oyashio base water throughout the year in the area 40–44°N, 141–150°E are shown in Fig. 4 based upon 210 GEK-BT stations. From this figure, one may see that

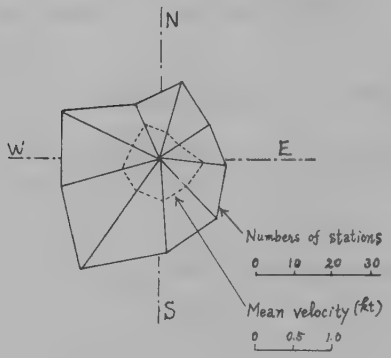


Fig. 4. Frequency and mean velocity in each current direction of the Oyashio base water throughout the year in the area 40–44°N, 141–150°E.
The solid line connects the numbers of stations in every 40° of direction and the broken line connects the mean velocity in every 40° of direction.

Table 6. Frequency in each velocity of the Oyashio base water in the area 40–44°N, 141–150°E throughout the year.

| Velocity (kt) | 0.1–0.2 | 0.3–0.5 | 0.6–1.0 | 1.1–1.5 | 1.6–2.2 |
|---|---|---|---|---|---|
| Frequency (%) | 24 | 46 | 26 | 3 | 1 |

the frequency and the mean velocity vary with the current direction nearly parallel each other. On the other hand the same GEK data of the Oyashio base water in Table 5–3 are sorted by their velocities as shown in Table 6. From the table, frequency of the velocity of 0.3–0.5 knot is 47%, and frequency of the velocity above 1.1 knot is only 4% throughout the year.

(3) Annual variations of the current of the Oyashio base water

The GEK data of the Oyashio base water shown in Tables 5–3, 5–4 and 6 are divided by their month and by their locality as shown in Table 7–1 to 7–3.

Table 7. Mean velocity of the Oyashio base water in various periods and in various localities.

| Table | Localities | Periods | No. of stations | Scalar mean velocity | Vector mean velocity | Stability |
|---|---|---|---|---|---|---|
| 7-1 | 40–43°N, 142–145°E | Feb.–Jun. | 79 | 0.49 kt | SSW 0.15 kt | 30 % |
| | | Jul.–Nov. | 19 | 0.40 | S 0.10 | 24 |
| | 40–44°N, 145–150°E | Feb.–Jun. | 47 | 0.46 | W 0.08 | 18 |
| | | Jul.–Nov. | 65 | 0.48 | S 0.11 | 23 |
| 7-2 | 42–43°N, 145–150°E | Feb.–Jun. | 25 | 0.46 | SW 0.12 | 27 |
| | | Jul.–Nov. | 34 | 0.54 | SSW 0.25 | 47 |
| 7-3 | 42–43°N, 143–145°E | Feb.–Mar. | 17 | 0.47 | W 0.21 | 44 |
| | | May–Jun. | 14 | 0.57 | SW 0.42 | 73 |
| | 41–42°N, 143–145°E | Feb.–Mar. | 23 | 0.40 | S 0.18 | 45 |
| | | May–Jun. | 12 | 0.50 | E 0.05 | 10 |

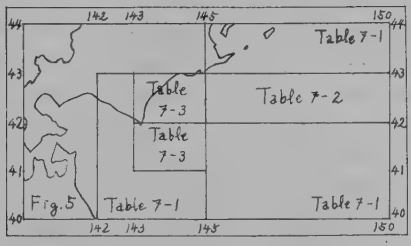


Fig. 5. The areas those have been referred in Tables 7–1, 7–2 and 7–3.

From these tables, seasonal variation of the mean current velocity of the Oyashio base water is seen to be different with locality. In the area 40–43°N, 142–145°E, the stability is larger in February through June (30%) than in July through November (24%), but in the area 40–44°E, 145–150°E and in the area 42–43°N, 145–150°E the stability is larger in July through November (23–47%) than in February to June (18–27%). On the other hand in the area 42–43°N, 143–145°E the stability is larger in May to June (73%) than in February to March (44%), but in the area 41–42°N, 143–145°E the stability is larger in February to March (45%) than in May to June (10%).

Throughout the periods and the areas above mentioned, the Oyashio base water flows with the scalar mean velocity of 0.40–0.58 knot, with the vector mean velocity of 0.05–0.42 knot and with the stability of 10–73%.

### *7. Current velocity of the Kuroshio water (velocity of the Oyashio front)*

The warm water with $T_{100}$ above 6.0°C in the sea north of 40°N, having large chlorinity as shown in Table 8–1, corresponds to the Kuroshio water (in most cases transmuted) or to the Tsugaru current water. But it is difficult to divide these two water mases by the T-Cl diagram only. In this paper, for convenience, the warm water with $T_{100}$ above 6.0°C in the sea to the east of 144°E is defined as the "Kuroshio water of the northern branch of the Kuroshio Extension" and the similar water in the sea to the west of 144°E as the "Tsugaru current water".

The Kuroshio water extends as far as 42°N in the period February through

Table 8-1. Relation between $T_{100}$ and $Cl_{100}$ of the warm water with $T_{100}$ above 6.0°C in the area 40–46°N, 141–151°E throughout the period from September 1955 through June 1959.

| No. of stations | $T_{100}$ (°C) | $Cl_{100}$ (‰) |
|---|---|---|
| 61 | 6.0–9.9 | 18.58–18.92 |
| 39 | 10.0–17.9 | 18.68–19.13 |

Table 8-2. Frequency (%) of the Kuroshio water among the GEK stations in the area 40–43°N, 144–151°E in four periods.

| Period | Feb.–Mar. | May–Jun. | Jul.–Sept. | Oct.–Nov. | Total |
|---|---|---|---|---|---|
| Frequency (%) | 14 | 12 | 36 | 33 | 25 |
| Total No. of GEK St. | 115 | 66 | 147 | 55 | 383 |

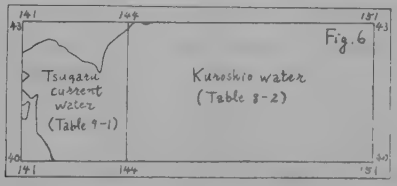


Fig. 6. The areas those have been referred in Table 8-2 and Table 9-1.

Table 8-3. Current velocity of the Oyashio front in two periods.

| Period | $T_{100}$ (°C) | No. of stations | Scalar mean velocity | Vector mean velocity | Stability | Max. velocity | Frequency (%) above 1.0 kt |
|---|---|---|---|---|---|---|---|
| Feb.-Jun. | 6.0-14.0 | 24 | 0.54 kt | E 0.28 kt | 53 % | 1.1 kt | 16.7 |
| Jul.-Nov. | 6.0-9.9 | 45 | 0.47 | SSE 0.02 | 5 | 1.3 | 6.7 |
| | 10.0-16.2 | 26 | 0.65 | SSE 0.23 | 35 | 1.8 | 19.3 |

June and as far as 43°N in the period July through November. Frequency of the Kuroshio water in the area 40-43°N, 144-151°E in each periods is shown in Table 8-2. It is 12-14% in the period February through June and 33-36% in July through November. The GEK data in Table 8-2 are divided into three by their month periods and their $T_{100}$ as shown in Table 8-3. From the table, in the period February through June the Kuroshio water with $T_{100}$ of 6.0-14.0°C flows to the E with fairly larger stability (53%). In the period July through November, the transmuted Kuroshio water with $T_{100}$ of 6.0-9.9°C is nearly at a standstill and the Kuroshio water with $T_{100}$ of 10.0-16.2°C flows to the SSE with small stability (35%).

The so-called Oyashio front (Kawai 1955) corresponds to the E or SSE flow of the Kuroshio water above mentioned. From Table 8-3, the maximum velocity of the Oyashio front is seen to be 1.1 knot in the period February through June and 1.8 knot in the period July through November. And the frequency of the strong current above 1.0 knot is 17-19% in the Kuroshio water.

Comparing Table 7-1 and Table 8-3, the mean velocity of the Kuroshio water in the sea north of 40°N is larger and more stable than the mean velocity of the Oyashio water.

### *8. Current velocity of the Tsugaru current water*

As above mentioned, the Tsugaru current water is defined here as the warm water with $T_{100}$ above 6.0°C in the area 40-43°N, 141-144°E. The frequency of the Tsugaru current water in the area 40-43°N, 141-144°E is about 75% except in the period February to March as shown in Table 9-1.

From Table 9-2, the Tsugaru current water with $T_{100}$ above 10.0°C has larger velocity and stability than the water with $T_{100}$ of 6.0-9.9°C throughout the year.

Table 9-1. Frequency (%) of the Tsugaru current water among the GEK stations in the area 40-43°N, 141-144°E in four periods.

| Period | Feb.-Mar. | May-Jun. | Jul.-Sept. | Oct.-Nov. | Total |
|---|---|---|---|---|---|
| Frequency (%) | 38 | 73 | 74 | 77 | 68 |
| Total number of GEK stations | 47 | 74 | 70 | 63 | 254 |

Table 9-2. Mean velocity of the Tsugaru current water in the area 40-43°N, 141-144°E throughout the year.

| $T_{100}$ (°C) | Number of stations | Scalar mean velocity (kt) | Vector mean velobity (kt) | Stability (%) |
|---|---|---|---|---|
| 6.0-9.9 | 93 | 0.60 | ESE 0.15 | 25 |
| 10.0-18.1 | 79 | 1.02 | SE 0.45 | 44 |

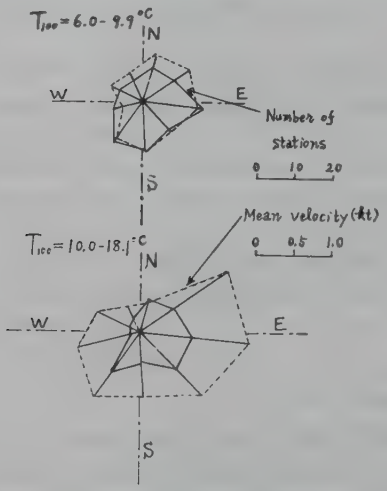


Fig. 7. Frequency and mean velocity in each current direction of the Tsugaru current water throughout the year in the area 40-43°N, 141-144°E.
Upper figure correspends to $T_{100}$ of 6.0-9.9°C and lower does to $T_{100}$ of 10.0-18.1°C.
The explanations are the same with Fig. 4.

From Fig. 7, the frequency of current direction of the Tsugaru current water is small in W, NW and N directions and mean velocity is large in E direction throughout the year.

From Table 9-3 and 9-4, current velocity of the Tsugaru current is small

Table 9-3. Mean velocity of the Tsugaru current water in the area 40-43°N, 141-144°E in four periods.

| $T_{100}$ (°C) | Periods | Number of stations | Scalar mean velocity (kt) | Vector mean velocity (kt) | Stability (%) |
|---|---|---|---|---|---|
| 6.0-9.9 | Feb.-Mar. | 18 | 0.65 | SE 0.25 | 39 |
| | May-Jun. | 39 | 0.59 | E 0.10 | 18 |
| | Jul.-Sept. | 23 | 0.64 | SE 0.24 | 37 |
| | Oct.-Nov. | 13 | 0.49 | SE 0.01 | 3 |
| 10.0-18.1 | May-Jun. | 15 | 0.59 | S 0.30 | 51 |
| | Jul.-Sept. | 29 | 1.14 | SE 0.54 | 47 |
| | Oct.-Nov. | 35 | 1.10 | ESE 0.47 | 43 |
| 6.0-18.1 | Feb.-Mar. | 18 | 0.65 | SE 0.25 | 39 |
| | May-Jun. | 54 | 0.59 | SE 0.13 | 22 |
| | Jul.-Sept. | 52 | 0.92 | SE 0.40 | 44 |
| | Oct.-Nov. | 48 | 0.94 | ESE 0.35 | 37 |

Table 9-4. Maximum velocity and the frequency of the strong current above 1.0 kt of the Tsugaru current water in the area 40-43°N, 141-144°E in four periods.

| $T_{100}$ (°C) | 6.0-9.9 | | 10.0-18.1 | |
|---|---|---|---|---|
| Period | Max. velocity (kt) | Frequency (%) above 1.0 kt | Max. velocity (kt) | Frequency (%) above 1.0 kt |
| Feb.-Mar. | 1.2 | 22 | — | — |
| May-Jun. | 1.3 | 10 | 1.2 | 27 |
| Jul.-Sept. | 2.0 | 13 | 2.6 | 62 |
| Oct.-Nov. | 1.6 | 8 | 3.0 | 49 |

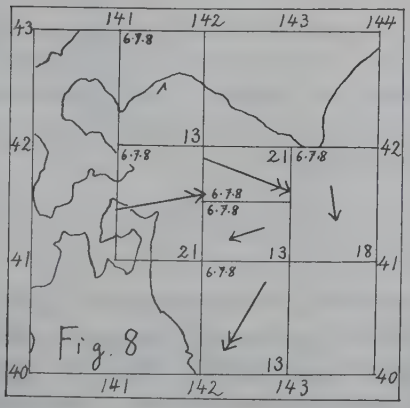


Fig. 8. Current chart of the Tsugaru current water in the period from July through November.
The explanations are the same with Fig. 2.

in the period February through June and large in the period July through November.

In the period July through November, the stream axis is seen clearly in the current chart for the warm water with $T_{100}$ above 6.0°C, Fig. 8.

*9. Discussion*

The results above outlined are subject to the following restrictions:

(1) GEK data include the effect of temporary wind drift current.

(2) As only 3–4 years data have been obtained, so inter-annual variation over a period longer than 5 years may yield some error in the results.

(3) In sections 7 and 8 above, the Kuroshio water and the Tsugaru current water are divided conveniently by the meridian of 144°E, but in May to June the Kuroshio water flows into the area to the west of 144°E on occasions. So the figures on the mean velocity of the Tsugaru current water in May to June contain some error.

(4) As the number of GEK stations is not sufficiently large especially to the east of 145°E, it is difficult to differentiate the seasonal variation and the local variation of the currents over the whole area.

Nevertheless, the mean velocity data of the Oyashio, the Kuroshio and the Tsugaru current waters north of 40°N above mentioned are the most reliable ones ever obtained. Furthermore, the vector mean velocity and its stability for each water mass in the area north of 40°N are presented for the first time.

It is ascertained from the GEK data that the Oyashio current does not form a distinct and continuous stream axis. The strong current which is found occasionally in the Oyashio water may be due to some isolated local eddy: in the investigated area the Oyashio base water flows to SSW very slowly (at 0.1 knot) in the average throughout the year.

*10. Comparison of the current velocity by GEK and the velocity obtained by dynamic computation*

(1) In Table 10–1, the velocity of the Oyashio current obtained by dynamic computation Vc (Sugiura 1957, 1958b) and the mean velocity observed by GEK Vo in the same area and the same period are compared. From this table, Vc values in an interval of 10–20 naut. miles are larger than Vo, but Vc values

Table 10-1. Vc and Vo in the Oyashio current

| Vc | | | | | Vo | | | | |
|---|---|---|---|---|---|---|---|---|---|
| Month | Locality | Interval of the stations | Mean velocity between the stations | Level referred | Period | Area | Number of stations | Scalar mean velocity (kt) | Vector mean velocity (kt) |
| | | naut. mile | kt | m | | | | | |
| Feb. | 42.2°N 144.6°E | 20 | 1.07 | 1,000 | Feb.-Mar. | 42-43°N 143-145°E | 17 | 0 47 | 0.21 |
| Mar. | 40.5°N 143.6°E | 11 | 0.76 | 800 | Feb.-Mar. | 41-42°N 143-145°E | 23 | 0.40 | 0.18 |
| Mar. | 42.2°N 145.5°E | 16 | 0.58 | 1,200 | Feb.-Jun. | 42-43°N 145-150°E | 25 | 0.46 | 0.12 |
| May | 41.5°N 143.8°E | 14 | 0.66 | 1,200 | May-Jun. | 41-42°N 143-145°E | 12 | 0.54 | 0.05 |
| Jul. | 44.0°N 149.2°E | 135 | 0.08 | 800 | Jul.-Nov. | 40-44°N 145-150°E | 65 | 0.48 | 0.11 |
| Jul.-Aug. | 43.8°N 149 9°E | 56 | 0.40 | 1,500 | | | | | |
| May-Jun. | 43.1°N 149.2°E | 260 | 0.13 | 1,500 | Feb.-Jun. | 40-44°N 145-150°E | 47 | 0.46 | 0.08 |

Table 10-2. Vc and Vo in the Tsugaru current

| Vc | | | | | Vo | | | | |
|---|---|---|---|---|---|---|---|---|---|
| Month | Locality | Interval of the stations | Mean velocity between the stations | Level referred | Period | Area | Number of stations | Scalar mean velocity (kt) | Vector mean velocity (kt) |
| | | naut. mile | kt | m | | | | | |
| Oct. | 41.8°N 141.8°E | 35 | 1.1 | 400 | Jul.-Nov. | 41-42°N 141-142°E | 21 | 1.3 | 1.0 |
| Oct. | 40.8°N 142.8°E | 39 | 1.3 | 600 | 〃 | 40-41°N 142-143°E | 13 | 1.0 | 0.9 |
| Nov. | 41.5°N 142.7°E | 23 | 1.4 | 800 | 〃 | 41-42°N 142-143°E | 21 | 1.2 | 1.0 |

in an interval larger than 100 naut. miles agree with Vo fairly well.

(2) In Table 10-2, Vc and Vo values for the Tsugaru current in the same area and in the same period (SUGIURA 1958a) are compared; as shown in the table, Vc and Vo agree with each other fairly well.

(3) As shown in Fig. 4, 26% of the GEK data from the Oyashio base water in the area 40-44°N, 141-150°E show that the currents flows to the direction of 0°-110° throughout the year. The stability of the mean current of the transmuted Oyashio water in the area 40-44°N, 141-150°E throughout the year is only 1%. These results substantiate the existence of the counter current of the Oyashio base water and the transmuted Oyashio water which has been pointed out on the basis of the geopotential topography (SUGIURA 1957).

## *11. Summary*

(1) In the sea to the north of 40°N, the most rapid and stable flow of water is the Tsugaru current. In the period July through November the Tsugaru current has the vector mean velocity of 0.9-1.0 knot and the stability of 80-90%.

(2) The so-called Oyashio front to the north of 40°N flows to E-SE with the vector mean velocity of 0.2-0.3 knot and the stability of 40-60% in the average of the area 40-42°N, 144-151°E.

(3) The transmuted Oyashio water with $T_{100}$ of 3.0-5.9°C is at a standstill with a vector mean velocity of 0.01 knot and the stability of 1% on the average in the area 40-44°N, 141-150°E throughout the year.

(4) The Oyashio base water with $T_{100}$ below 2.9°C flows to SSW with a vector mean velocity of 0.11 knot and the stability of 23% on the average in the area 40-44°N, 141-150°E throughout the year.

(5) The most distinct current of the Oyashio base water is found from May to June in the area 42-43°N, 143-145°E off the coast of Kushiro-Tokachi flowing to SW with the vector mean velocity of 0.42 knot and with large stability of 73%.

*Acknowledgements*: In conclusion, the author wishes to express his thanks to Mr. Z. YASUI for his continuous encouragement and to Dr. K. YOSHIDA for his kind advices and suggestions. Thanks are also due to Prof. HAROLD M. LANE for reading the manuscript.

## References

HIDAKA, K. (1955): The ocean current (in Japanese). Tokyo, Iwanami Book Co. 30pp.

KAWAI, H. (1955): On the polar frontal zone and its flucutuation in the waters to the northeast of Japan (I). (in Japanese). *Bull. Tohoku Regional Fisheries Research Laboratory*, **4**, 1-46.

Maritime Safety Agency (1951): Coastwise passage pilot (in Japanese). 62pp. Fig. 30.

SHOJI, D. (1955): Droop correction of GEK (in Japanese). *Hydrographic Bull.*, Special Number 17, 33-34.

SUGIURA, J. (1957): On the Oyashio Current in the sea adjacent to Hokkaido. *Oceanogr. Mag.*, **9**, 133-142.

SUGIURA, J. (1958a): On the Tsugaru Warm Current. *Geophys. Mag.*, **28**, 399-409.

SUGIURA, J. (1958b): On the sea conditions to the east off the Kurile Islands. *Oceanogr. Mag.*, **10**, 169-178.

SUGIURA, J. (1959): On the currents south off Hokkaido in the western North Pacific. *Oceanogr. Mag.*, **11**, 1-11.

von ARX, W. (1950): An electromagnetic method for measuring the velocities of ocean currents from a ship under way. *Pap. Phys. Oceanogr. Met.*, **11**, 1-62.

The Oceanographical Magazine
Vol. 11. No. 2, March 1960

# On the Deep Water in the Western North Pacific*

By

Takashi Ichiye

*Oceanographic Institute, Florida State University*

**Abstract:** The temperatures of deep waters at 4000 m depth to the south of Japan indicate higher values west than east of the ridge. In the Kuroshio region salinity at 1000 m depth which corresponds to the minimal layer is higher west than east of the ridge. Correspondingly, the oxygen at the minimal oxygen layer is higher west of the ridge. The level of no motion in the Kuroshio is estimated as 1000 m to 1200 m from comparison of surface velocity measured by GEK and obtained by dynamic calculation. With such reference level the counter current under the Kuroshio is found to transport almost the same amount of the water as the Kuroshio. It is discussed that the counter current may cause formation of the cyclonic vortex along the northern edge of the Kuroshio west of the ridge as well as differences in properties of waters east and west of the ridge.

## *1. Introduction*

The hydrographic studies of the Kuroshio or the western North Pacific in general are far behind those of the Gulf Stream as far as deep waters are concerned. Recent systematic surveys of Woods Hole Oceanographic Institution have revealed various important features of the deep circulation owing to close networks of stations, dense sampling layers in the deep and extensive use of high precision salinometers. On the other hand, in the western North Pacific stations yielding hydrographic data below 2000 m were only occasionally occupied after the World War II. The data available were mostly collected by the Japanese Navy Hydrographic Office vessels from 1930 to 1939. However, these hydrographic stations are scattered at random in time and space. Also sampling depths at the stations were taken usually at intervals of about 1000 m below 2000 m. Yet some features of deep waters can be derived by adequate interpretation of such data, although they are incomplete from today's standard.

* Contribution No. 134, Oceanographic Institute, Florida State University.

The purpose of this study is to show how these data are useful in some respects and to urge future observations of deep waters which are so valuable in oceanography. In this study the distribution of deep waters is discussed in relation to the effect of the submarine ridge south of Japan.

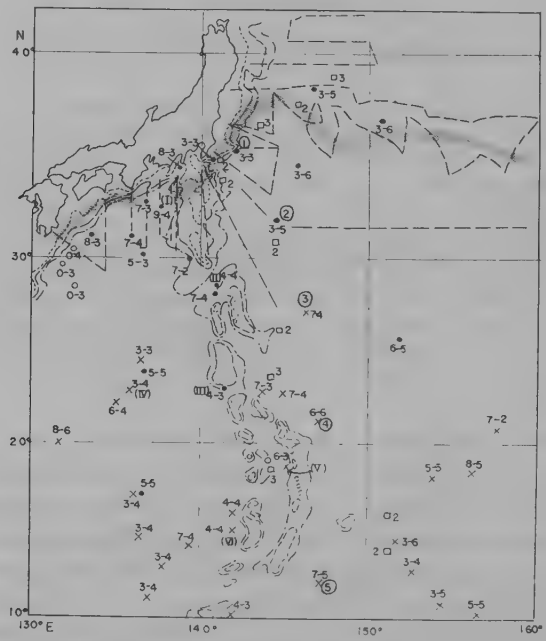


Fig. 1. Bottom topography of the Western North Pacific and locations of stations and sections studied. Bottom contours of 1000 m are shown in dotted lines, those of 2000 m in broken lines and those of 3000 m in chain lines. Thick broken lines indicate the sections of NORPAC Operation. Keys for hydrographic stations: ○ for the Manshū, × for the Koshū, ● for the Komahashi and □ for the Carnegie. The figures attached to stations indicate the year of observation (the last figure of 1930 to 1939) and the maximal depth of observation (in 1000 m). At the Carnegie stations only the maximal depth is shown. The Roman number in parenthesis or Arabic number in a circle means the station, oxygen-temperature correlations of which are shown in Fig. 6. The stipled zone indicates the course of the Kuroshio in August, 1955, obtained from the NORPAC data.

## 2. *Comparison of T-S diagrams in deep waters*

The locations of deep sea stations including Carnegie stations (Fleming et al, 1945) used in this study are shown in Fig. 1 with the bottom contours copied from the Russian chart "Morskoi Atlas" Tom 1, Plate 56 (1950). At each station the maximal depth and year of observation are indicated. All these stations are within a region of the Western North Pacific Central Water as defined in the "Ocean" (Sverdrup et al, 1942).

As the first step, T-S points at 4000 m, 3000 m and 2000 m of these stations are plotted in Fig. 2. The points of stations east and west of the Bonin Ridge (hereafter referred as the Ridge) south of Japan are indicated by different symbols. Also the T-S diagrams are divided into three latitudinal sections, 30° to 38°N, 20° to 30°N and 10° to 20°N, because these sections have different

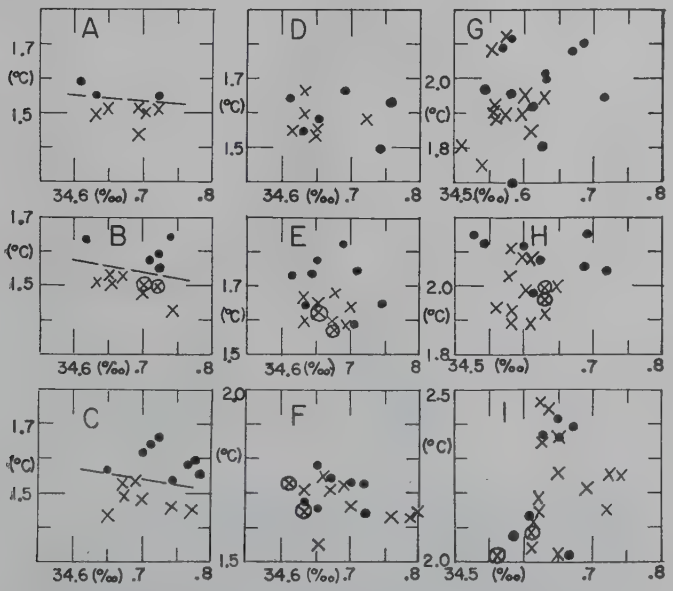


Fig. 2. T-S correlations at 4000 m (A, B and C), 3000 m (D, E and F) and 2000 m (G, H and I). The figures A, D and G are from stations between 30° and 38°N; B, E and H are from those between 20° and 30°N; C, F and I are from those between 10° and 20°N. Keys: ● West of, × east of, ⊗ on Ridge.

oceanographic features. The northernmost section represents the swift flowing Kuroshio region, the middle section the stagnant region corresponding to the Sargasso Sea in the North Atlantic and the southernmost section the subtropical region.

This figure indicates that there is almost no latitudinal difference at 3000 m and 4000 m depth but apparently the temperatures at 2000 m depth increase to the south. The water at 4000 m depth has definitely higher temperature west than east of the Ridge, but no east-west difference in the distributions of T-S points can be recognized at 2000 m depth. Those at 3000 m depth are intermediate between those two depths. The reason is almost obvious, because at 4000 m depth the Ridge forms a barrier separating the water east and west of it completely. At 2000 m depth the water masses of

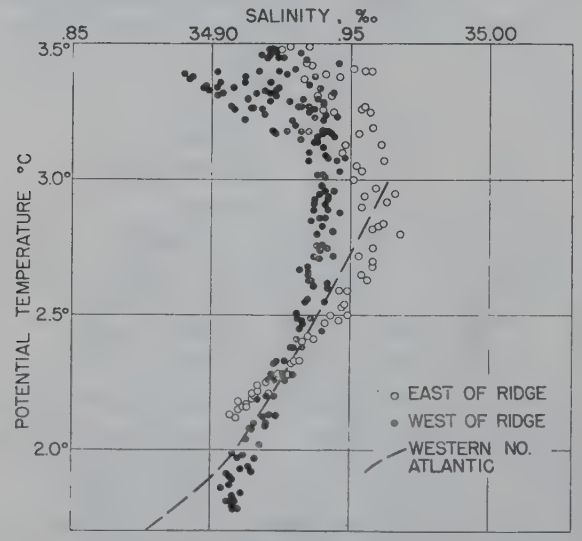


Fig. 3. Potential temperature versus salinity diagrams obtained by WORTHINGTON (1957) (The dashed line is the average curve from 805 measurements, west of 50°W up to April, 1957. The solid and open circles are from the Discovery data).

both sides of the Ridge can mix through many gaps in the Ridge. As an exception of this situation, east-west difference in temperature can be recognized up to 2000 m depth in the section between 20° and 30°N. This is perhaps due to the stagnant water in the area which corresponds to the Sargasso Sea. It is noted that the temperature of the water at the stations right upon the Ridge is intermediate between those of the stations east and west at 4000 m depth.

The scatter of salinity is large compared with the recent data obtained in the North Atlantic by use of salinometers which is reproduced in Fig. 3

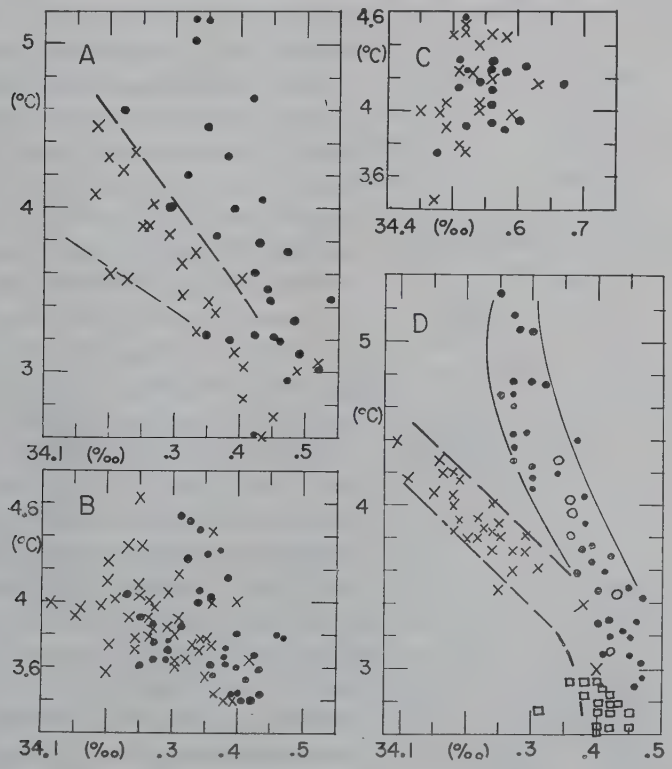


Fig. 4. T-S correlations at 1000 m. The figures A, B and C are from stations between 30° and 38°N, between 20° and 30°N and between 10° and 20°N. The figure D is from the NORPAC data. Keys: ● west of, × east of, ○ on Ridge, □ in the Oyashio (east of Ridge).

(WORTHINGTON, 1957). There is no information about the accuracy of titration at the time of observations of the data discussed. This scatter seems to be larger than attributed solely to errors of titration which might be at most ±0.05%. However it is worth while to check in future observations whether this scatter is actual or due to errors of titration.

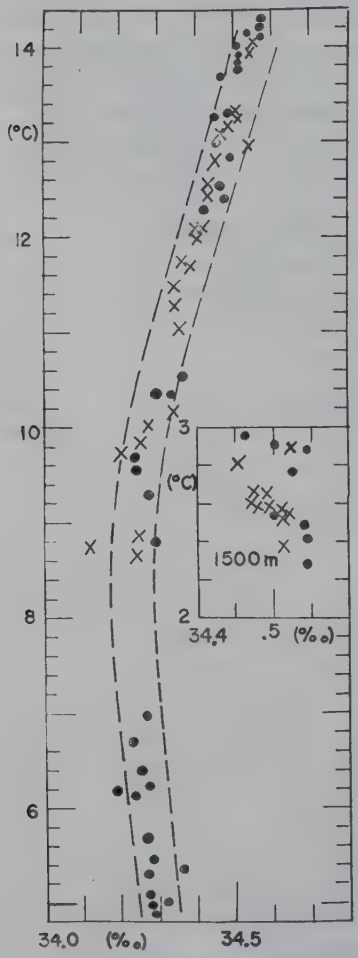


Fig. 5. T-S correlations at 500 m and 1500 m (an inserted figure) from the NORPAC data. Keys: ● west of, × east of Ridge.

The hydrographic data of 1000 m depth are more abundant than those of 2000 m and deeper depths. In Fig. 4(A) to (C), therefore, T-S points from all data obtained by the Hydrographic Office during the same period as those of Fig. 2 are plotted in the same way as Fig. 2. The scatter of the points is larger than in deeper layers. Also there is no distinction between the points east and west of the Ridge south of 30°N. But the points in the section of 30° to 38°N have apparently different T-S correlation in the east and west of the Ridge. In order to confirm this, T-S points of 1000 m layer are plotted from the data of NORPAC Operation in 1955 in Fig. 4(D). In this figure the data of the stations east of the Ridge are indicated by different symbols according to their location which is either in the Kuroshio region or in the Oyashio region. This criterion is based on the current chart obtained by dynamic calculation. The sections of NORPAC Operation are shown in Fig. 1. It is clearly seen that the T-S correlations are different in the Kuroshio water between east and west of the Ridge. Also both cor-

relations converge into the cluster of points representing the Oyashio water. The T-S points of the stations right upon the Ridge belong to those west of the Ridge.

For comparison, T-S diagrams of 1500 m and 500 m from the NORPAC data are plotted in Fig. 5. This figure again indicates difference between east and west of the Ridge. What effect cause the east-west difference in T-S relations at 1000 m depth? As revealed later, the depth of no motion in the Kuroshio lies at 1000 m to 1200 m. The movement and horizontal mixing in 1000 m layer are expected to be weak compared with layers below and above it. On the other hand, the intermediate water which sinks north of the polar front spreads to the south at about 800 m to 1100 m in the region east of the Ridge, forming minimal salinity layer (Ichiye, 1955b and 1956b). However, this water does not mix well with the water west of the Ridge at about 1000 m owing to sluggish flow there. Therefore the salinity at the depths near the minimal salinity layer is smaller in the east than in the west of the Ridge. This tendency is generally seen in T-S curves of individual stations (Ichiye, 1956b). The difference in the T-S diagrams at 1000 m depth is merely a reflection of this tendency.

### *3. Oxygen and temperature relations*

The oxygen data are also important in the water mass analysis in the deep sea, when they are used together with temperature and salinity data (Stommel, 1958). However, the oxygen data in the area are too scarce to construct oxygen-temperature diagrams similar to the T-S diagrams shown in Fig. 2. Therefore, instead, oxygen-temperature curves of a few representative stations are indicated in Fig. 6.

The east-west difference of oxygen-temperature correlations is most conspicuous at the portion of minimal oxygen which is found at the depths of 1000 m to 1200 m east and of 800 m to 1000 m west of the Ridge. Apparently the minimal value of oxygen increases from the north to the south in the section east of the Ridge (Ichiye, 1954b, 1956a). The minimal oxygen is larger west than east of the Ridge but in the section south of 20°N there is almost no west-east difference in this value.

It is shown that the sill-depth effect of the Ridge on the distributions of temperatures seems to be limited below 3000 m in the T-S diagrams of Fig. 2.

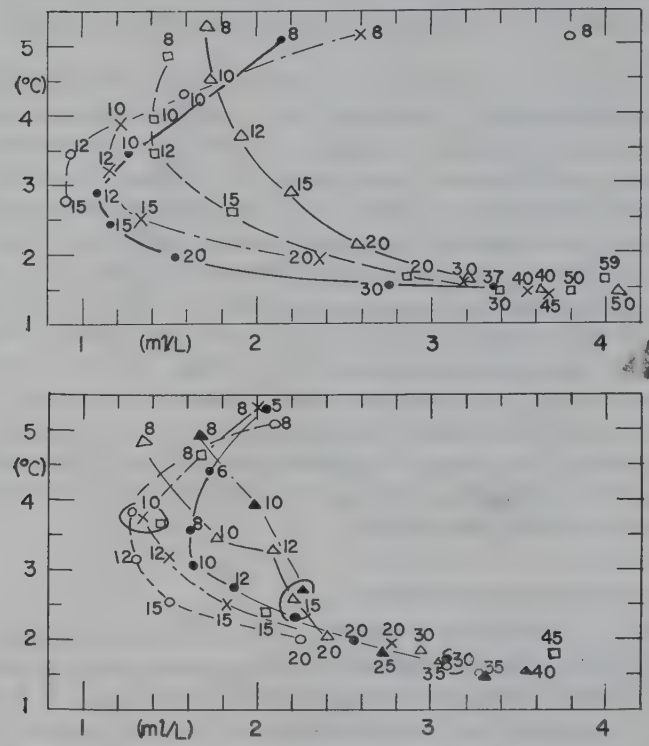


Fig. 6. Temperature (°C) and oxygen (ml/L) correlations at the stations east of the Ridge (upper) and west of the Ridge (lower). The location of the stations is indicated in Fig. 1 with Arabic numbers in circles (eastern stations) and with Roman numbers in parentheses (western stations). Keys to stations: Upper, ● for ①, ○ for ②, × for ③, □ for ④, △ for ⑤; Lower, ● for (I), ○ for (II), × for (III), □ for (IV), △ for (V), ▲ for (VI).

Thus the west-east difference in the minimal oxygen is due to more intense spread of the intermediate water in the east than west of the Ridge. This effect also causes the difference in T S diagrams at 1600 m depth as shown in Fig. 4.

*4. The level of no motion and the effect of the Ridge on circulation*

The movement of the Kuroshio must be greatly influenced by the Ridge which rises up to the depth of 1000 m or less in the course of the current. One of phenomena which are supposed to be due to the Ridge is the periodic appearance of a cyclonic vortex to the north of the Kuroshio west of the Ridge (Ichiye, 1954a, 1955a and 1957). This vortex was observed from 1936 to 1944 and again since 1954 (Ichiye, 1957). When it exists, the Kuroshio makes a detour around it to the south. Certainly this vortex was produced by the effect of the Ridge but no theory is established yet about the dynamics of its formation and dissipation. Also there is no general theory about the effect of a ridge on a flow which has the same order of vertical and horizontal scales as the Kuroshio. However, theories of an atmospheric flow over a mountain range can be applied to this problem if some modifications are done. Bolin's theory (1950), one of those about the effect of a mountain on an air flow, indicates that the narrow current deviates to the right when it crosses over a mountain range of an infinite length. Therefore if the Kuroshio flowed eastward down to the bottom, the effect of the Ridge would deviate the current to the south east of the Ridge but not west of it as observed.

The velocity of the current near the bottom is one of the most important factors governing the effects of bottom topography. However, again there is no direct measurement of the current in deep layers of the area. Therefore the indirect method, dynamical calculation of temperature and salinity data, has to be used to determine deep currents. The difficulty inherent to this method is undeterminedness of the depth of a reference level. One of the procedures to avoid this difficulty is to use the surface velocity measured with GEK as the standard in dynamic calculation. Then the absolute values of a velocity profile can be determined.

During the NORPAC Operation some ships carried out four to six GEK measurements between stations which yield the data for dynamic calculation. Actually the current speed measured with GEK is generally too weak and variable outside the Kuroshio to be reliable. Thus the procedure was applied to the stations in the Kuroshio only which is also the main current of interest in this study. The depths of no motion determined from velocity profiles west and east of the Ridge are indicated in the following table.

| | West of the Ridge | | | | East of the Ridge | | | | |
|---|---|---|---|---|---|---|---|---|---|
| Depth ranges (in 100 m) | 9–10 | 10–11 | 11–12 | >12 | 8–9 | 9–10 | 10–11 | 11–12 | >12 |
| Nnmbers of station-pairs | 1 | 1 | 2 | 3 | 1 | 2 | 4 | 3 | 2 |

This table shows us that the depths of no motion are slightly deeper west than east of the Ridge but the numbers of pairs of stations are too small to reach a definite conclusion. However certainly the depths of no motion in the whole area of the Kuroshio are at around 1000 to 1200 m. It is interesting to note that these depths are almost the same as those of no meridional motion in the North Pacific determined by a procedure derived from dynamic consideration (ICHIYE, 1959). In the Gulf Stream the level of no motion is at about 1600 m (STOMMEL, 1956) which is deeper than in the Kuroshio as estimated here.

There is few hydrographic stations which yield deep hydrographic data for dynamic calculation. In Fig. 7 the vertical profiles of volume transports from two pairs of such stations are plotted. The location of the stations is also indicated in the inserted chart of the figure. One pair of the stations was observed by the Komahashi and the other by the Carnegie. In the curves of Fig. 7 the level of no motion is taken at 1200 m. Apparently the volume transports from the Komahashi stations are much larger than those of the Carnegie. The reason of such difference is unknown.

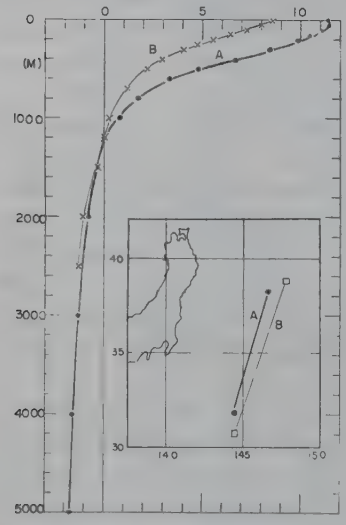


Fig. 7. Volume transports (in $10^6$ $m^3$/sec per 100 m) for Section A (thick line) and Section B (fine line).

The transports below the level of no motion are larger than has been expected heretofore. In the Komahashi section the transport to the east above the level of no motion is $56.6 \times 10^6$ $m^3$/sec but the westward transport below it reaches $45.2 \times 10^6$ $m^3$/sec. These curves suggest two important features which have been neglected

in the past. First, the flow below the mid-depth of the Kuroshio is westwards with relatively large transport. Thus the cyclonic vortex to the west of the Ridge becomes leeward phenomenon behind the Ridge for this undercurrent. Secondly, the variation in the transport of this undercurrent may influence greatly the course and speed of the Kuroshio overlying it.

Therefore hydrographic data of deep layers as well as of the upper layer are needed to understand the mechanism of variation of the Kuroshio. Unfortunately there was no systematic deep observations in the past as stated already. This means that any theory concerning the variation of the Kuroshio is a mere speculation until more deep data are available.

However one of such theories will be proposed as an example stressing the importance of the deep current on the variation of the Kuroshio. This is an explanation about the formation of the cyclonic vortex to the west of the Ridge (Ichiye, 1954a and 1955a). In this model the counter current under the Kuroshio is considered to be deflected to the north by the Ridge, owing to the vertical concentration of the water column (Bolin, 1950). The deflecting angel $\alpha$ of the current after passing the Ridge is given by

$$\sin\alpha \sim f U_0^{-1} \int_{x_0}^{x} h dx$$

in which $f$ is the Coriolis' parameter, $U_0$ is the initial volume transport per unit width and $h$ is the change of the depth of the current at the Ridge.

When $U_0$ decrease below a certain value, this angle $\alpha$ becomes larger than a critical value. Then the undercurrent strikes at the southern coast of Japan. Near the coast this current piles up the deep water which upwells there and forms a cold water domain in the upper layer. The Kuroshio will then make a detour around the cold water, producing a cyclonic vortex. This system becomes stable after the balance between the divergence term $f(\partial u/\partial x+\partial v/\partial y)$ and the increase of vorticity $D\zeta/Dt$ is established in the upper layer. (In the initial stage the divergence is positive, because it is equal to the vertical velocity $w_0$ at the bottom of the upper layer which is positive due to upwelling. Thus $D\zeta/Dt<0$ and cyclonic vorticity increases in the upper layer.)

## 5. *Concluding remarks*

The effects of the Ridge on the distribution of water masses in deep waters south of Japan will be revealed in many ways other than the east-west

difference in temperature if more deep data are available. Also the deep circulation in the area seems to be important as one of the causes of long period fluctuation of the Kuroshio. The formation of the vortex west of the Ridge will also be proved to be associated with the Ridge when more deep observations are carried out. This vortex has no counter part in the Gulf Stream. However, the study of its dynamics will help better understanding of both currents.

*Acknowledgements*: The author expresses his best thanks to Dr. SIDNEY W. FOX and Dr. F.C.W. OLSON for their encouragement throughout the present work.

## *References*

BOLIN, B. (1950): On the influence of the earth's orography on the westerlies. *Tellus*, **2**(3), 184–195.

FLEMING, J.A. et al (1945): Scientific results of cruises of the Carnegie during 1928–29. Oceanography, 1–B, Carnegie Institute of Washington, Pub. 545.

ICHIYE, T. (1954a): On the variation of oceanic circulation (VI). *Geophys. Mag* **25**(3 to 4), 185–217.

ICHIYE, T. (1954b): On the distributions of oxygen and their seasonal variations in the adjacent seas of Japan (I) and (II). *Oceanog. Mag.* **6**(2), 41–100.

ICHIYE, T. (1955a): On the variation of oceanic circulation (V). *Geophys. Mag.* **26**(4), 283–342.

ICHIYE, T. (1955b): On the possible origin of the intermediate water in the Kuroshio. *Rec. Oceanog. Works in Japan*, **2**(2), 82–89.

ICHIYE, T. (1956a): On the distributions of oxygen and their seasonal variation in the adjacent seas of Japan (IV). *Oceanog. Mag.*, **8**(1), 1–28.

ICHIYE, T. (1956b): On the properties of the isolated cold and fresh water along the edge of the Kuroshio (Hydrography of the polar front region, IV). *Oceanog. Mag.* **8**(1), 53–64.

ICHIYE, T. (1957): On the variation of oceanic circulation in the adjacent seas of Japan. Proc. UNESCO Symposium on Oceanog. in 1955, Tokyo, 116–129.

ICHIYE, T. (1959): A note on determination of the depth of no meridional motion. *J. Oceanog. Soc. Japan* **15**(4).

STOMMEL, H. (1956): On the determination of the depth of no meridional motion. *Deep-Sea Res.*, **3**, 273–278.

STOMMEL, H. (1958): The abyssal circulation (Letters to the Editors). *Deep-Sea Res.* **5**, 80–82.

SVERDRUP, H.U. et al (1942): The Oceans. Prentice Hall Inc.

VOENNO-MORSKOE MINISTERSTOVO, USSR (1950): Morskoi Atlas. Tom 1.

WORTHINGTON, L.V. (1957): A study of the deep water masses of the North Atlantic (Unpublished manuscript of the paper presented at the eleventh General Assembly of IUGG at Toronto).

The Oceanographical Magazine
Vol. 11. No. 2, March 1960

# On Water Budget in a Two-Layered Ocean*

By

Takashi Ichiye

*Oceanographic Institute, Florida State University*

**Abstract:** A two-layered ocean bounded with east and west coasts is envisaged. The regimes of flow in the upper and lower layers are divided into a narrow western boundary current and an inner geostrophic flow. The wind stresses act upon the inner flow in the upper layer. The water budget in a part of the ocean bounded with two coasts and two latitude circles is determined by meridional transports of the western inner flows across two latitudes and the vertical transports through the interface. The equation of conservation of mass leads to the differential equation about the integrated vertical current along a latitude. The latter equation can be solved when the western transports and wind stresses are known. The result is applied to the data of the Atlantic and the North Pacific to determine the transports of the inner flow in both layers, the vertical transport and the western transport in a lower layer from the wind stresses and western transport in a upper layer. In the Atlantic Ocean the meridional transport of the inner flow is southward in the upper layer and northward in the lower layer in most latitudes. The vertical motion is upward in the North Atlantic and downward in the South Atlantic. In the North Pacific the inner transport is southward in both layers and is much smaller in magnitude than in the Atlantic. The vertical motion in the middle latitudes of the North Pacific is downward, in contrast to the North Atlantic.

## *1. Introduction*

As Stommel pointed out (1958), the theory of thermohaline circulation in the ocean has not been well developed yet compared with the theory of wind-driven circulation. This is partly due to the condition that the heating-cooling process over the ocean is less known than the momentum transport process by the wind stress but mostly due to the non-linearity of the equations involved in the thermohaline theory. However, the serious discrepancy between the observed transports of the western current and those derived from the wind driven circulation theory confirms the importance of the thermohaline process

* Contribution No. 133, Oceanographic Institute, Florida State University.

in oceanic circulation.

One approach to the problem is mathematical handling of the non-linear equations which was provided by the author (1959) and SAINT-GUILY (1959). Another approach is to use a two-layered ocean model with a vertical current at the interface. In this model the thermohaline process is implicitely represented by the vertical current. STOMMEL (1958) already applied this model to the Atlantic to explain the discrepancy between the observed and theoretical transports of the western current. In this paper is used the same model as his. The equation of conservation of mass is applied to a basin surrounded by east and west coasts and two latitudinal circles. The result gives the relation among the wind stress curl, the western transport and the vertical transport, under the assumptions that the wind acts upon the upper layer only and that the inner current is governed mostly by geostrophic relation.

## 2. *Fundamental relations*

The model ocean is divided into the upper and lower layer. All quantities in the lower layer are designated with primes. The equations of motion and continuity in the upper layer are

$$-fv=-\partial p/\partial x+\partial\tau_x/\partial z \qquad (1)$$

$$fu=-\partial p/\partial y+\partial\tau_y/\partial z \qquad (2)$$

$$\partial u/\partial x+\partial v/\partial y+\partial w/\partial z=0 \qquad (3)$$

in which $x$-, $y$- and $z$-axis are positive toward the east, the north and upwards, respectively. These equations of motion are valid in the inner region of the ocean excluding the western current. The vertical shearing components $\tau_x$ and $\tau_y$ becomes equal to the wind stress at the surface and vanish at the bottom of the upper layer. The corresponding equations in the lower layer are obtained by replacing velocity components and pressure by primed letters and by deleting the shearing terms.

Crossdifferentiating (1) and (2) and integrating the result with $z$ from the surface to the bottom, of the upper layer, we have

$$f(\partial M_x/\partial x+\partial M_y/\partial y)+\beta M_y=\mathrm{curl}\,\boldsymbol{\tau} \qquad (4)$$

in which $M_x=\int u dz$ and $M_y=\int v dz$. The wind stress vector is expressed by $\boldsymbol{\tau}$. In this derivation the depth of the upper layer $H$ is assumed to be constant. The integration of (3) with $z$ gives

$$\partial M_x/\partial x+\partial M_y/\partial y-w_H=0 \qquad (5)$$

in which $w_H$ is the vertical velocity at the interface. Substituting (5) into (4) we have

$$fw_H+\beta M_y=\mathrm{curl}\,\tau \qquad (6)$$

The corresponding equation in the lower layer is

$$-fw'_H+\beta M'_y=0 \qquad (7)$$

in which the relation $w'_H=-w_H$ is used.

### 3. *Water budget in a surrounded section of the ocean*

The ocean is assumed to be bounded with east and west coasts as schematically shown in Fig. 1. The coasts are almost north-south and the $x$-coordinates of the east and west coast are $b(y)$ and $a(y)$, respectively. At first it is assumed that the ocean is also bounded to the north as is the case in the North Pacific and the Indian Ocean.

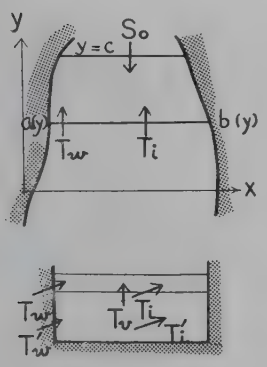


Fig. 1. Schematic representation of a model ocean. (Upper; horizontal plane: lower; cross-section.)

Consider the water budget in an area surrounded by these three boundaries and one latitude circle. In the upper layer meridional transports due to the western current and inner flow are expressed by $T_w$ and $T_i$, respectively. The upward transport across the interface is put to $T_v$. The conservation requirement (Stommel, Arons and Faller, 1958) gives the relation

$$T_i+T_w+T_v=0. \qquad (8)$$

In the lower layer we have the corresponding relation

$$T_i'+T_w'+T_v'=0 \qquad (9)$$

in which $T_v'=-T_v$ represents the downward transport across the interface.

The transports $T_i$ and $T_v$ are expressed by $M_y$ and $w_H$ from the definition like

$$T_i=\int_a^b M_y dx, \quad T_v=\int_y^c\int_a^b w_H dxdy \qquad (10)$$

in which $c$ is the $y$-coordinate of the northern boundary. Substitution of (6) into $M_y$ gives

$$T_i=\beta^{-1}\int_a^b (\mathrm{curl}\,\tau-fw_H)\,dx \qquad (11)$$

These equations are given by

$$T_i' = f\beta^{-1}\int_a^b w_B dx, \qquad T'_s = -T_s \tag{12}$$

in the lower layer. In these equations the lower limit of integration $a$ is understood to exclude the region of the western boundary current.

For brevity we put

$$W(y) = \int_a^b w_B dx \tag{13}$$

$$T_s = \beta^{-1}\int_a^b \mathrm{curl}\,\tau dx. \tag{14}$$

After substituting (10) and (11) and using (13) and (14), the equation (8) becomes

$$T_w + T_s = f\beta^{-1}W(y) - \int_y^e W(y)\,dy. \tag{15}$$

This equation (15) determines the function $W(y)$ in terms of the western transport $T_w$ and the wind stress curl. Since $T_w$ and $T_s$ are determined directly, the vertical velocity can be computed from this relation through measurable quantities.

In order to obtain more convenient form for computation, the variable $y$ of the function in (15) is transformed into latitude $\theta$. The relation between $y$ and $\theta$ is $y=R\theta$, in which $R$ is the radius of the earth. Differentiating (15) with $\theta$ we have

$$dW(\theta)/d\theta + \cot\theta\,(1+\sec^2\theta)\,W(\theta) = R^{-1}\cot\theta\,dF(\theta)/d\theta \tag{16}$$

in which

$$F(\theta) = T_w + T_s. \tag{17}$$

In this derivation the relation $f\beta^{-1}=R\tan\theta$ is used.

The value of $W(\theta)$ at a latitude $\theta=\theta_1$ is denoted by $W_1$. The integral of (16) becomes

$$RW(\theta) = \cot\theta\,\mathrm{cosec}\,\theta\left\{RW_1\sin\theta_1\tan\theta_1 - F(\theta_1)\sin\theta_1 + F(\theta)\sin\theta + \int_\theta^{\theta_1} F(\lambda)\cos\lambda\,d\lambda\right\}. \tag{18}$$

At the northern boundary $T_w=0$ and $T_i=0$, because the transports across it are assumed to vanish. When $\theta_1$ is put as the latitude of northern boundary, these boundary conditions lead to

$$F(\theta_1) = T_s(\theta_1),$$
$$R\tan\theta_1 \cdot W_1 = F(\theta_1). \tag{19}$$

Substituting (19) into (18) we have

$$RW(\theta)=\cot\theta\,\mathrm{cosec}\,\theta\left\{F(\theta)\sin\theta+\int_{\theta}^{\theta_1}F(\lambda)\cos\lambda\,d\lambda\right\}. \qquad (20)$$

*4. Application and modification of the water budget relations*

The relation (18) can be applied to determine $W(\theta)$ when $T_w$, $T_s$ and the value of $W(\theta)$ at a certain latitude are known. The relation (20) can be applied to the oceans which have a northern boundary. After determining $W(\theta)$, the quantities $T_i$, $T_v$ and $T_i'$ can be derived from the relation (8), (12) and

$$T_i=T_s-\tan\theta\cdot RW. \qquad (21)$$

When $T_i$ are known at all latitudes, the relation (21) gives the values of $W(\theta)$ and thus the relation (15) gives $T_w$.

In the Atlantic Ocean reliable hydrographic data are available to determine both $T_i$ and $T_w$. The hydrographic data for $T_w$ are abundant and more reliable than those for $T_i$, because mostly pairs of stations in the western current are available from the data of the same cruises. Then the relation (18) or (20) can be checked by comparing the values of $T_i$ derived from (21) and those computed directly from the hydrographic data.

When there is no latitudinal boundary preventing meridional transports, the relations (8) and (9) must be modified. Consider the water budget in an area bounded by a fixed latitude $\theta_1$ and a variable one $\theta$. The transport entering the area at the latitude $\theta_1$ is put to $S_1$. This is equal to the value of $-(T_i+T_w)$ at $\theta_1$, if $\theta_1$ is taken to the north of $\theta$. The relation (8) then becomes

$$T_i+T_w+T_v+S_1=0. \qquad (8')$$

Similarly in the equation (9) must be added $S_1'$ which represents the transport entering the area at $\theta_1$ in the lower layer.

The equation (16) is changed by taking

$$F(\theta)=T_w+T_s+S_1. \qquad (17')$$

The solution of (16) is expressed by (20) by use of the function $F(\theta)$ defined by the relation (17') under the conditions that

$$S_1=-T_i(\theta_1)-T_w(\theta_1)$$

and that the vorticity equation (6) is valid at the latitudes $\theta_1$.

In the southern hemisphere there is no latitudinal boundary across which

meridional transports vanish. Therefore the area bounded by two latitudinal circles must be considered for the water budget problem. When the fixed latitude $\theta_1$ is taken at the southernmost section, the northward transport across the latitude $\theta_1$ is inward flow to the area considered. Thus, if $S_1$ is taken as the northward (that is, inward) transport at $\theta_1$, the relation (8) becomes

$$T_s - T_t - T_w + S_1 = 0. \qquad (8')$$

In this equation $T_t$ and $T_w$ are taken positive northwardly. Also

$$T_s = \int_{\theta_1}^{\theta} RW d\theta$$

in which $\theta$ is understood as negative. The equation (17) is replaced with

$$F(\theta) = -S_1 + T_w + T_s. \qquad (17'')$$

The solution of (16) with modification about the fixed latitude is again given by (20) in which the function $F(\theta)$ is expressed by (17'').

## 5. *Application to the Atlantic Ocean*

The function $T_s$ is determined at each five degrees over the Atlantic Ocean from the data of the wind stress by HIDAKA (1958). The western transport $T_w$ is obtained by dynamic calculation of hydrographic data at pairs of stations which are located on both sides of the western current and almost at the same latitude. As predicted deductively by STOMMEL (1957) and proved later by an observation (SWALLOW and WORTHINGTON, 1957), the level of no motion in the Gulf Stream is at about 1600 m depth. This level is taken as the interface of two layers in this study. Further the reference level of dynamic calculation of the western current is also taken at this depth.

The numbers of hydrographic data which are available for this calculation are not sufficient even in the North Atlantic. Collections of data from various sources only make it possible to compute $T_w$ at about five degrees intervals. The sources of such data are as follows: the Evergreen (SOULE and MORSE, 1958), the Discovery II (WORTHINGTON, 1958), the Crawford (FUGLISTER, 1957), and the Meteor (DEFANT, 1936) as well as the data referred by STOMMEL (1958). The location of sections used for computation is shown in Fig. 2.

The values of $T_w$ and $T_s$ are plotted in Fig. 3. It is obvious that the extremely large amount of northward transport of $T_w$ between 30° and 45° N is due to the Gulf Stream. In the southern hemisphere there is no correspond-

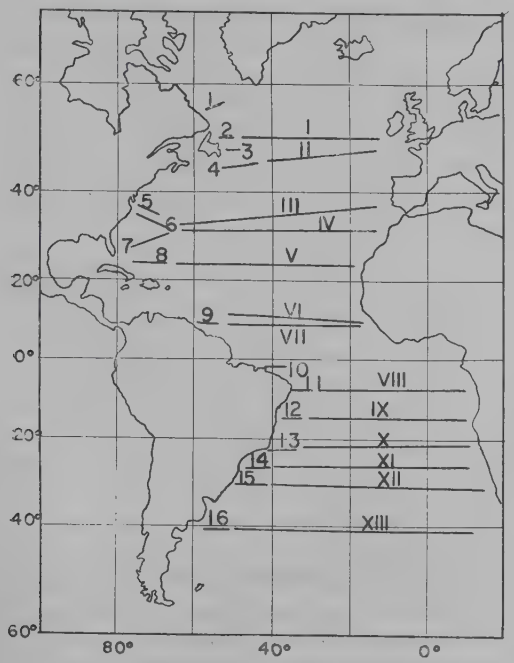


Fig. 2. Locations of hydrographic sections used for dynamic calculation of $T_w$ and $T_t$. Keys to western sections for $T_w$: 1, 2 and 3 by the Evergreen (SOULE and MORSE, 1958); 4 by the Discovery II and 6 and 8 by the Atlantis (WORTHINGTON, 1958); 5 and 7 from sections used by STOMMEL (1958); 9, 11 and 12 by the Crawford (FUGLISTER, 1957); 11, 13, 14, 15 and 16 by the Meteor (DEFANT, 1936). Keys to the inner sections for $T_t$: I, III and VI from STOMMEL's sections (1958); II, IV and V by the Discovery II; VII, VIII and IX by the Crawford; X; XI, XII and XIII by the Meteor.

ing strong transport in the region of the Brazil Current (STOMMEL, 1958). On the other hand, the distribution of $T_s$ is almost antisymmetric about the equator.

The value of $WR\tan\theta$ is finite at the equator only when

$$\lim_{\theta\to 0}\int_{\theta}^{\theta_1} F(\lambda)\cos\lambda\, d\lambda \to 0 \qquad (22)$$

as seen from the relation (20). Also the value of $W(\theta)$ is finite there only when

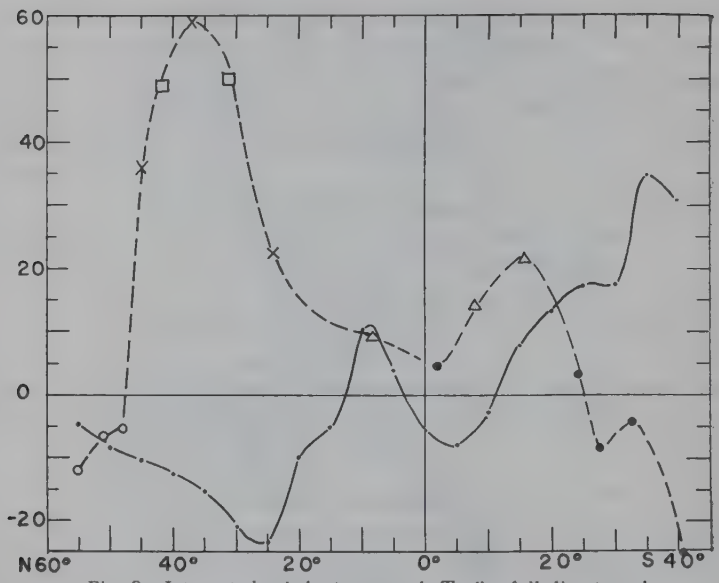


Fig. 3. Integrated wind stress curl $T_s$ (in full lines) and western transport $T_w$ (in broken lines) in $10^6$ m$^3$/sec. Keys to the symbols representing the western sections: ○ for 1, 2 and 3; × for 4, 6 and 8; □ for 5 and 7; △ for 9, 11 and 12; ● for 10, 13, 14, 15 and 16.

$$F(0) = -\lim_{\theta \to 0} \operatorname{cosec} \theta \int_0^{\theta_1} F(\lambda) \cos \lambda \, d\lambda. \tag{23}$$

In the region close to the equator the validity of the equation (1) and (2) is doubtful because the inertia terms neglected become more important than the Coriolis' terms. However the vorticity equation is valid at the equator as the first approximation when $M_y$ does not vanish there. Therefore the equation (16) holds near the equator under the condition that

$$F'(0) = 0. \tag{24}$$

Then the conditions (22) and (23) should be satisfied so that the solution (21) might be valid near the equator.

The values of $W(\theta)$ can be computed from (21) by use of the values of $T_w$ and $T_s$ plotted in Fig. 3. When $l$ is taken as the width of the ocean at $\theta$, the average vertical velocity $\bar{w}$ is given by

$$\bar{w} = W(\theta)/l. \tag{25}$$

From the values of $W(\theta)$ the distributions of $T_t$ and $T_t'$ are determined by

$$T_t = T_s - RW\tan\theta, \quad T'_t = RW\tan\theta. \tag{26}$$

The western transport $T'_w$ in the lower layer is given by

$$T'_w = -(T_s + T_w + S'_1 + S_1). \tag{27}$$

If there is no net transport from the surface to the bottom at the latitude $\theta_1$, $S_1 + S_1'$ vanishes. Then (27) becomes

$$T'_w = -(T_s + T_w). \tag{27'}$$

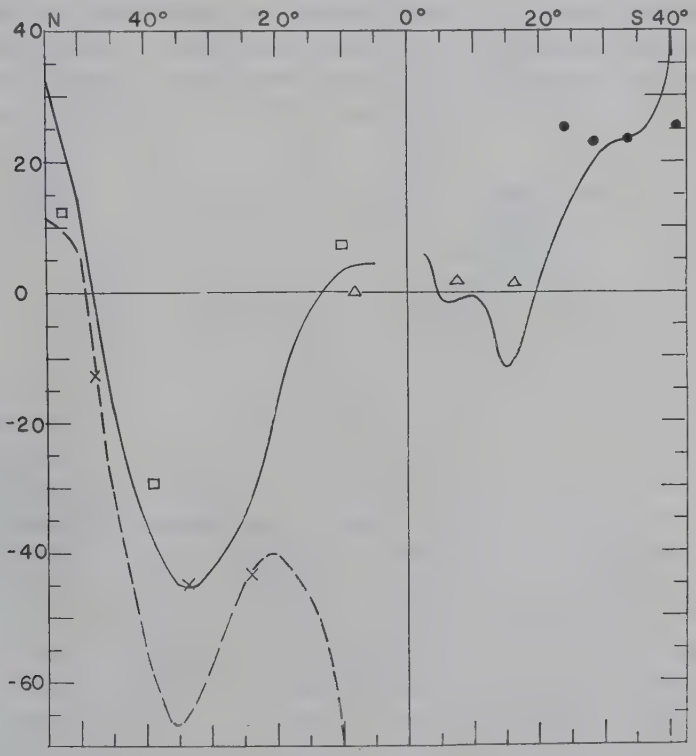


Fig. 4. Theoretical curves and estimated values from the data of $T_t$ in $10^6$ m$^3$/sec. (In the North Atlantic the curves for $T_t$ with $S_1 = -15.1$ and $S_1 = 0$ are indicated in full and broken line, respectively.) Keys to symbols representing the inner sections: □ for I, III and VI; × for II, IV and V; △ for VII, VIII and IX; ● for X, XI, XII and XIII.

The results of computation are plotted in Fig. 4, 5 and 6. The fixed latitude $\theta_1$ is taken at 55° N and 33° S. In the North Atlantic the values of $RW$ and $RW\tan\theta$ become extremely large near the equator, say at 5° N, when $S_1$ is put to zero. When $S_1$ is assumed to be finite, the condition (22) leads to $S_1=-15.1\times10^6$ m³/sec where the function $F(\theta)$ is given by (17′) and the condition (24) is used. On the other hand, the total transport between Cape Farvel, Greenland and Cape Wrath, Scotland is about $12.2\times10^6$ m³/sec (northward) above the reference level between 800 m and 1500 m (DIETRICH, 1957). The transport across the section between South Wolf Island, Labrador and Cape Farewel, Greenland is $2.1\times10^6$ m³/sec (northwestward) above 1600 m as computed from the data of 1957 (SOULE and MORSE, 1958). Therefore the total transport to the north at the latitude of about 55° to 60° N is equal to

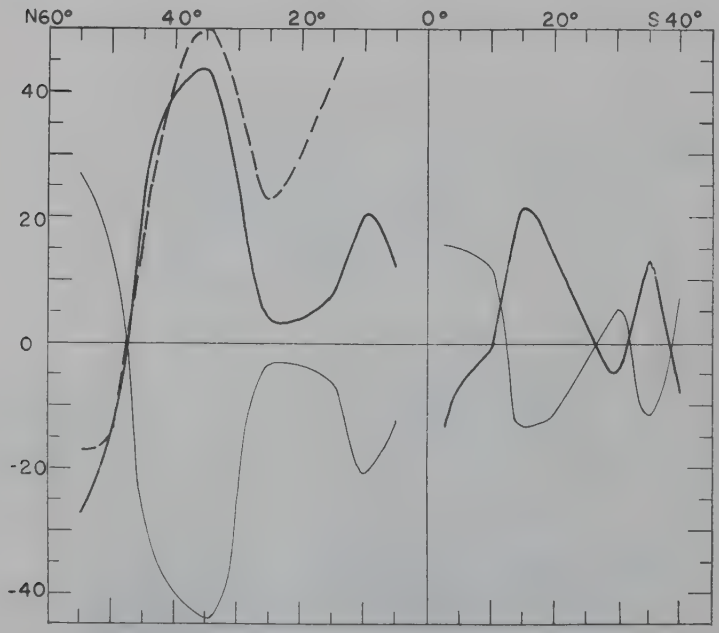


Fig. 5. Curves of $T_t'$ (in thick line) and $T_w'$ (in fine line) in $10^6$ m³/sec. (In the North Atlantic the curve of $T_t'$ for $S_1=0$ is indicated in broken line.)

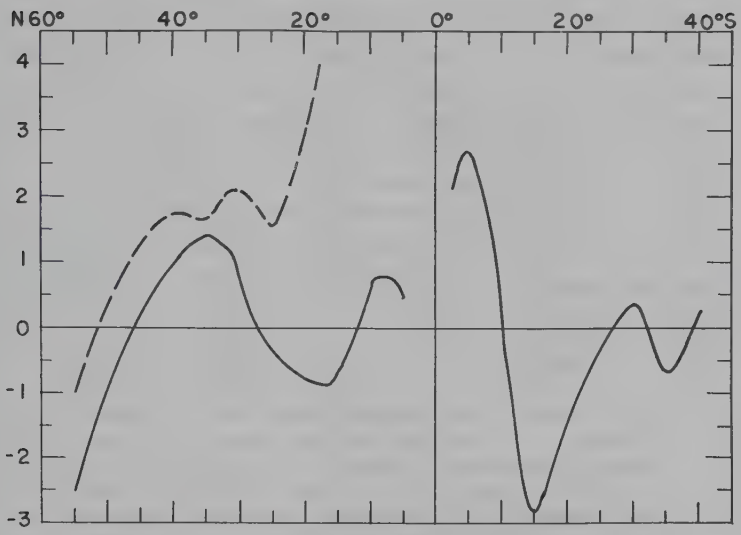


Fig. 6. Curves of $\bar{w}$ in $10^{-4}$ cm/sec. (In the North Atlantic a broken curve indicates $\bar{w}$ for $S_1=0$, and a full line for $S_1=-15.1\times10^6$ m$^3$/sec.)

$14.3\times10^6$ m$^3$/sec which is very close to the estimated value of $S_1$ mentioned above.

In Fig. 5 to 7 two kinds of curves in the North Atlantic corresponding to $S_1=0$ and $S_1=-15.1\times10^6$ m$^3$/sec are shown for comparison. The curves in the South Atlantic are based on the value of $S_1$ at 33° S which is taken as the sum of $T_w$ and $T_t$ determined by dynamic calculation of the data by the Meteor. The values of $T_w'$ are obtained with the assumption that $S_1+S_1'=0$. In Fig. 4 the curves of $T_t$ determined by dynamic calculation are plotted. The sections used for this calculation are shown in Fig. 2. In the calculation the interface of two layers is taken at 1600 m as in the western transport but the reference level is determined by STOMMEL's method (STOMMEL, 1956; ICHIYE, 1959a).

The agreement of theoretical curves of $T_t$ with the values computed from the hydrographic data in Fig. 4 seems to be good considering the crude nature of the assumptions involved. Also this figure suggests that the estimated value of $S_1$ at 55° N is not far from the actual value. Fig. 5 and Fig. 6

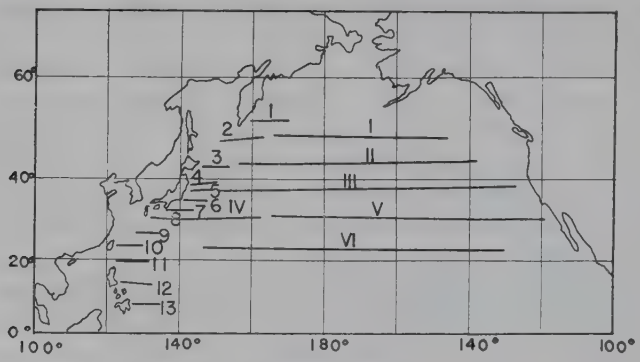


Fig. 7. Location of hydrographic sections used for dynamic calculation of $T_w$ and $T_t$ in the North Pacific. Keys to the symbols representing the western sections: 1 by the Oshoro in NORPAC; 2 and 4 by the Carnegie (FLEMING, 1945) and the Komahashi; 3, 5 and 6 by the Ryōfū (Japan Meteorol. Agency, 1956) and the Satsuma in NORPAC; 7 by the Komahashi; 8 and 9 by the Shumpu in NORPAC; 10 and 11 by the Cruise 99 of Japanese Hydrographic Office (1954); 12 and 13 by the Cruise 98 of J.H.O. All inner sections were occupied by the Carnegie.

indicate that the vertical motion at 1600 m depth divides the North Atlantic into four zones; the polar and subtropical zone of downward motion and the temperate and tropical zone of upward motion. In the South Atlantic the temperate zone of upward motion is reduced its extent. Instead, the vertical motion in the tropical and sub-tropical zone increases its magnitude in the southern hemisphere.

The western transport of the lower layer is southward in the North Atlantic as seen in Fig. 5, in agreement with the deduction of STOMMEL (1957) and the result of the observation (SWALLOW and WORTHINGTON, 1957). In the South Atlantic the western transport is almost equal to $-T_t$ since $T_w' = -T_w \sim -S_1'$. It is desirable to confirm this by future observations (WÜST, 1955).

### 6. *Application to the North Pacific*

The same procedure is applied to the North Pacific where the hydrographic data are abundant next to the Atlantic Ocean. In Fig. 7 are shown the

sections for which $T_{ts}$ and $T_t$ are determined by dynamic calculation. It is found that the depth of no meridional motion is about 1200 m in the inner

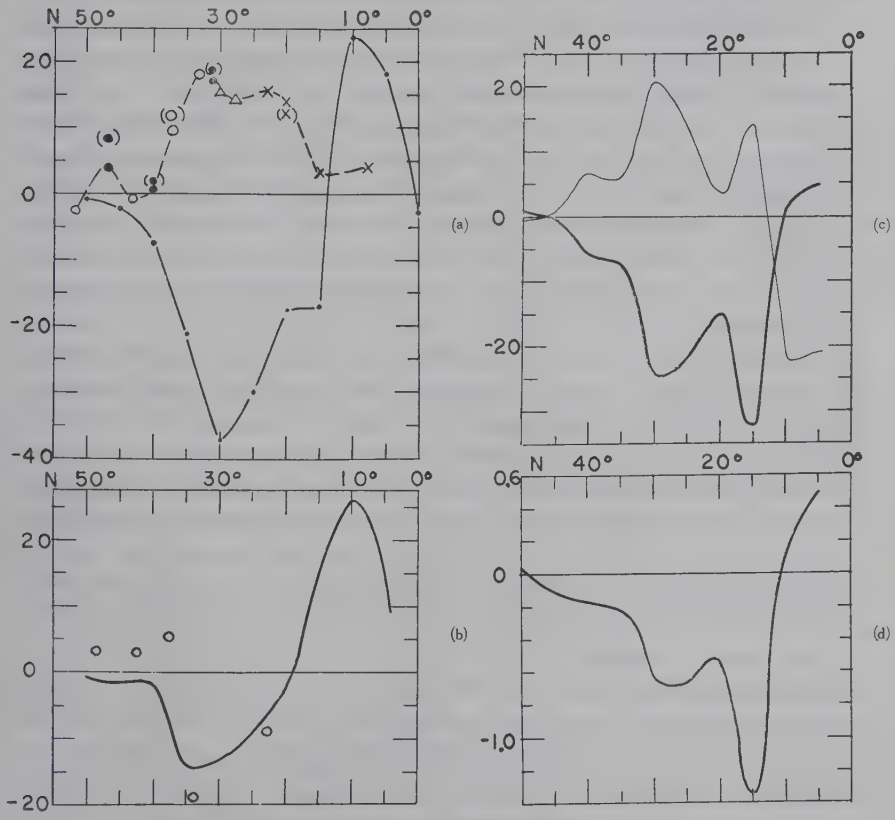


Fig. 8. (a) The latitudinal distributions of $T_s$ and $T_w$ in $10^6$ m$^3$/sec. Keys to the symbols for the western sections: ○ for 1, 3, 5 and 6; ● for 2, 4 and 7; △ for 8 and 9; × for 10, 11 12 and 13. The symbols of $T_w$ in parenthesis indicate the western transports above 1600 m. (Upper left.)
(b) Theoretical curves of $T_t$ and estimated values from the data in $10^6$ m$^3$/sec. (Lower left.)
(c) Curves of $T_t'$ (in thick line) and $T_w'$ (in fine line) in $10^6$ m$^3$/sec. (Upper right.)
(d) Curves of $\bar{w}$ in $10^{-4}$ cm/sec. (Lower right.)

region of the North Pacific (Ichiye, 1959b). The interface of two layers and the reference level of the dynamic calculation of $T_w$ are taken at 1200 m. The refenence levels for $T_t$ are determined by Ichiye's method (1959a).

The values of $T_s$ and $T_w$ are plotted in Fig. 8(a). The northward transport of the Kuroshio is less than one third of the Gulf Stream. In this figure the transport $T_w$ above 1600 m in several sections is also plotted. The large difference in the transport between the Kuroshio and the Gulf Stream cannot be explained by the difference of the thickness of the layer, since the transport above 1600 m is seen to be slightly larger than above 1200 m in the Kuroshio. The reason is as follows: The Kuroshio increases its transport near the coast of Japan and after leaving it. Thus the transport increased is predominantly to the east, while the transport considered here is its northward component.

The fixed latitude $\theta_1$ is taken at 50° N. The value of $S_1$ determined from the condition (22) is equal to $0.62\times10^6$ m$^3$/sec which is almost negligible amount. This is in good agreement with a general conception that there is almost no transport through the Bering Straits. In Fig. 8(b) are plotted the curve of $T_t$ obtained from (26) and the values of $T_t$ determined from dynamic calculation. The agreement between two quantities is good. The latitudinal distribution of the theoretical curve of $T_t$ has the same tendency as that of the North Atlantic, although the amplitudes are much smaller in the North Pacific.

The western transport $T_w'$ of the lower layer is plotted in Fig. 8(c). In most latitudes of the North Pacific this has a northward component, contrary to the North Atlantic. Again the distribution of the vertical current of Fig. 8(d) indicates slight downward motion all over the North Pacific except near the equator, with contrast to the North Atlantic. Such differences in both oceans are remarkable to understand the circulation of the ocean.

## 7. *Concluding remarks*

The water budget method can be applied to actual oceans in different ways from those discussed here. For instance, when the inner transports $T_t$ are known instead of $T_w$, this method will give a good estimation of $T_w$. The procedure of determining the level of no meridional motion (Stommel, 1956; Ichiye, 1959a) is applicable only in the inner region where the geostrophic

relation is valid. Thus the dynamic calculation can yield more accurate value of $T_i$ than $T_w$ because the reference level can be determined in the inner region more conclusively than in the western current. Then this alternate approach will give better estimation of $T_w$ than the conventional dynamic calculation if more hydrographic data are available for determining $T_i$. Also the budget method will yield the estimation of vertical transport at different depths by changing the depth of the interface.

Weak points in the method are as follows: (1) The transport across the the northern or southern boundary, if any exists, must be determined accurately from hydrographic data, because the whole solution is sensitive to this value. (2) Near the equator the values of $W(\theta)$ computed by the solution become extremely large. This suggests us that the inertia terms may be important there in the vorticity equation. (3) The vertical transport at the surface due to evaporation and precipitation was neglected. The water removed from the upper layer by excess of evaporation over precipitation is equal to 0.34 and $0.65\times10^6$ m$^3$/sec in the area between 40° and 10° N (which yields the maximal vertical transport by this process) of the North Atlantic and the North Pacific, respectively, from crude estimation (Wüst et al., 1954). Therefore the neglect of this process in the water budget seems to be allowed.

*Acknowledgement:*—The author wishes his thanks to Dr. Sidney W. Fox and Dr. F. C. W. Olson for their encouragement throughout the present work.

## *References.*

Defant, A. (1936): Schichtung und Zirkulation des Atlantischen Ozeans: Die Troposphäre. *Wiss. Erg. Dtsch. Atl. Exp. "Meteor"* 1925-27, Bd. **6**, 1.

Dietrich, G., (1951): Schichtung und Zirkulation der Irminger-See im Juni 1955. *Ber. Dtsch. Wiss. Komm. Meeresforsch.*, **14** (4), 255-312.

Fleming, J.A. et al, (1945): Scientific Results of Cruises of the Carnegie during 1928-29. *Oceanography 1-B, Carnegie Institute of Washington Pub.* 545.

Fuglister, F.C., (1957): Oceanographic Data from Crawford Cruise Ten obtained for IGY of 1957-58. *W.H.O.I. Ref.* No. 57-54.

Hidaka, K., (1958): Computation of the wind stresses over the oceans. *Rec. Oceanog. Works in Japan, New Ser.* **4** (2), 77-123.

Ichiye, T., (1958): On convective circulation and density distribution in a zonally uniform ocean. *Oceanog. Mag.*, **10** (1), 97-135.

Ichiye, T., (1959a): A note on determination of the depth of no meridional motion. (To be published).

Ichiye, T., (1959b): A theory on the formation of the intermediate water in the North

Pacific. (Paper presented at the International Oceanographic Congress in New York).

Japanese Hydrographic Office, (1954): The results of oceanographic observations in the North-Western Pacific Ocean, No. 6, 1938-40. *Hydrg. Bull. Spec.* No. 13.

Japan Meteorological Agency, (1956): *The Results of Mar. Met. and Oceanog. Obs.* No. 17.

SAINT-GUILY, B., (1959): Note sur l'action de la force de Coriolis dans la circulation convective. *Bull. de l'Inst. Oceanog. Monaco.* No. 1148.

SOULE, F.M. and R.M. MORSE, (1958): Physical oceanography of the Grand Banks region and the Labrador Sea in 1957. *U.S. Coast Guard Bull.* **43**, 81-131.

STOMMEL, H., (1956): On the determination of the depth of no meridional motion. *Deep-Sea Res.*, **3**, 273-278.

STOMMEL, H., (1957): A survey of ocean current theory. *Deep-Sea Res.*, **4**, 149-184.

STOMMEL, H., (1958): The Gulf Stream. University of California Press, Los Angeles and Berkeley.

STOMMFL, H., A.B. ARONS and A.J. FALLER, (1958): Some examples of stationary planetary flow in bounded basins. *Tellus*, **10** (2), 179-187.

SWALLOW, J.C. and L.V. WORTHINGTON, (1957): Measurements of deep currents in the Western North Atlantic. *Nature*, 179, 1183-84.

WORTHINGTON, L.V., (1958): Oceanographic data from the R.R.S. Discovery II. IGY Cruise One and Two, 1957. *W.H.O.I. Ref.* No. 58-30.

WUST, G., W. BROGMUS and E. NOODT, (1954): Die zonale Verteilung von Salzgehalt, Niederschlag, Verdunstung, Temperatur und Dichte an der Oberfläche der Ozeane. *Kiel. Meeresforsch.* 10.

WUST, G., (1955): Stromgeschwindigkeiten im Tiefen-und Bodenwasser des Atlantischen Ozeans. Supplement to Vol. 3 of *Deep-Sea Res.*

The Oceanographical Magazine
Vol. 11. No. 2, March 1960

# An Analysis on the Mechanism of the Cold Water Mass Appearance in the Enshu-nada

By

Jiro Fukuoka

*Meteorological Research Institute, Tokyo*

## 1. *Introduction*

We know several examples of the appearance of the cold water mass since 1934 when it appeared for the first time in the offing of the Enshu-nada. Such cold water mass is one of the most characteristic phenomena in the Kuroshio. We cannot recognize the persistence of the cold water mass in any ocean currents other than the Kuroshio, for example, in the Gulf Stream regions of the Atlantic Ocean corresponding to the Kuroshio regions of the Pacific Ocean. It is natural that oceanographers in our country are strongly interested in this phenomenon. The author has collected all data about the cold water mass and analyzed the mechanism of its appearance, in order to search for the method to forecast the appearance of the cold water mass.

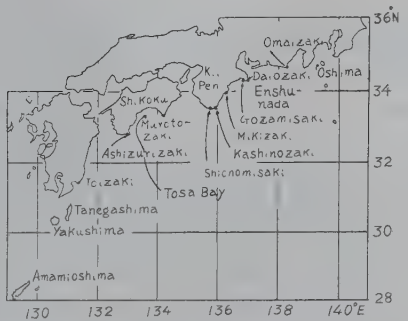


Fig. 1. Map showing names of island and cape.

The present analysis has hardly established any theory about the appearance of cold water mass, but it may be important to pursue the observational data conscientiously and to study the anomalies in the Kuroshio. (The positions of island and cape in this paper are indicated in Fig. 1.)

## 2. *The appearance of the cold water mass in 1959*

In 1959 we observed an abnormal state of the Kuroshio flow pattern. That

is, in March the Kuroshio streamed very near Shikoku from west to east, but in May the offshore receding of the Kuroshio axis is found by oceanographical observations on board the Shumpu Maru, Kobe Marine Observatory[1].

This offshore receding of the Kuroshio axis is very curious, never seen before (Fig. 2). In company with the offshore receding of the Kuroshio axis, a low water-temperature region is formed between Shikoku and the Kuroshio axis (Fig. 3).

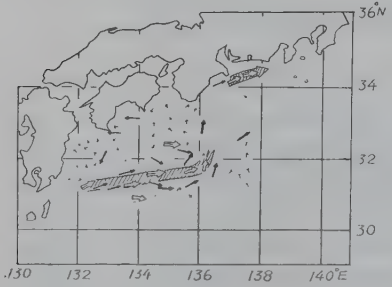


Fig. 2. Surface ocean current, May, 1959. (Shumpu Maru.)
Kuroshio axis.
<1 kt. 2~3 kt.
1~2 kt. 3~4 kt.

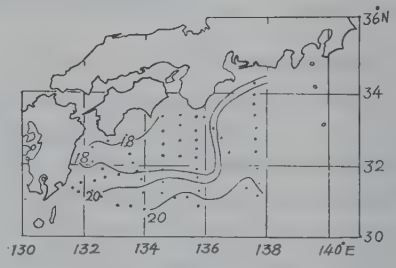


Fig. 3. Isotherms on 100 m layer, May, 1959. (Shumpu Maru.)

In June the Kuroshio flow pattern presents an abnormal mode (Fig. 4). Namely, the meandering of the Kuroshio seems to go eastward, and the low

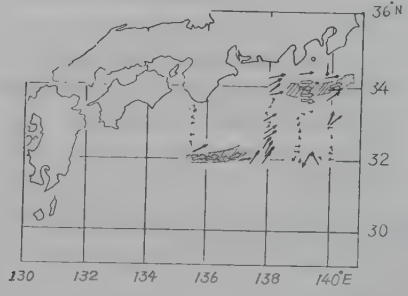


Fig. 4. Surface ocean current, June, 1959. (Hydrographic Department.)
Kuroshio axis.

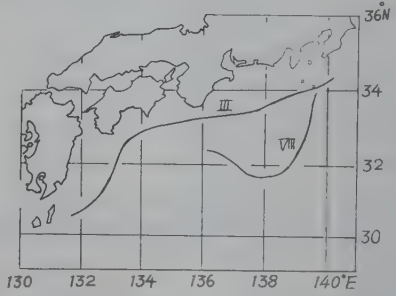


Fig. 5. Variations of the Kuroshio positions from Mar. to Aug., 1959.

water-temperature region shifts from south of Shikoku to south of the Kii peninsula[2]. At last the variation of the Kuroshio flow pattern attains a typical cold water mass pattern that the cold water mass occupies the offing of the Enshu-nada. The variations of the Kuroshio axis are shown in Figure 5. Summarizing these variations, we can probably assume the abnormal state of the Kuroshio off Shikoku to be a presage of the appearance of the cold water mass in the Enshu-nada.

We have already two examples of the cold water mass appearance, i.e. in 1934 and 1954. So it is necessary to know from the observational data whether the presage of the cold water mass appearance is shown by the abnormal state of the Kuroshio off Shikoku or not.

### 3. *The cold water mass in 1934*

We have some rather accurate oceanographical data since 1927. For analyzing the mechanism of the cold water mass, the data before 1927 can not be utilized, because serial oceanographical observations were not sufficiently carried out at that time and the data are very scanty.

At first the author has minutely studied the report of the ocean current in the Hydrographic Bulletin[3] published by the Japanese Hydrographic Department and the general state of the seas delivered in the Oceanographical Investigation[4] published by the Imperial Fisheries Experimental Station with the view to find an abnormal ocean current and a presage of the cold water mass. These ocean current reports are summarized in Table 1.

From 1927 to 1933 the Kuroshio off Shikoku is noticed to stream normally, eastward and almost along the Pacific coast of Honshu (Japanese Main Island). Figure 6(a) shows the summarized ocean states mentioned above. The flow pattern is shown by the distribution of isotherms at 100 m layer (Fig. 6(b), (c)). The most characteristic features in Figure 6 are the straight streaming of the Kuroshio and the existence of the Kuroshio axis near Honshu. Such a Kuroshio flow pattern is generally said to be normal. In January 1933 the cruiser Chokai of the Japanese Navy reported the abnormal state in the Kuroshio near Shikoku for the first time. Although the Kuroshio flow pattern reverted to be normal thereafter, observations of westward counter current in the Kuroshio region off Shikoku were often reported (see Table 1). Oceanographical observations off Gozamisaki in February 1934 seems to suggest

Table 1. Abnormal state of the Kuroshio by reference to ocean current reports and water temperature reports.

(After Hydrographical Bulletin from 1927 to 1943 and Oceanographical Investigation from 1931 to 1943.)

| Hydrographic Bulletin | | | Oceanographic Investigations | |
|---|---|---|---|---|
| Year Month | Sea region and ocean current | Observer | Year Month | State of seas |
| 1927 Feb. | The offing of Shionomisaki, E 2~3 kts. | Hydrographic Dep. | | |
| 〃 Aug. | The north margin of the Kuroshio approaches the Kii pen. | Seito | | |
| 〃 Nov. | Shionomisaki~Murotozaki, E 1 kt.<br>Murotozaki~Ashizurizaki, ocean current weak. | Naka | | |
| 1928 July~ Aug. | Kuroshio normal. | H D. | | |
| 1929 Sept. | Kuroshio approaches Shikoku. | H. D. | | |
| 1930 Jan. | 〃 | H. D. | | |
| 1931 | Kuroshio normal. | | 1931 July~ Dec. | Kuroshio 50 N. M. south of Gozamisaki. Aug., Oct., the Kuroshio approaches near Shikoku. |
| 1932 | 〃 | | 1932 | Kuroshio 40~70 N.M. south of Gozamisaki. Feb., Apr., June, Oct., Kuroshio approaches near Shikoku. |
| 1933 Jan. | 31° 10′ N, 131° 35′ E ~ 30° 57′ N, 132° 00′ E, 165° 2 kts. | Chokai | 1933 Feb. Mar. | Rather offshore receding of the Kuroshio axis south of Ashizurizaki. |
| 〃 〃 | 30° 57′ N, 132° 00′ E ~ 31° 18′ N, 132° 18′ E, 193° 1.2 kts. | 〃 | Mar. Apr. May Nov. | Kuroshio, 20~70 N.M. south of Gozamisaki. |
| 〃 Feb. | 32° 35.5′ N, 134° 21′ E, 62° 2.8 kts. | 〃 | Nov. | Kuroshio 50 N. M. south of Ashizurizaki. |
| 〃 Mar. | 32° 18′ N, 134° 08′ E ~ 31° 40.5′ N, 134° 11′ E, 355° 0.7 kts. | 〃 | | |
| 〃 〃 | Ashizurizaki~Murotozaki, counter current 0.4 kts. | Tairyu maru | | |
| 〃 〃 | Toizaki~Ashizurizaki, ocean current is not seen. | Ganges maru | | |
| 〃 May | South of the Kii pen., ocean current is not seen. | Heimei maru | | |

| Hydrographic Bulletin | | | Oceanographic Investigations | |
|---|---|---|---|---|
| Year Month | Sea region and ocean current | Observer | Year Month | State of seas |
| 1933 Dec. | Toizaki～33° 04′ N, 134° 57′ E 247° 0.7 kts. | Gyoko maru | | |
| 〃 〃 | Toizaki～Shionomisaki, ocean current is not seen. | Osaka maru | | |
| 1934 May | Murotozaki～Shionomisaki, counter current 0.6 kts. | Tomiura maru Amazon maru | 1934 Feb. | Remarkable offshore receding of the Kuroshio south of Ashizurizaki. |
| 〃 Sept. | 〃 counter current. | H D. | 〃 May | 〃 〃 (80 N. M.) |
| | | | 〃 Aug. | Cold water mass appeares and continues to Dec. |
| 1935 May | Ashizurizaki～Shionomisaki, counter current. South off Shionomisaki, northward Kuroshio is seen. | Kojun maru | 1935 Feb. | Offshore receding of the Kuroshio south of the Kii pen. |
| | | | 〃 June | Water temperature south of Gozamisaki is highest since 1919. |
| | | | 〃 Oct | Cold water mass developes. |
| | | | 〃 Nov. | High water temperature south of Gozamisaki. |
| 1936 Feb. | Tanegashima～32° 45′ N, 134° 54′ E ～ Shionomisaki, 245° 1 kt and 249° 1.9 kts. | Senzan maru | 1936 Feb | Low water temperature and offshore receding of the Kuroshio south of Ashizurizaki (90 N. M.). |
| 〃 〃 | 31° 27′ N, 132° 15′ E ～ 33° 20′ N, 135° 43′ E 239° 1 kt. | Aso maru | Jan～ Oct. | Cold water mass. |
| 〃 〃 | Shionomisaki light house～ Mikizaki, 60° 3～4kts. | Kanda maru | Apr. Sept. Oct. | High water temperature south of Gozamisaki. |
| 〃 〃 | The offing of Daiozaki, 55° 3 kts. | Tatsutasan maru | | |
| 〃 Sept. | The offing of Omaezaki 65° 2.4 kts, Shionomisaki 85° 2 kts, Daiozaki 68° 4 kts, Kashinozaki 58° 4 kts. | Chieago maru | | |
| 〃 Oct. | 32° 31′ N, 133° 52′ E 111° 0.6 kts. | France maru | | |
| 〃 〃 | Rather west of Shionomisaki, 275° 0.6 kts. | Isuzu | | |
| 〃 〃 | East of Shionomisaki～Oshima, 70° 2.3 kts. | Sanramon maru | | |
| 1937 Feb. | South of Ashizurizaki, the Kuroshio normal, but in the offing of Murotozaki and Shionomisaki southward current. | Shunsho maru | 1937 Feb. | Kuroshio near Shikoku. Cold water mass south of Shionomisaki. |
| | | | Apr. May June | Cold water mass south of Shionomisaki. High water temperature south of Gozamisaki. |

| Hydrographic Bulletin | | | Oceanographic Investigations | |
|---|---|---|---|---|
| Year Month | Sea region and ocean current | Observer | Year Month | State of seas |
| | | | 1937 July Aug. Oct. Nov. | Cold water mass. |
| 1938 Jan | 33° 35′ N 137° 46′ E 342° 0.6 kts. | Kaijo maru | 1938 through a year | Cold water mass. |
| 〃 July | Shionomisaki~Kashinozaki light house, 234° 1.9 kts. | Taihozan maru | 1939 through a year | Cold water mass. |
| 〃 Sept. | 30° 40′ N 136° 56′ E ~ 32° 05′ N 135° 11′ E 127° 2 kts. | Shintoku maru | | |
| 1940 Nov. | 32° 41′ N 143° 13′ E ~Kashinozaki light house, 308° 0.35 kts. | Kyushu maru | 1940 Apr~ Aug., Dec. | Cold water mass. |
| | | | 1941 through a year | Cold water mass. |

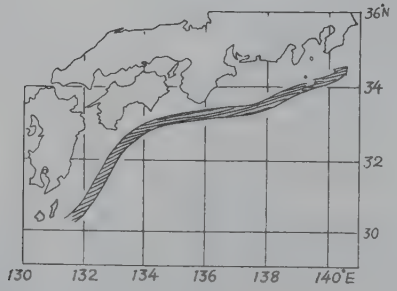


Fig. 6(a). Mean position of the Kuroshio axis from 1927 to 1933.

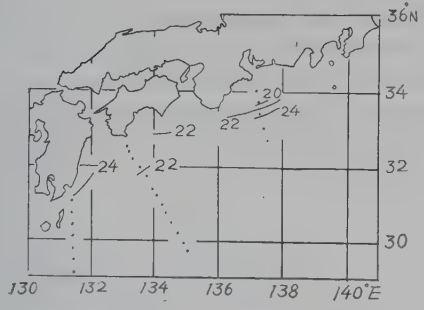


Fig. 6(b). Isotherms on 100 m layer, June, 1932. [After Oceanographical Investigation.]
●: Observational station.

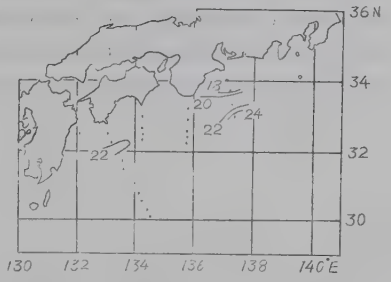


Fig. 6(c). Isotherms on 100 m layer, Oct., 1933. [After O.I.]

the appearance of cold water mass may appear off the Kii peninsula, but the observational data are too scanty to assert the occurrence of the cold water mass.

In August 1934 the cold water mass appeared distinctly off the Kii peninsula (Fig. 7).

According to these data, it is seen that the abnormal state off Shikoku might occur several months (from 2 or 3 months to about a year) before the appearance of cold water mass off the Kii peninsula. The offshore receding of the Kuroshio axis in 1933 and 1934 is also ascertained in the offing south of Shikoku by the report of General State of Seas in the Oceanogra-

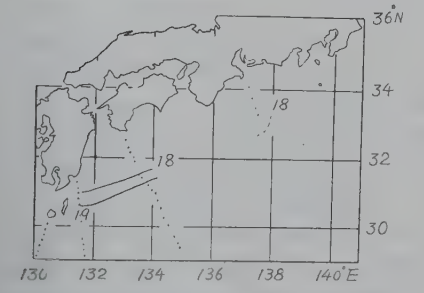


Fig. 7(a). Isotherms on 100 m layer, Feb., 1934. [After O.I.]

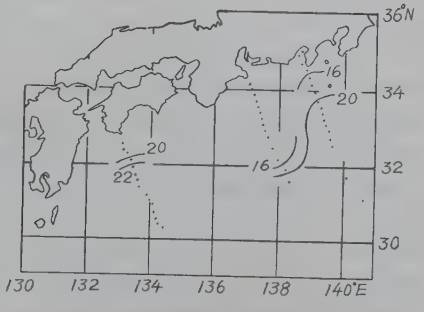


Fig. 7(b). Isotherms on 100 m layer, Aug., 1934. [After O. I.]

phical Investigation (see Table 1). Namely, this phenomenon is similar to the offshore receding of the Kuroshio axis south of Shikoku in 1959.

In the early stage of the cold water mass, its location varies with seasons. An example of the variations of the loacation is shown in Figure 8.

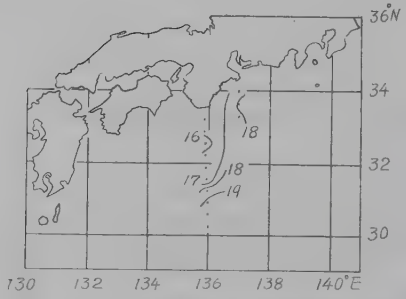


Fig. 8(a). Isotherms on 100 m layer, Jan., 1936. [O. I.]

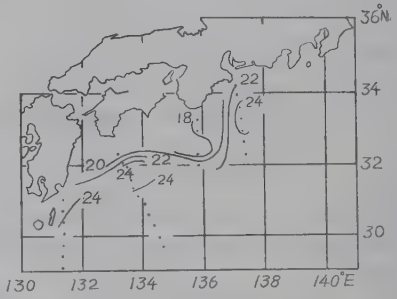


Fig. 8(b). Isotherms on 100 m layer, Nov., 1936. [O. I.]

For example, in June and November 1935, the water temperature south of Gozamisaki is higher than the mean, but there is always the cold water mass in February, March, August and October. Besides, in June and November we have some data for assuming a region of the low water temperature south of the Kii peninsula. From these phenomena it is seen that the cold water mass moves sometimes from west to east, and sometimes from east to west. When the cold water mass is transferred from east to west, the northward or northeastward Kuroshio is observed near Gozamisaki (see Table 1, February and September, 1936). This northward strong Kuroshio naturally necessitate an isothermal distribution at 100m layer of low temperatures south of the Kii peninsula and high temperature south of Gozamisaki. Eastwestward movement of the cold water mass such as these is seen until the end of 1937. However, in 1938 the cold water seems to occupy its settled location. The locations of cold water mass from 1938 to 1941 are shown in Figure 9, from which we can deduce that the developed cold water mass occupies a constant

space. Through 1941 the cold water mass may exist in the same space. Thereafter, during the 2nd World War the oceanographical observations could not be carried out sufficiently. It is said, however, that the cold water mass surely in 1943 by referring to data observed by the Japanese Navy and the report of fishing boats. After the War this cold water mass disappeared.

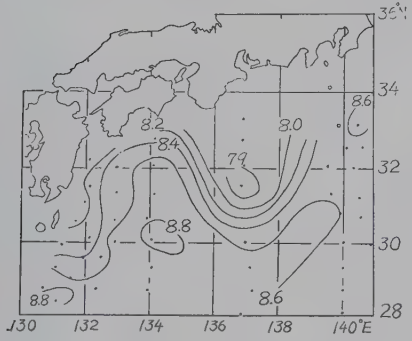


Fig. 9(a). Dynamical Topography Aug., 1938. (0-800db, +700) [H.D.]

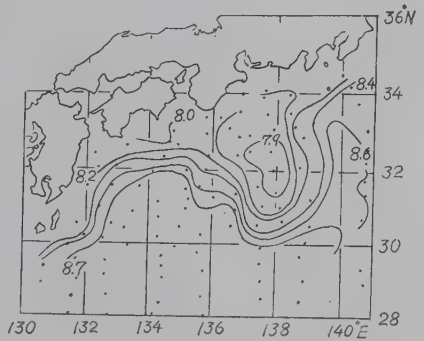


Fig. 9(b). Dyn. Top. July, 1939. (0-800db, +770) [H.D.]

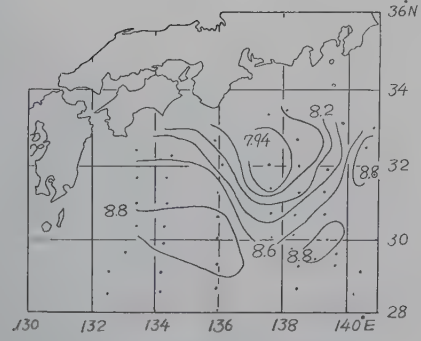


Fig. 9(c). Dyn. Top. Aug., 1939. (0-800db, +770) [H.D.]

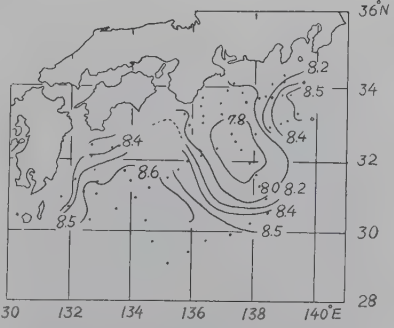


Fig. 9(d). Dyn. Top. Nov.~Dec., 1839. (0-800db, +770) [H.D.]

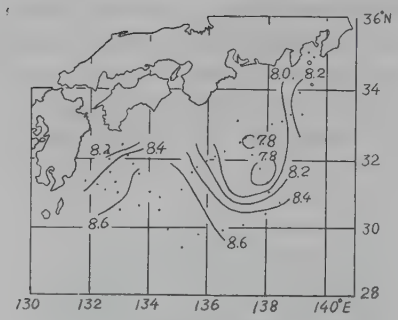


Fig. 9(e). Dyn. Top. Jan.~Feb., 1940. (0-800db, +770) [H.D.]

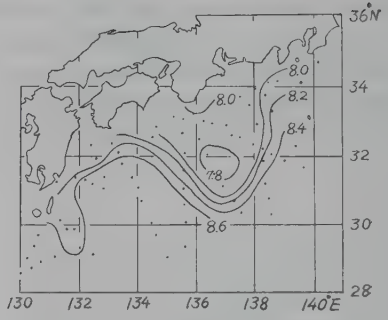


Fig. 9(f). Dyn. Top. June, 1940. (0-800db, +770) [H.D.]

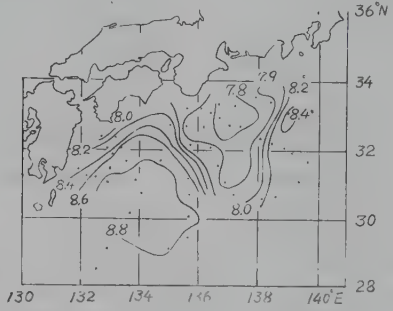


Fig. 9(g). Dyn. Top. Aug., 1940. (0-800db, +770) [H.D.]

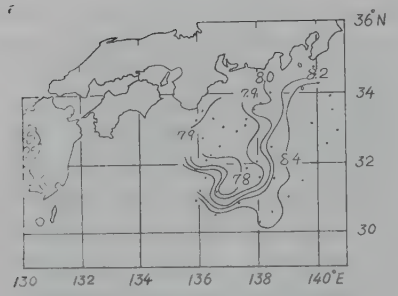


Fig. 9(h). Dyn. Top. Nov., 1940. (0-800db, +770) [H.D.]

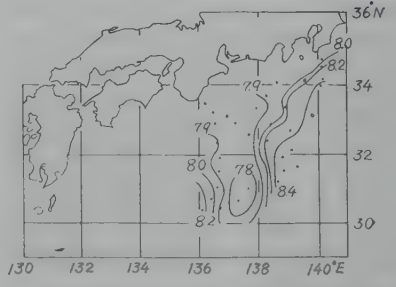


Fig. 9(i). Dyn. Top. Jan., 1941. (0-800db, +770) [H.D.]

*4. The cold water mass of 1954*

After the 2nd War we did not see the cold water mass developed in the offing of the Enshu-nada and could not recognize the cold water mass until April 1954. But in May it was reported by the Shumpu Maru, and the Atsumi, an ocean weather ship, respectively, that the cold water mass appeared. This cold water mass was existing through 1954 and 1955 (Fig. 10). (From Figure 10 we can find the similarity between pattern of dynamical topography on the sea surface and pattern of isotherms of 100m layer.) So we would like investigate on the presence of presage of cold water mass.

From 1947 to 1951 the Kuroshio flow patterns are normal, as shown by Fig. 11, the Kuroshio axis approaches Shikoku and the Kii peninsula. In order to clarify the approaching of the Kuroshio axis, descriptions[5] published by the Kochi Fisheries Experimental Station are reproduced on Table 2. According to Table 2, it is known that in November and December 1953 the Kuroshio axis receded to the south off Shikoku. On examining these phenomena stated above, it might be correct to conclude that the offshore receding of the Kuroshio axis occurs several months before the appearance of the cold water mass in the Enshu-nada. But in the February 1952 the cold water mass made an abrupt appearance in the Enshu-nada, and then in May the scale of this cold water mass was reduced, and finally the Kuroshio[6] flow pattern returned

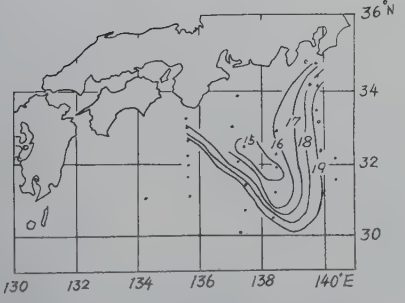


Fig. 10(a). Isotherms on 100m layer, May~June, 1954.

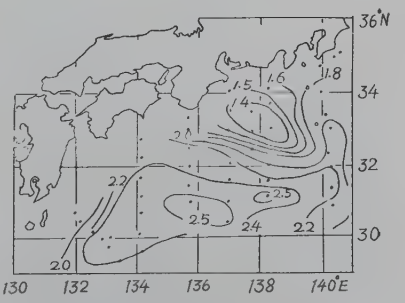


Fig. 10(b). Dyn. Top. Aug., 1955. (0-1000db, anomaly.)

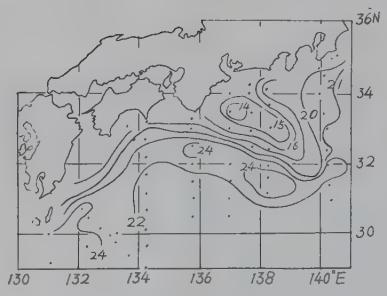


Fig. 10(c). Isotherms on 100m layer, Aug., 1955.

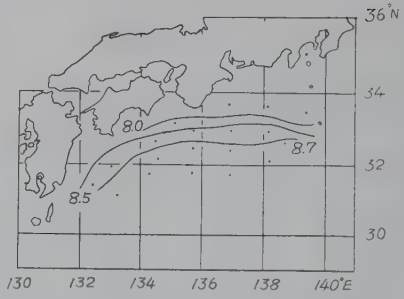


Fig. 11(a). Dyn. Top. Oct.~Nov., 1948. (0-800db, +770) [H.D.]

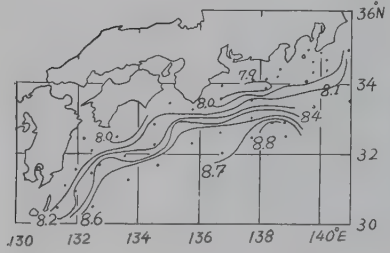


Fig. 11(b). Dyn. Top. July~Aug., 1950. (0~800db, +770) [H.D.]

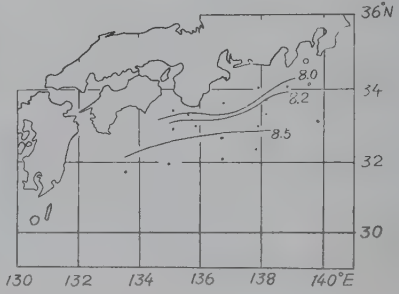


Fig. 11(c). Dyn. Top. Feb.~Mar., 1951. (0-800db, +770) [H.D.]

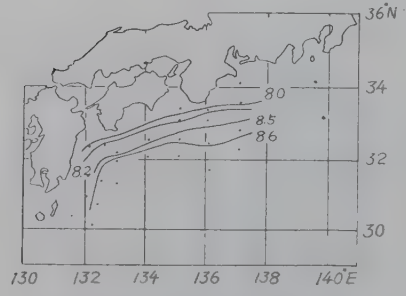


Fig. 11(d). Dyn. Top. May, 1951. (0-800db, +770) [H.D.]

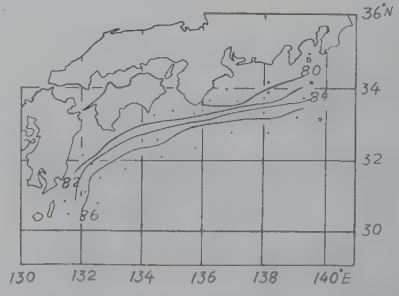


Fig. 11(e). Dyn. Top. Nov.~Dec.. 1951. (0-800db, +770) [H.D.]

Table 2. State of the Kuroshio South of Ashizurizaki since 1952
(After the Report of Kochi Fisheries Experimental Station)

| Year | Month | State of the Kuroshio |
|---|---|---|
| 1952 | June | Branch of the Kuroshio flows west of Shikoku. |
| | Sept. | Branch of the Kuroshio streams widely in the Tosa Bay. |
| | Oct. | The Kuroshio approaches near Ashizurizaki (17 N. M.). |
| | Dec. | The Kuroshio approaches near Ashizurizaki but its velocity is slow. |
| 1953 | Feb. | Branch of the Kuroshio approaches near Ashizurizaki. |
| | Mar. | The Kuroshio, 30~40 N. M. south of Ashizurizaki and its velocity 3 kts. |
| | Apr. | Branch of the Kuroshio appproaches near Ashizurizaki. |
| | July | Branch of the Kuroshio flows into the Tosa Bay. |
| | **Nov.** | **Kuroshio does not approach near Ashizurizaki.** |
| | **Dec.** | **Kuroshio flows eastward farther south of Ashizurizaki and from Nov. to half of Dec. the Kuroshio does not approach near Shikoku.** |

to the normal state in summer and autumn (Fig. 12). In this case we can not see the presage in the Kuroshio region near Shikoku several months before the appearance of cold water mass in the Enshu-nada. So far as the author researches, we can not notice the abnormal states of the Kuroshio near Shikoku before the appearance of the cold water mass. However, it is uncertain whether the presage does not exist at all or is not distinct because of the scantiness of data.

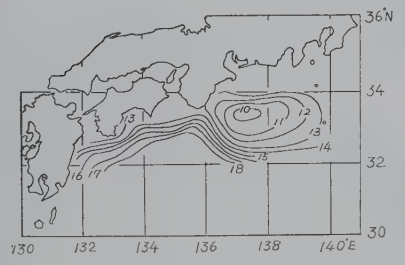


Fig. 12(a). Isotherms on 200 m layer Feb., 1952. [H.D.]

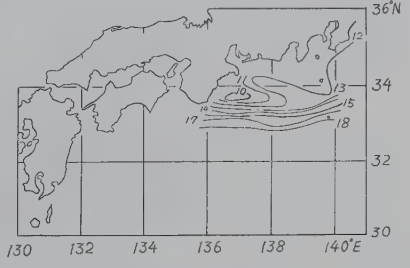


Fig. 12(b). Isotherms on 200m layer, May, 1952. [H.D.]

As the life of the cold water mass in 1952 is very short, the characteristic of this water mass may be different from the persistent cold water mass stated above. Although the difference between temporary and persistent cold water masses must be studied, study of this difference is a difficult and important problem which remains to be solve in future.

### 5. *Speculation about the occurrence of the offshore receding of the Kuroshio axis south of Shikoku*

In the above paragraphs it is stated that the offshore receding of the Kuroshio axis south of Shikoku may be connected with the appearance of the cold water mass. It is necessary to consider why the offshore receding of the Kuroshio axis occurs. As such problem is analyzed only by use of plentiful and systematic data, it is most suitable to use the data of oceanographical observations in 1959, because in 1934 and 1954 oceanographical observations were made less widely and less systematically than in 1959.

In January 1959 the Kuroshio transport was most abundant since 1954, according to the routine oceanographical observations by the Nagasaki Marine Observatory in the East China Sea. The value[7] is about $50\times10^6$ $m^3/s$, one and half times as much as the mean value. As the width of the current is rather smaller than the mean, the current velocity may be about 1.7 times as much as the mean. In the case of the strong Kuroshio, the north eastward currents in the sea east of the Ryukyu Islands which are observed always in normal years are not noticed. As the current velocity below 500m depth in this sea area is low, it can be assumed that the Kuroshio in the East China Sea reaches the 500m depth. In the present paper also it is considered that the lower boundary of the Kuroshio is 500m.

When we study the mean current velocity of water column of 500m, the value is from 80 cm/s to 120 cm/s in the East Chine Sea. From the observations in January 1959, current velocity of 120 cm/s is not unexpected. Now we take it into consideration that this Kuroshio traverses over the Ryukyu submarine ridge. The depth of the submarine ridge between Yakushima and Amamioshima is about 400m. So the Kuroshio should traverse a mound 100m high.

When we study the case where a current traverses a mountain, we may adopt the following formula[8] in the simple form:

$$\sin\alpha=-\frac{f}{CD}\int_{x_1}^{x_2}h\,dx$$

$$\Delta x=x_2-x_1.$$

Where $C$ is the current velocity, $f$ Coriolis parameter, $h$ the mountain height, $\Delta x$ the width of submarine ridge, $D$ the current thickness under undisturbed

state, $\alpha$ the deflecting angle when the current traverses the top of the mountain. $\alpha$ is calculated in Table 3.

Table 3.

$f=7.29\times10^{-5}$ $D=500$ m
$h=100$ m $\Delta x=30$ km

| Current velocity | Deflecting angle |
|---|---|
| $C=80$ cm/s | $\alpha=-34°$ |
| $C=120$ cm/s | $\alpha=-19°$ |

From this table it is known that the deflecting direction across the submarine ridge is remarkable, when the ocean current velocity is weak. Such phenomena are often observed near Yakushima. In case of a strong current direction is not so deflected.

In the mean state of the Kuroshio in the East China Sea the north eastward current to the east of the Ryukyu Islands is fairly predominant, but in the case of strong Kuroshio the northeastward current is not developed (for example, January 1959). In the former case the northeastward current approaches Shikoku in company with the meandering Kuroshio through the channel between Yakushima and Amamioshima. Meanwhile, when the Kuroshio is strong, there is no northeastward current to the east of Ryukyu Is., and the strong ocean current coming from the sea region between Yakushima and Amamioshima has a trend of straight flowing from west to east

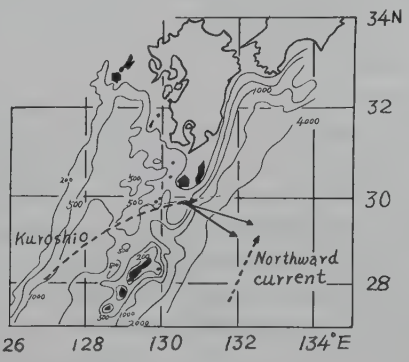


Fig. 13. Deflecting current on the submarine ridge. (Small numerals showing bathymetric depth in meter.)

(Fig. 13). So that, the Kuroshio flows almost eastnortheast-ward from the sea region between Yakushima and Amamioshima and then the axis of the Kuroshio tends to recede offshore to the south of Shikoku.

The above analysis is only a speculation based on the oceanographical observations of 1959. Different analyses [9][10][11] about the mechanism of the cold water mass have been offered by many oceanographers. The author intends to clarify the mechanism of the appearance by making reference to various analyses in future.

### *6. The future problem to clarify the occurrence of the cold water mass and the conclusion*

The easiest and most effective method which we can begin for clarifying the mechanism of the cold water mass is to collect and arrange the reports of ocean current observed by merchant ships and fishing boats. Unfortunately we have not reports of the ocean current at all, because any institution now does not gather reports of the ocean current. If we can collect and arrange these reports, they should offer us continuous informations about abnormal states of the current. So the author is strongly in the hope that reports of ocean current should be collected and then up to date charts of ocean current should be prepared. Such systems are one of the best methods to clarify the mechanism of cold water mass. It is natural that the continuous record of ocean current is suitable for an analysis of the cold water mass. If a tide gauge is installed at Yakushima, the record of this tide gauge will give a continuous information of the state of the Kuroshio in cooperation with the tide gauge at Amamioshima which the Hydrographic Department has established.

In oceanographical observations it is desirable to carry out simultaneous observations in the East China Sea and in the Pacific Ocean south of Shikoku and of the Kii peninsula. Besides, current profiles should be obtained for the East China Sea, for the Ryukyu submarine ridge and for the Kuroshio south of Shikoku. And it is an important problem in future to know how the effects of submarine ridges will be manifested in various flow patterns of the Kuroshio, by using an electronic computer.

*Acknowledgment*: It is a pleasure to record authors thanks to Dr. Y. TAKENOUTI, Dr. T. NANNITI, Dr. J. MASUZAWA, Dr. Y. SAITO and Dr. K. YOSHIDA for their encouragements in this work and to Mr. K. WADA for his assistance in the polishment of this paper and to Miss K. OKADA for her toil of drawing figures of this paper.

## *References*

(1) *Oceanographical Report* No. 14, 1959: Kobe Marine Observatory (in Japanese, Mimemograph).
(2) *Oceanographical Report* No. 2, 1959: Hydrographic Department (in Japanese, Mimemograph).
(3) *Hydrographic Bulletin* Vol. **6**, 1927～Vol. **22**, 1943: Hydrographic Department (in Japanese).
(4) *Oceanographical Investigation* No. 48, 1933～No. 72, 1943, 44: Imperial Fisheries Experimental Station (in Japanese).
(5) *Annual Reports of the Kochi Experimental Station* 1952, 53 and 54 (in Japanese).
(6) YOSHIDA, S.: Currents and other phenomena in the southern area of Honshu, in February through May (in Japanese). *Hydrog. Bull.* No. 981, Oct. 1952, pp 172-175.
(7) Data of the 11th forecasting meeting of the oceanic conditions, Nagasaki Marine Observatory (in Japanese, Mimemograph) 1959.
(8) BOLIN, B.: On the influence of the earth's orography on the general character of the westerlies. *Tellus* Vol. **2**, pp 184-195, 1950
(9) NANNITI, T.: A theory of the mechanism of the generation of the cold water region in the offing of Enshunada. *Pap. Met. Geophys.* Vol. **8**, pp 317-331, 1958.
(10) UDA, M.: On the recent anomalous hydrographical conditions of the Kurosio in the south waters off Japan Proper in relation to fisheries (in Japanese). *Jour. Imp. Fisher. Exper. St.* No. 10, Mar., 1940.
(11) FUKUOKA, J.: On the variations of the Kuroshio current south of Honshu (Japanese Main Island). *Geophys. Mag.*, Vol. **28**, pp 343-355, 1958.

The Oceanographical Magazine
Vol. 11. No. 2, March 1960

# Introductory Remarks of Japanese Expeditions of Deep Sea*

By

Kazuhiko TERADA and Hidetaka FUTI

*Japan Meteorological Agency*

## *1. Historical sketch*

During his stay in United States of America in 1956, Dr. Y. MIYAKE, chief of Geochemical Branch of Meteorological Research Institute, have had the preliminary negotiation with the Rockefellor Foundation about the financial aid for the Japanese deep sea researches.

Along the line of this negotiation, Dr. R. K. ANDERSON of Reckefellor Foundation came to Japan and inspected various research organizations. On 18th Dec. 1956 he suggested to Dr. K. WADATI, Directior-General of JMA, to contact officially to the Rockefellor Foundation.

So Dr. K. WADATI had organized the Planning Committee for Deep Sea Research on 10 Apr. 1957 for the purpose of exploring the Japan Trench and the neighbouring deep seas and the leading oceanographers in Japan were participated to the committee. He wrote on 12 April to the Foundation that "from the present financial conditions of Japan, it is very difficult to us to get necessary fund from governmental and/or private sources to make the deep sea research. Therefore we would like to get a grand totaling 123,250 from your Foundation" attaching the reason and research items and list of budget as follow :—

> Japan is one of the countries, such as the United States, the United Kingdom and Scandinavian countries which have greatly contributed to the development of the modern oceanography since the end of the 19th century. To our regret, however, Japanese oceanographers have had little chance to carry out the deep sea research which is regarded as the most important and interesting problem in the advanced study of the ocean. On the other hand, after World War II, Sweden, Denmark, the United Kingdom, the United States and the U.S.S.R. have accomplished great expeditions to clarify the deepest part of the ocean which covers the larger part of the earth.

* JEDS Contribution No. 1.

Along the Japanese Islands there extends the deepest trench in the Pacific, and we have not been able to explore it due to the lack of equipments to reach the bottom of the Japan Trench which is often close to 10,000 meters deep. The length of the longest wire rope now available in Japan is only, 6,000 meters, and it is quite essential to provide a new tapered wire rope of 15,000 meters long together with powerful winch.

From the geographical point of view, we believe that it is our duty as well as responsibility to exploit the Japan Trench by ourselves with the capability of Japanese oceanographers. This is also earnestly desired by leading oceanographers in the rest parts of the world.

For the reasons mentioned above, we apply for the grant, from the Rockefeller Foundation, for assisting the deep sea research conducted by Japanese scientists. Japan Meteorological Agency has a number of oceanographers and research ships. The MS Ryofu Maru of 1200 tons is one of them. The Oceanographers of our Agency are carrying on the extensive oceanographic observations in the western North Pacific in cooperation with other institutions in Japan and those in the United States and Canada.

If the MS Ryofu Maru could be provided with a big winch and modern instruments for deep sea study, we, the Japanese oceanographers of various govermental and civilian agencies and institutions, would be able to begin right now under the close cooperation the exploration of neighboring sea area. That will surely contribute to increase the common knowledge of mankind about the unknown world and to exploit the undeveloped resources in the ocean. We are very glad to add here that the Oceanographical Society of Japan and National Committee on Oceanography in Japan Science Council are much interested in this problem and they have pledged to give their earnest support to our plan when it is realized.

It would be our greatest pleasure if you could take our plan into your consideration and help our earnest desire to explore the deep sea around us.

**Research items we are planning are as follows:**

1. Movement of deep waters
2. Chemistry of deep waters
3. Geological studies
4. Deep sea fauna
5. Microbiological studies
6. Geophysics of the ocean floor

**List of Budget**

| | |
|---|---|
| DEEP SEA WINCH | |
| Diesel engine for electric generator, 160 HP. | $18,000 |
| Generator, 120 KW | 14,000 |
| Motor, 100 KW | 12,500 |
| Motor, Attachments | 1,400 |
| Drum | 4,200 |
| Derick | 5,600 |
| Equipment | 7,000 |
| | ($62,700) |

| | | | |
|---|---|---|---|
| TAPERED WIRE-ROPE | | | |
| (8m/m 32m/m$\phi$×15 000m) | | | ($11,000) |
| ECHO SOUNDER | | | |
| Echo sounder | | | $8,200 |
| Equipment | | | 1,700 |
| | | | ($9,900) |
| CORE SAMPLER | | | |
| Piston core, 6m | 3 | 1,400 | 4,200 |
| Piston core, 2m | 5 | 220 | 1,100 |
| Gravity core, 2m | 5 | 160 | 800 |
| Dredge | 3 | 180 | 540 |
| Plastic tubes, 6m | 150 | 12 | 1,800 |
| Plastic tubes, 2m | 300 | 4 | 1 200 |
| | | | ($9,640) |
| INSTRUMENTS FOR SEISMIC INVESTIGATIONS OF THE OCEAN FLOOR | | | (20,000) |
| DEE-SEA CAMERA | | | (10,000) |
| | | | $123,240 |

Answering this inquiry, Dr. WADATI received the letter dated on June 3, 1957 from Dr. R.K. ANDERSON, of the following contents:—

"Since my return from Japan, I have had an opportunity to discuss your request for equipment for deep sea oceanography with several of our officiers. They were very much interested in your request, were favorably impressed by the program you outlined, by the caliber of people on your planning committee, and by the breadth of their interests. They were also impressed by the fact that you already have the ship, facilities, and personel to carry on deep sea oceanography and that all you need to go ahead is the equipment.

It is my understanding that you and your associates at the Japan Meteorological Agency would have direct responsibility for receiving and administering the grant, if and when made, and for general supervision of the program, including the installation of equipment in the ship, the investigations conducted at sea, and the subsequent laboratory work invloved. I presume, however, that the latter would be carried through in various laboratories, such as those of your Agency and related institutions, various departments at Tokyo University, Nagoya University, etc. Would it be possible to give us a little more specific information on the facilities and personnel available? We have no doubt about the competence of the members of the committee and their ability to supervise the work, but they are all extremely busy people who carry heavy responsibilities and may not be in a position to do much of the actual technical work themselves. We are, therefore, likely to be asked just where and by whom the various specialized aspects of this broad program of laboratory research would be conducted.

At this time I think it would also be in order for you to ask the appropriate authorities to send us an official request.

The request could be quite brief, perhaps merely an official statement that the Ministry endorses a request such as that contained in your letter to me of April 12 and that the Japan Meteorological Agency would be prepared to receive and administer such a grand, would see that it was used for the purpose specified, and would account for the expenditure of the funds."

So the Japan Meteorological Agency took the appropriate action for the endorsement of the Ministry of Transportation and also discussed some questionaries presented by Dr. ANDERSON for the effective operations of the deep sea researches.

In regard to this problem, Dr. R. Revelle, Director of Scripps Institution of Ooeanography had kindly written to Dr. ANLERSON to urge that the Rockefellor Foundation may give favorable consideration for the funds of the equipments of deep sea research on Ryofu Maru, showing the following philosophy :—

> "During the past five years American and Japanese marine scientists have cooperated closely and profitably in studying the Pacific Ocean, and this cooperating is now being further extended to include Russian ships and scientists. During the summer of 1955, for example, twelve Japanese ships and eight United States and Canadian ships carried out a synoptic survey of the entire North Pacific Ocean north of twenty degrees latitude. The results of this "Norpac" operation are now being issued as a joint publication by the University of Tokyo and the University of California. During 1956 a similar multiple ship expedition was carried out in the equatorial Pacific. In both these expeditions the work was confined largely to the biological and the physical and chemical oceanography of the top thousand meters of the sea, because the Japanese ships did not have the necessary winches and other equipment to explore the deeper waters. These deeper waters are becoming one of the main objects of modern oceanographic research.
>
> It seems to me essential that the Japanese should play their proper part in this work. We are just beginning to realize how important the deep waters are in the entire biological and physical regime of the sea. The exchange between the deep and surface layers, bringing untrient substances up from the depths, determines the variations in fertility of different parts of the ocean. We can think of the ocean and the atmosphere as interlinked heat engines of low efficiency, and the oceanic deep waters are one of the working fluids of these heat engines, which carry excess heat from the "firebox" of the tropics to the radiation-cooled "condenser" of the high latitudes. The oceanic circulation system is both more sluggish and more massive than of the atmosphere, and it is believed that it plays a large role in determining climate.
>
> From another point of view, the deep waters may become especially important to the Japanese. Because of their lack of fossil fuels and their industrial needs, a rapid development of power from nuclear fission will be necessary in Japan. In this small, heavily populated land with its long coastline, one can expect that much of the radioactive wastes will be dumped into the nearby deep ocean. (As you know, one of the deepest areas on earth, the Japan Trench, lies a few miles east of Hokkaido and Honshu.) If this material is to be safely disposed of, a good deal more must be known about the bottom topography, the sediments, and the deep waters in the western Pacific."

On September 16, 1957, Drs. ANDERSON, HARKER, CHANDER, and MORISON of Rockefellor Foundation came again in Japan for the full dicussions among the

members of Planning Committee and several staffs of Japan Meteorological Agency, and after he returned to America, the grant of the necessary fund was determined, on Dec. 7, 1957.

ROCKEFELLOR FOUNDATION GRANTS

Volume VIII Fourth Quarter, 1957 Number 4

**Extract**

Japanese Agency Plans Deep Sea Research

Because the depth of the deepest trenches in the ocean floor exceeds by roughly 6,500 feet the height of the world's lofties mountains, studies of the deep seas, the marine life they support, and their influence on such phenomena as tidal waves, have been limited. The Japan Meteorological Agency, Tokyo, will initiate research in the deep waters off the coast of Japan with the help of a two-year grant of $130,000 from The Rockefeller Foundation.

Scientists are increasingly impressed with the importance of deep waters to the entire biological and physical regime of the sea. The exchange between deep and surface layers appears to influence the fertility of different parts of the ocean, and the circulation of ocean water from the tropics to the high latitudes is believed to play an important part in the determination of climate. Better knowledge of the migration and habits of marine life in the lower levels of the ocean may well have practical results in an augmented food supply for the world's growing population. Atomic wastes cannot safely be dumped in deep waters until further information is obtained concerning the contour of the ocean floor and the overturn of ocean waters.

The Japan Meteorological Agency has appointed a committee composed of Japan's most distinguished geophysicists, geochemists, ichthyologists, oceanographers, planktologists, microbiologists, biochemists, and marine biologists to plan and carry out the proposed research program. In addition to its own facilities, the agency will have at its disposal the resources of the several institutions it operates and of various research laboratories in selected Japanese universities.

Now there necessarily occurred problems of two different directions, one is concerning to the discussion facilitating the deep sea research from various point of view and the another is concerning the design of the installation of the said equipments.

In order to promote effectively the deep sea research, a small committee of the deep sea research was established in the Science Council of Japan which includes naturally the members of Planning Committee as the leading members.

The latter problem is directly connected to the official works of the repair of Ryofu Maru, and so Dr. K. Terada, chief of Marine Divison of JMA,

is ordered to conduct the installation taking into consideration the opinions of the members of Deep Sea Research.

After careful and frequent discussions, the manufacturing of the installation of deep sea research was determined to order to Ishikawazima Heavy Industries Co. LTD, under the following specifications :—

June 4th, 1958

The specification and an estimate for installation of the lifting equipment of deep sea core sampler on MS Ryofu Maru

1. **The Specification for the Work**

A. **Outline of the Works**

Specification of lifting equipment of deep sea core sampler and outline of fitting work of the same to be installed on MS Ryofu Maru, a survey ship of Meteorological Bureau of Japanese Government, is as follows:

Being this equipment of considerable weight, it shall be installed in a sternside cargo hold to prevent a rise of ship's center of gravity. For this purpose, the permanent ballast located in the afore-mentioned hold shall be shifted to a certain suitable location and install an electric power source for driving winch and wire reel and established a refrigerated chamber for storing core samples in the said hold. The equipment is so designed as to have minimum measurement as the space of the hold is not big enough, by means of taking the smallest safety factor allowable for lifting rope to lessen load on winch. The lifting rope shall have larger diameter toward winch length by length and shall be wound in wire reel through a 2 drum-friction-driven winch.

As the space is quite insufficient, we can not provide enough distance between winch and wire reel. Thus the handling of wire in usual way is rather difficult, therefore the winding of wire shall be performed by moving its drum from left to right or right to left. As this equipment is designed to increase its winding speed when the remaining rope become short, the revolution of which and winding drum shall have to be changed accordingly.

And as the diameter of wire rope shall be also changed with its winding operation, it shall be necessary to change the speed of side movement of the winding drum too.

In order to obtain such complicated movement to the motors driving winch, driving and side movements of wire reel, a unit equipment of Wordleonard Generators, Amplydines and Magnetic Amplifiers shall be equipped. And each motor shall be controlled automatically by this control unit.

On the aft part of the upper deck, a mast and work platform shall be provided for the adjustment of lifting equipment.

In order to be lower the gravity of the vessel while in winding operation, and to avoid a heavy load on the mast, a leading block of rope to be lowered, through the guide rail of the mast, and fastened on the upper deck.

Beside the above, Echo Sounder, having a capacity of 11,000 m, and Hydrophone shall be provided, to detect the reach of core sampler on the sea bottom.

**B. Principal Particulars of Lifting Equipment**

a. Winch
- load (excl. rope weight) 1.0 t
- lifting speed max. (under 3.3 t load) 48.8 m/min
- min. (over 13.8 t load) 12.2 m/min.
- lift 13,000 m

b. Motor

| | | |
|---|---|---|
| for driving winch | DC 40 KW | 1 set |
| for driving wire reel | DC 15 KW | 1 set |
| for shifting wire reel | DC 1 HP | 1 set |

c. Generator

(1) Electric source for Leonard control

| | | |
|---|---|---|
| for winch | DC 220 V 50 KW | 1 set |
| for wire reel | DC 220 V 20 KW | 1 set |
| for exciter | DC 220 V 25 KW | 1 set |

(2) Motor generator for automatic control

| | | | |
|---|---|---|---|
| common bed | amplidyne generator for winch motor | 2.4 KW | 1 set |
| common bed | amplidyne generator for wire real motor | 1.0 KW | 1 set |
| common bed | motor for driving above generator | DC 7½ HP | 1 set |
| | amplidyne generator for winch generator | 1 5 KW | 1 set |
| | amplidyne generator for wire real shift motor | 1.0 KW | 1 set |
| common bed | generator for magnetic amplifier AC 100 V, 500 VA 60 cy | | 1 set |
| | motor for driving above generator | DC 7½ HP | 1 set |

d. Prime mover
- type: Vertical 4 cycle single acting airless injection diesel engine
- output × rpm: about 150 BHP × 900 rpm

e. Tapered rope
- construction of rope: 7×7 independent wire strand core (IWSC) galvanized, right hand ordinary lay, preformed rope
- material: 80c KPR (KOBE STEEL MFG.)
- breaking strength: 200 kg/mm²

| dia. (m/m) | breaking load (t) | length (m) | weight (t) | load at rope end (t) | safety factor |
|---|---|---|---|---|---|
| 9 | 6.68 | 2,400 | 0.826 | 3.326 | 2.01 |
| 10 | 8 25 | 1,800 | 0.765 | 4.091 | 2.01 |
| 12 | 11.90 | 3,000 | 1.794 | 5.885 | 2.02 |
| 14 | 16.10 | 2,500 | 2.084 | 7.960 | 2.02 |
| 16 | 21.10 | 2,300 | 2.510 | 10.479 | 2.01 |
| 17 | 23.80 | 1,100 | 1.353 | 11.709 | 2.02 |
| Total | | 13,100 | 9.332 | | |

**2. Estimated Price**

A. Winch and installation of the same. $19,000.—

B. Diesel motor for generator and installation of the same. $13,500.—

| | | |
|---|---|---|
| C. | Generator, electric motor, generator switch board, Leonard control system and installations of the same. (Including illumination apparatus) | $54,020.— |
| D. | Echo-sounder and installation of the same. | $14,100.— |
| E. | Wirerope. | $15,400.— |
| F. | The turret at the stern, working stage and installation of the david. | $11,280.— |
| G. | Refrigerator of the specimen and installation of the same. | $2,700.— |
| | Total: | $130,000.— |

3. **Time of Completion**

All work to be completed before March 31st 1959.

As we see from this specification we were obliged to change our schedule a little from that was shown to the Rockefellor Foundation.

So we were obliged to give up some instruments and to minimize the length of the tapered wire through frequent discussions among the researchers and the engineers of the shipyard. This change of the first design was made with consent of Rockefellor Foundation.

In the letter of the Rockefellor Foundation dated on June 16, 1958 Dr. K. WADATI wrote that :—

1. This sort of research is the first case in our country and took much time for investigation till we reach this conclusion.

2. As for the equipment listed in this requirement, it does not include all the items shown in the previous statement. Here, only deep sea winch, echo-sounder, wire-rope, tower and davit, and refrigerator for samples are listed.

3. The chief reason of difference in the list was caused by the change of specification of the winch. The winch, which can coil and recoil smoothly the 15,000-meter rope as requested by the Deep Sea Research Committee, has to be installed in the hold at the stern of the MS Ryofu Muru.

(1) The winch must be installed in conformity with the general rules of ship-building engineering, that is to keep the center of gravity of vessel as low as possible.

(2) On the decks of the Ryofu Maru, there are so many constructions that the enormous expence is necessary for drastic remodelling, such as taking out or removal of constructions, in case the winch is installed there.

With these two points, it was decided to fix the winch in the hold at the stern. However, as the hold is narrow, enough span cannot be expected. Also stable and smooth motion of the winch cannot be hoped from the ordinary winding system. That is why this winch was specially designed. It is operated by electric assembly of automatic control system which is usually used at the automatic compress-stretch factory of steel-plate trade, so that the winch can smoothly coil or uncoil the rope with changing diameter. It is of fairly advanced type of winch.

Even the Ishikawajima Heavy Industries Co., noted for its conscientious service,

stated that it can furnish the said five equipment only within the cost of $130,000 You must have recognized that the length of wire is not longer than 13,000 meters. It is also due to the same financial reason.

4. Accordingly, this requirement does not contain instruments for biological studies, core sampler and deep sea camera etc. as listed in the previous list. It is impossible to provide these items within the grant. Therefore, in order to perform the deep sea research as scheduled in the initial plan, we are now exerting ourselves to obtain financial resources in Japan and the negotiation is expected to be completed shortly.

As to the design of the installation of the deep sea equipments, the enginneers of the shipyard have had the frequent discussions among the members of Marine Division of JAM, including Dr. K. TERADA, the chief of the division and also the member of deep sea research committee.

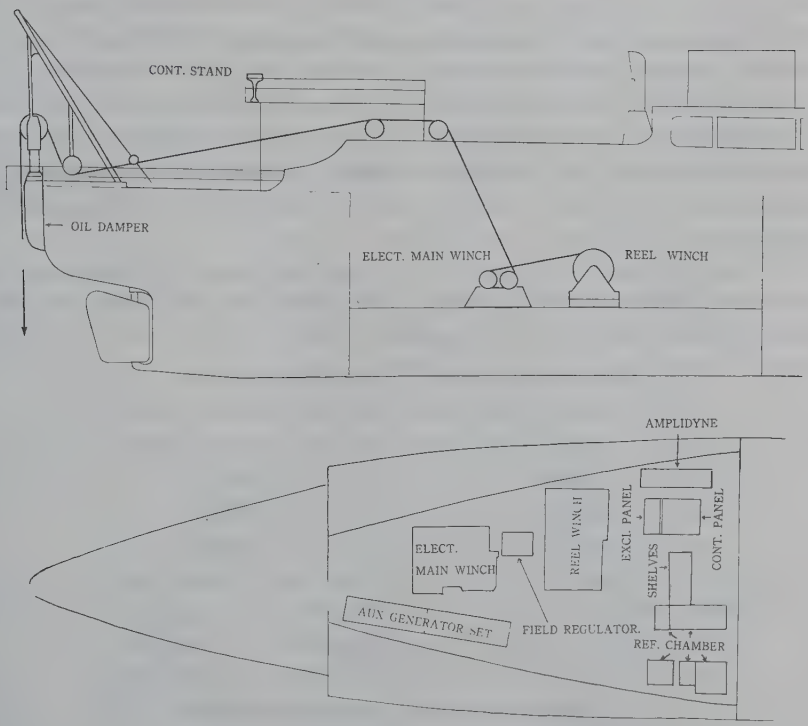


Fig. 1. Stationing diagram of Deep Sea Plant.

Accordingly some points were remedied and one of them was the installation of the oil damper at the rear side of the ship, which acted very effectively for the decrease of the amplitude of vibrations of the tapered wire.

As Ryofu Maru is a research ship constantly working in the neighbouring sea, the manufacturing period was limited to be only one month. But through the good collaboration of the shipyard and Japan Meteorological Agency, the construction was over perfectly during one month and the final installation was completed on 31st March, 1959.

*2. Deep Sea Research Committee*

In order to promote effectively the oceanic researches in Japan, the Science Counsil of Japan has decided to install a research committee in April, 1958. This committee is corresponding to the Special Committee of Oceanic Research (SCOR) of the International Counsil of Scientific Union (ICSU) and is nominated as "National Committee of Oceanic Research (NCOR)" and has a responsibility to act as the mother body for the promotion of oceanic research, specially for the interrelation with the foreign countries and international affairs concerning the oceanic research. Dr. K. HIDAKA was elected as the president of NCOR.

In the meeting of 23 July 1858, the Deep Sea Research Committee was installed in NCOR and the members of this committee were nominated from those of NCOR and those not belonging to NCOR.

The members were: (*member of NCOR)

| | | |
|---|---|---|
| *Dr. K. WADATI | (Chairman) : | Director-General of JMA. |
| *Dr. K. TERADA | (Convener) : | Marine Division, JMA. |
| *Dr. K. YOSHIDA | ( ,, ) : | Tokyo University |
| *Dr. K. HIDAKA | : | Tokyo University |
| *Dr. Y. MATSUE | : | Tokyo University |
| *Dr. H. NIINO | : | Tokyo Univ. of Fisheries |
| *Dr. M. UDA | : | Tokyo Univ. of Fisheries |
| *Mr. T. KUMAGORI | : | Tokyo Univ. of Fisheries |
| *Dr. Y. MIYAKE | : | Tokyo Univ. of Education |
| *Dr. K. SUGAWARA | : | Nagoya University |
| *Dr. D. MIYAJI | : | Kyoto University |
| *Dr. K. SUDA | : | Hydrog. Div. Maritime Safety Board |

| | | |
|---|---|---|
| *Dr. T. Suyehiro | : | Tokyo University |
| Mr. N. Taga | : | Tokyo University |
| Dr. N. Nasu | : | Tokyo University |
| Dr. Y. Tekenouti | : | Meteorological Research Inst. |
| Dr. Y. Saito | : | Osaka City University |
| Dr. T. Sasaki | : | Tokyo Univ. of Fisheries |
| Dr. Y. Okada | : | Miye University |
| Mr. S. Takayama | : | Tokai Regional Fisheries Research Laboratory |
| Mr. R. Komukai | : | Hydographic Div., M.S.B. |

*Mr. U. Tsukamoto has charged as the Chief of Hydographic Div., M.S.B. in 1959.

The members of this committee proposed many valuable suggestions for the installation of deep sea equipments, and also discussed the ways and methods of obtaining the financial aid for the construction of the equipments, which could not be supplied by the grant of Rockefellor Foundation, and for various expenses to promote the deep sea research. (This point was a little overcome by the voluntary aid from the Yomiuri Press).

According to the progress of the installation of the deep sea equipment on Ryofu Maru, this committee began to discuss the precise schedules of the researches. To do so it was inevitable to add some staffs of Ryofu Maru, the actual observers and the engineers of shipyard. And so the new committee was established for the actual promotion of the researches in Japan Society for the Promotion of Science and the main problem of the implementation of the research works was took over this new committee.

This new committee is consisted from the members of Deep Sea Research Committee in NCOR and the acting staffs of various agencies, as follows:

| | | |
|---|---|---|
| Dr. K. Wadati | : | Chairman, Director-general, JMA. |
| Dr. K. Terada | : | Convener, Chief, Marine Division, JMA. |
| Mr. T. Araya | : | Secretary, Japan Society for the Promotion of Science |
| Dr. K. Hidaka | : | Prof. Tokyo University. |
| Dr. Y. Matsue | : | Prof., Tokyo University. |
| Dr. Y. Suyehiro | : | Prof., Tokyo University. |
| Dr. K. Yoshida | : | Assist. Prof., Tokyo University. |

| | | |
|---|---|---|
| Dr. N. Nasu | : | Assist. Prof., Tokyo University. |
| Mr. N. Taga | : | Tokyo University. |
| Mr. H. Iwai | : | Tokyo University. |
| Dr. K. Futi | : | Chief, Oceanographical Section, JMA. |
| Mr. K. Nakano | : | Chief, Ship Operation Section, JMA. |
| Mr. N. Suzuki | : | Ship Operation Section, JMA. |
| Mr. T. Suenaga | : | Captain, Ryofu Maru. |
| Dr. J. Masuzawa | : | Oceanographical Section, JMA. |
| Dr. R. Marumo | : | Oceanographical Section, JMA. |
| Mr. M. Yasui | : | Oceanographical Section, JMA. |
| Mr. H. Akamatsu | : | Oceanographical Section, JMA. |
| Mr. A. Suwa | : | Seismological Section, JMA. |
| Dr. Y. Takenouti | : | Meteorological Research Institute. |
| Mr. T. Shimada | : | Meteorological Research Institute. |
| Mr. T. Kumagori | : | Prof., Tokyo Univ. of Fisheries. |
| Dr. M. Uda | : | Prof., Tokyo Univ. of Fisheries. |
| Dr. H. Niino | : | Prof., Tokyo Univ. of Fisheries. |
| Dr. T. Sasaki | : | Prof., Tokyo Univ. of Fisheries. |
| Mr. M. Ishino | : | Tokyo Univ. of Fisheries. |
| Dr. Y. Miyake | : | Prof., Tokyo University of Education. |
| Dr. H. Hamaguchi | : | Prof., Tokyo University of Education. |
| Mr. M. Horikoshi | : | Ochanomizu Women's Univ. |
| Dr. D. Miyaji | : | Prof., Kyoto University. |
| Dr. Y. Okada | : | Prof., Miye University. |
| Dr. Y. Saito | : | Prof., Osaka City University. |
| Mr. Y. Tsukamoto | : | Head, Hydrogr. Div. M.S.B. |
| Mr. T. Matsuzaki | : | Chief. Oceanogr. Sec. Hydrogr. Div. M.S.B. |
| Mr. S. Kishi | : | Oceanogr. Sec. Hydrogr. Div. M.S.B. |
| Mr. T. Sato | : | Oceanogr. Sec. Hydrogr. Div. M.S.B. |
| Dr. K. Sugawara | : | Prof., Nagoya University. |
| Mr. S. Takayama | : | Tokai Regional Fisheries Research Laboratory. |
| Dr. K. Suda | : | Former Head, Hydrogr. Div. M.S.B. |

The members of this new committee of the similar name are generally divided into four branches according to their specialities as follows :—

(1) Physical oceanography

(2) Chemical oceanography
(3) Biological oceanograshy
(4) Geological oceanography

Thus divided members were constructed their special plans of researches respectively and these plans were altogether discussed taking into the schedule of Ryofu Maru.

The similar processes will be taken in the coming researches, too.

After the researches in 1959, the committee decided the following points as to the various points such as the publication of the result of the researches.

(1) The samples obtained from the deep sea research will be regulated under the heading:

JEDS-2-S

implying that the sample of the point S of the 2nd research of "Japan Expedition of Deep Sea".

(2) The result of the researches concerning the deep sea investigations will be published, as the

Collected Paper

from this Committee.

(3) If the precise points are published in every branches, the note of

JEDS Contribution No.-

is preferable to be added.

(4) In such case the summary should be printed in

Oceanographical Magazine

of Japan Meteorological Agency.

*3. Deep Sea Researches in the year 1959.*

In July the preliminary tests of various equipments installed on Ryofu Maru were performed at the Japan Trench. All the equipments were newly designed and constructed in various factories in Japan, each of them having no experiences. So in the preliminary tests the researchers and engineers of Ishikawajima shipyard and allied companies and the related officers of Japan Meteorological Agency were on board with many researchers.

As is expected from the specifications of tapered wire, the lowering or lifting speed was designed to be of the order of 40m/min. or so and such speed is to be controlled by the electric devices. First of all, such a

controll system relating to the observed speed of the wire was examined carefully attaching the core sampler at the end of the wire.

After several tests of lowering and lifting of wire in rather shallow sea,

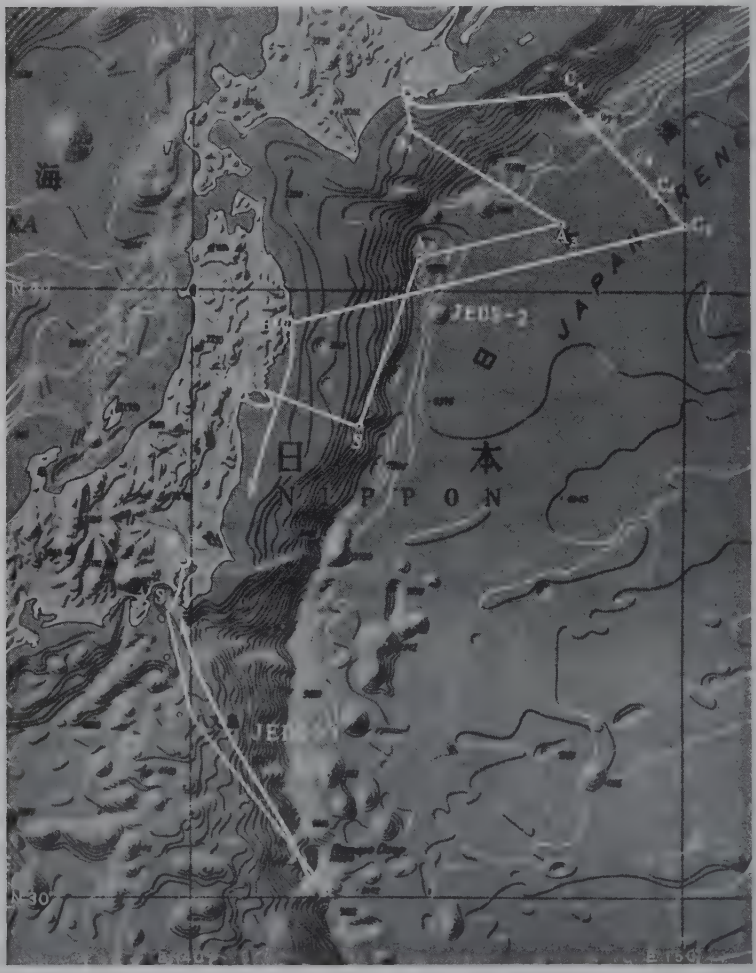


Fig. 2. Expedition Routs of Deep Sea in 1°5°.

the precise test was performed on 26th, at the Japan Trench, by drifting the ship.

Wire began to be lowered at 8h 29m and it seemed to reach the bottom of 8450m at 17h 11m after several tests of the control system. The ship was shifted southward about 10km due to the ocean current.

We began to wind the wire at 18h 00m and we worked all the night and at 01h 08m of 27th we found a large kink on the tapered wire at about 120m from the end, where the core sampler was attached. Due to this kink we could not wind the wire through the pulley. We endeavoured to overcome this trouble by shifting the kinked part by catching tightly the wire using the stopper designed for the core sampler. Fortunately we could overcome this difficulty and moreover we could get good samples of bottom specimens, ever obtained bottom sample by the Japanese researchers and by Japanese instruments.

The course of ship and other related phenomena will be shown in this table. This test is nominated JEDS-1. (See Fig. 2)

Schedule of JEDS-1.

| Date | Time | Departure | Arrival | Testing Instrument | Bottom Sampling (Depth, Location) |
|---|---|---|---|---|---|
| June 23 | 1700 | Tokyo | — | | |
| 〃 24 | 0500 | — | Sagami Bay | piston core sampler | 50 cm (700 m) |
| 〃 24 | 1850 | Sagami Bay | — | dredge | |
| 〃 26 | 0520 | — | Ramapo Deep | piston core sampler | 22 cm (8540 m) |
| 〃 27 | 1145 | Ramapo Deep | — | | (30°24.6′N, 142°18.7′E) |
| 〃 29 | 0800 | — | Tokyo | | |

Remarks: (1) A new designed echo sounder was fully operated during navigation and a deepest depth of 9695 m was observed at the point of 31°4.8′N, 142° 09.5′E.

(2) The working of ball-breakers of different types was tested on several layers of different depths.

(3) The sea noise from the new designed hydrophone was recorded on magnetic tapes.

In September we made the deep sea research in the northern part of Japan Trench in the period about 25 days. In this case many researchers of various branches were participated after the careful preparations. This test was nominated JEDS-2 and the general feature of this test will be shown in the table. (See Fig. 2)

Schedule of JEDS-2.

| Date | Time | Departure | Arrival | Bottom Sampling | Biological Sampling | Water Sampling | Echo Sounding |
|---|---|---|---|---|---|---|---|
| Sept. 5 | 1400 | Tokyo | — | | | | |
| 7 | 0800 | — | Shiogama | | | | |
| 8 | 1500 | Shiogama | — | | | | |
| 10 | 2100 | — | S | dredge (2350 m) | trawl (2230 m) | | |
| 12 | 1200 | | $A_2$ | | pl-net (6000 m) | 50 *l* (300 m, 6000 m) | |
| 15 | 1245 | | $A_3$ | | pl-net (3000 m) | | |
| 16 | | | | | larval net (2500 m) | | |
| 17 | 0730 | | $B_1$ | drege | | | |
| | 1040 | $B_1$ | — | | | | |
| | 1300 | — | Kushiro | | | | |
| 21 | 0900 | Kushiro | | | | | |
| 22 | 0020 | — | $C_1$ | | | | 8677 m (corrected) 42°46′N, 148°10′E |
| | 0640 | — | $C_2$ | piston core sampler 85 cm (8005 m) | pl-net (3000 m) | 50 *l* (6000 m) 20 *l* (200, 500, 3000 m) | |
| 24 | 0303 | $C_2$ | — | | | | |
| | 0800 | — | $C_3$ | | | 20 *l* (0, 500, 3000 m) | |
| | 1340 | $C_3$ | — | | | | |
| | 1830 | — | $C_4$ | | | | |
| | 2230 | $C_4$ | — | | | | |
| 25 | 0320 | | $C_5$ | | | 20 *l* (200, 500, 3000 m) | |
| | 0820 | $C_5$ | — | | | | |
| 27 | 0130 | — | Yamada | | | | |
| 28 | 1700 | Yamada | — | | | | |
| 30 | 0800 | — | Tokyo | | | | |

In this test also the researchers and ship officers and crews encountered many difficulties by the kink and the severe weather. As we easily notice, the test should necessitate long time continuations of rather good condition of the state of sea.

So it will be inevitable to omitt some scheduled points or research items due to various unexpected cases. But generally speaking the deep sea research of September was successful by obtaining many valuable data and samples.

General view of MS Ryofu Maru (1200 tons).
(See Fig. 1)

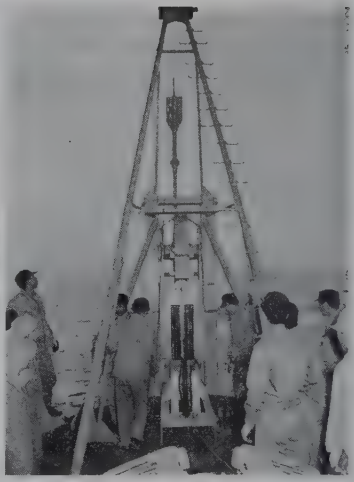

A-frame and damper.

Control tower. (↑)
and driving winch. (→)

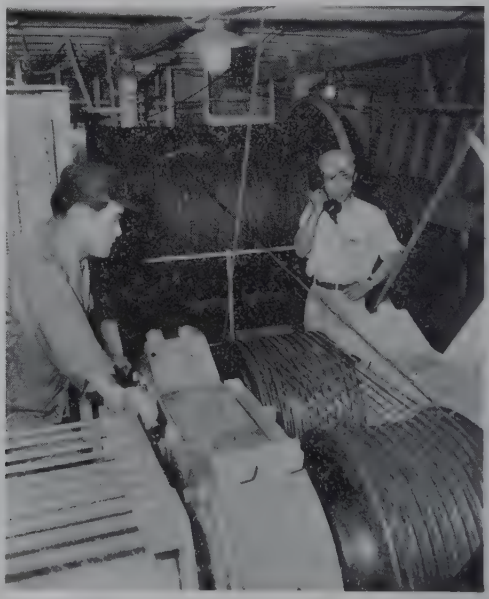

Wire reel and its motor.

Generator for driving winch and wire reel.

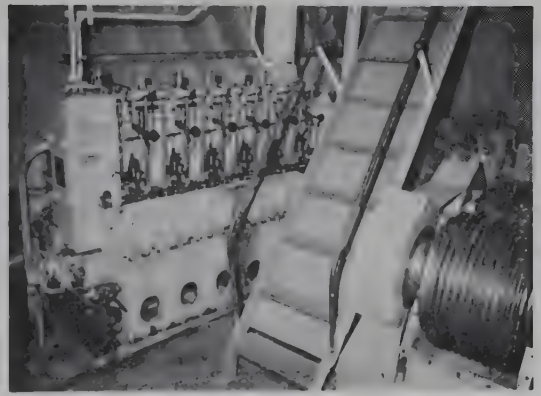

Vertical 4 cycle single acting airless injection diesel engine (150 HP).

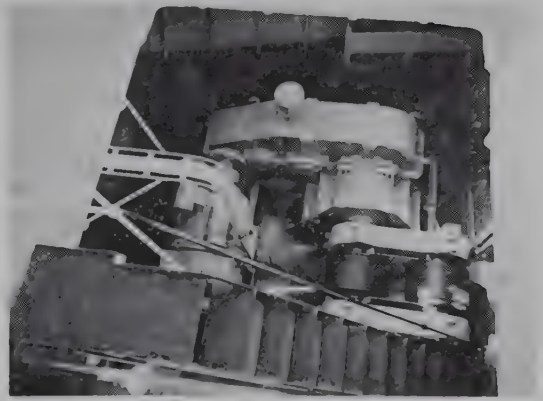

Driving winch and its motor.

The Oceanographical Magazine
Vol. 11. No. 2, March 1960

# A Hydrographic Section across the Kurile Trench*

By

Jotaro Masuzawa, Masashi Yasui and Hideo Akamatsu

*Japan Meteorological Agency*

## *1. Introduction*

It was planned to obtain two hydrographic sections on board the research vessel Ryofu Maru, the one across the northern part of the Japan Trench

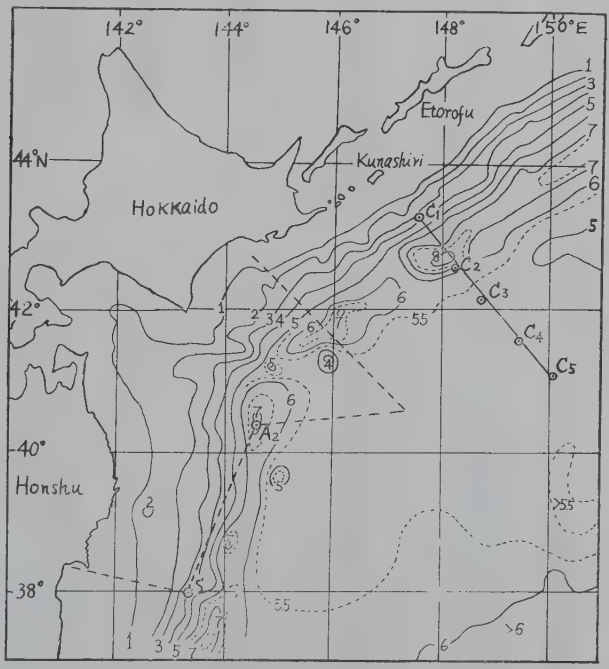


Fig. 1. Stations of serial oceanographic observations and the bathmetric chart reproduced from Chart No. 6901 of the Japan Hydrographic Office. Figures show thousand meters.

* JEDS Contribution No. 2.

Table 1. Results of serial observations in JEDS-2, September 1959 (*value doubtful).

| St. JEDS-2-S Sept. 10-11 1959 37°58′N, 143°24′E | | | | St. JEDS-2-$A_2$ Sept. 13 1959 40°22′N, 144°34′E | | | |
|---|---|---|---|---|---|---|---|
| Depth (m) | T (°C) | Cl (‰) | $O_2$ (m$l$/$l$) | Depth (m) | T (°C) | Cl (‰) | $O_2$ (m$l$/$l$) |
| 0 | 22.0 | 18.965 | 4.84 | 0 | 18.7 | 18.410 | 5.54 |
| 10 | 22.01 | 18.965 | 5.14 | 10 | 18.32 | 18.390 | 5.52 |
| 20 | 21.97 | 18.955 | 5.31 | 20 | 17.41 | 18.370 | 5.80 |
| 30 | 20.05 | 19.150 | 5.54 | 30 | 9.38 | 18.520 | 6.28 |
| 50 | 17.09 | 19.145 | 5.01 | 50 | 8.10 | 18.620 | 5.88 |
| 75 | 15.28 | 19.095 | 4.61 | 75 | 5.03 | 18.450 | 6.86 |
| 93 | 14.64 | 19.135 | 4.42 | 98 | 3.82 | 18.470 | 6.23 |
| 138 | 12.74 | 19.075 | 4.59 | 147 | 3.15 | 18.510 | 5.79 |
| 182 | 11.61 | 19.030 | 5.04 | 196 | 2.32 | 18.520 | 5.09 |
| 270 | 10.57 | 18.970 | 5.12 | 294 | 3.42 | 18.675 | 3.63 |
| 352 | 8.35 | 18.830 | 4.81 | 393 | 2.90 | 18.705 | 2.60 |
| 432 | 6.04 | 18.750 | 4.62 | 491 | 3.16 | 18.800 | 1.78 |
| 510 | 5.02 | 18.775 | 3.61 | 589 | 3.29 | 18.860 | 1.32 |
| 660 | 3.30 | 18.770 | 2·28 | 786 | 3.23 | 18.970 | 1.01 |
| 812 | 3.82 | 18.930 | 1.55 | 983 | 2.88 | 19.010 | 0.98 |
| 975 | 3.25 | 19.000 | 1.05 | 1181 | 2.55 | 19.050 | 1.09 |
| 1328 | 2.64 | 19.065 | 0.85 | 1615 | 2.17 | 19.100 | 1.30 |
| 1788 | 2.18 | 19.105 | 1.32 | 2163 | 1.81 | 19.145 | 2.11 |
| 2259 | 1.83 | 19.165 | 2.18 | | | | |
| 2739 | 1.63 | 19.160* | 2.55 | | | | |
| 3225 | 1.54 | 19.195 | 3.15 | | | | |

| St. JEDS-2-$C_1$ Sept. 22 1959 43°16′N, 147°32′E | | | | St. JEDS-2-$C_2$ Sept. 22-24 1959 42°48′N, 148°10′E | | | |
|---|---|---|---|---|---|---|---|
| Depth (m) | T (°C) | Cl (‰) | $O_2$ (m$l$/$l$) | Depth (m) | T (°C) | Cl (‰) | $O_2$ (m$l$/$l$) |
| 0 | 15.7 | 18.220 | 5.83 | 0 | 15.2 | 18.305 | 5.83 |
| 10 | 15.78 | 18.180 | 5.86 | 10 | 15.33 | 18.255 | 5.73 |
| 20 | 15.72 | 18.200 | 5.85 | 20 | 15.39 | 18.295 | 5.79 |
| 30 | 14.76 | 18.260 | 5.86 | 30 | 11.98 | 18.720 | 6.00 |
| 50 | 7.28 | 18.600 | 6.65 | 50 | 8.85 | 18.765 | 5.72 |
| 75 | 5.87 | 18.595 | 6.05 | 75 | 6.90 | 18.675 | 5.70 |
| 98 | 3.51 | 18.455 | 6.35 | 104 | 5.14 | 18.595 | 6.17 |
| 147 | 2.48 | 18.480 | 6.01 | 146 | 3.58 | 18.545 | 6.66 |
| 195 | 2 56 | 18.535 | 5.15 | 197 | 2.61 | 18.530 | 5.91 |
| 293 | 2.11 | 18.565 | 4.43 | 300 | 1.80 | 18.530 | 4.76 |
| 391 | 2.32 | 18.655 | 3.45 | 401 | 2.42 | 18.625 | 3.82 |
| 488 | 2.82 | 18.740 | 2.33 | 501 | 2.73 | 18.705 | 2.73 |
| 586 | 2.99 | 18.805 | 1.73 | 600 | 2.87 | 18.760 | 1.85 |
| 782 | 3.06 | 18.925 | 0.92 | 796 | 3.11 | 18.885 | 1.01* |
| 980 | 2.92 | 18.995 | 0.96 | 994 | 2.98 | 18.955 | 1.05 |
| 1178 | 2.66 | 19.050 | 0.90 | 1189 | 2.76 | 19.025 | 0.84 |
| 1416 | 2.44 | 19.070 | 0.98 | 1524 | 2.40 | 19.080 | 0.95 |
| 1902 | 2.05 | 19.125 | 1.46 | 2050 | 2.05 | 19.130 | 1.43 |
| 2394 | 1.78 | 19.175 | 2.17 | 2583 | 1.77 | 19.160 | 2.16 |
| 2788 | 1.62 | 19.180 | 2.60 | 2902 | 1.64 | 19.175 | 2.57 |
| | | | | 3125 | 1.60 | 19.180 | 2.64 |
| | | | | 3400 | 1.52 | 19.190 | 2.94 |
| | | | | 3800 | 1.50 | 19.195 | 2.96 |

| St. JEDS-2-$C_3$ Sept. 24 1959 42°08′N, 148°42′E | | | | St. JEDS-2-$C_4$ Sept. 24 1959 41°34′N, 149°24′E | | | | St. JEDS-2-$C_5$ Sept. 25 1959 41°05′N, 150°04′E | | | |
|---|---|---|---|---|---|---|---|---|---|---|---|
| Depth (m) | T (°C) | Cl (‰) | $O_2$ (ml/l) | Depth (m) | T (°C) | Cl (‰) | $O_2$ (ml/l) | Depth (m) | T (°C) | Cl (‰) | $O_2$ (ml/l) |
| 0 | 14.9 | 18.260 | 6.07 | 0 | 14.8 | 18.085 | 6.06 | 0 | 16.7 | 18.315 | 5.52 |
| 10 | 14.24 | 18.215 | 6.18 | 10 | 14.74 | 18.090 | 6.00 | 11 | 16.73 | 18.335 | 5.60 |
| 20 | 12.86 | 18.140 | 6.47 | 20 | 14.28 | 18.085 | 6.11 | 21 | 16.68 | 18.375 | 5.58 |
| 30 | 7.41 | 18.245 | 6.91 | 30 | 5.89 | 18.275 | 7.50 | 31 | 15.08 | 18.470 | 5.93 |
| 50 | 3.74 | 18.325 | 6.73 | 50 | 2.48 | 18.325 | 7.42 | 50 | 7.26 | 18.655 | 6.30 |
| 75 | 2.51 | 18.160* | 6.16 | 75 | 1.41 | 18.350 | 6.99 | 74 | 6.62 | 18.705 | 6.02 |
| 100 | 1.98 | 18.445 | 5.77 | 120 | 1.46 | 18.425 | 6.15 | 92 | 5.89 | 18.670 | 5.99 |
| 150 | 1.91 | 18.475 | 5.12 | 180 | 2.05 | 18.575 | 4.30 | 138 | 5.08 | 18.650 | 5.59 |
| 200 | 1.69 | 18.520 | 4.89 | 240 | 2.52 | 18.660 | 2.84 | 184 | 3.61 | 18.640 | 4.74 |
| 300 | 2.00 | 18.610 | 3.78 | 360 | 3.04 | 18.805 | 1.22 | 262 | 3.60 | 18.710 | 3.39 |
| 400 | 2.14 | 18.705 | 2.96 | 480 | 3.02 | 18.880 | 1.09 | 340 | 3.78 | 18.790 | 2.29 |
| 500 | 2.79 | 18.825 | 1.63 | 600 | 3.09 | 18.940 | 0.95 | 418 | 3.63 | 18.850 | 1.72 |
| 600 | 2.82 | 18.870 | 1.25 | 720 | 2.99 | 19 000 | 0.88 | 496 | 3.49 | 18.910 | 1.21 |
| 800 | 2.94 | 18.965 | 0 92 | 960 | 2.62 | 19.055 | 0.88 | 649 | 3.15 | 18.960 | 0.91 |
| 1010 | 2.81 | 19.015 | 0.97 | 1200 | 2.31 | 19.090 | 0.99 | 829 | 2.92 | 19.010 | 0.86 |
| 1220 | 2.52 | 19.060 | 0.89 | 1295 | 2.25 | 19.100 | 1.14 | 1007 | 2.67 | 19.055 | 0.88 |
| 1555 | 2.22 | 19.105 | 1.18 | 1623 | 2.14 | 19.135 | 1.30 | 1120 | 2.52 | 19.080 | — |
| 2049 | 1.93 | 19.155 | 1.71 | 2171 | 1.80 | 19.165 | 1.97 | 1656 | 2.08 | 19.150 | 1.40 |
| 2546 | 1.72 | 19.165 | 2.37 | 2720 | 1.60 | 19.185 | 2.60 | 2219 | 1.76 | 19.175 | 1.90 |
| 3359 | 1.52 | 19.180 | 3.00 | 2907 | 1.55 | 19.175* | 2.73 | 2796 | 1.59 | 19.185 | 2.52 |
| 3858 | 1.50 | 19.195 | 3.26 | 3407 | 1.49 | 19.195 | 3.07 | 3384 | 1.48 | 19.190 | 3.18 |
| | | | | 3907 | 1.45 | 19.195 | 3.34 | | | | |

and the other across the southern part of the Kurile Trench in the second Japanese Expedition of Deep Sea (JEDS-2, September 1959). However, owing to an accident of the tapered wire, the former section could not be completed as previously arranged. Furthermore, although the hydrographic cast was intended to be performed from the surface to the bottom with remodeled Nansen bottles so as to be attached to the tapered wire and released without the messenger, remodeled Nansen bottles did not work as designed. Therefore, the hydrographic cast was obliged to be limited to 4000 m depth from the sea surface.

To the southeast of Kunashiri-to Island, a hydrographic section (Section C) was set up across the Kurile Trench, along which five serial stations were occupied in 40 to 50 nautical miles interval (Fig. 1). The salinity was determined particularly more accurately than usual so as to calculate dynamic depth anomalies exactly in deep depths (Table 1).

## 2. *Results*

### (1) *Temperature*

The vertical distribution of temperature shows some typical features in

the subartic region. Namely, the minimum temperature lower than 2°C is found at depths between 50 m and 300 m and the intermediate warmer layer exists between the subsurface coldest layer and the deep cold water (Fig. 2a). In the deep water below 1000 m depth, the temperature decreases with depth, being about 1.5°C at 4000 m depth and it is highest at St. $C_2$ near the center of the trench, to the south-east of which is becomes lower in all deep depths.

(2) *Chlorinity*

The chlorinity decreases with depth from the sea surface at Stations $C_3$ and $C_4$, where there exists the lowest temperature (<1.5°C) in the subsurface layer. At other stations, on the contrary, rather higher chlorinity is found in the surface layer immediately below the surface. The chlorinity distribu-

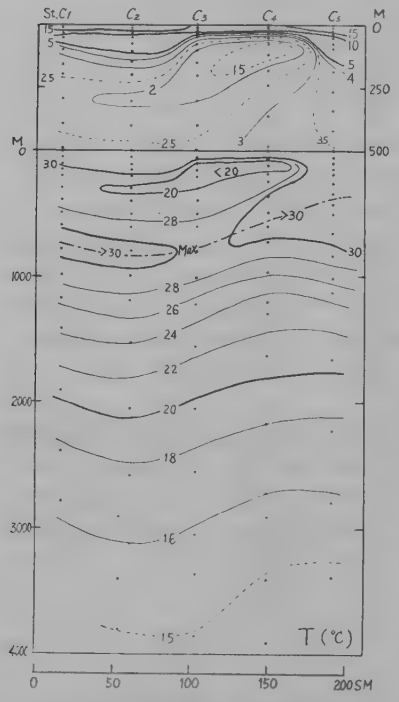


Fig. 2 (a). Section of temperature.

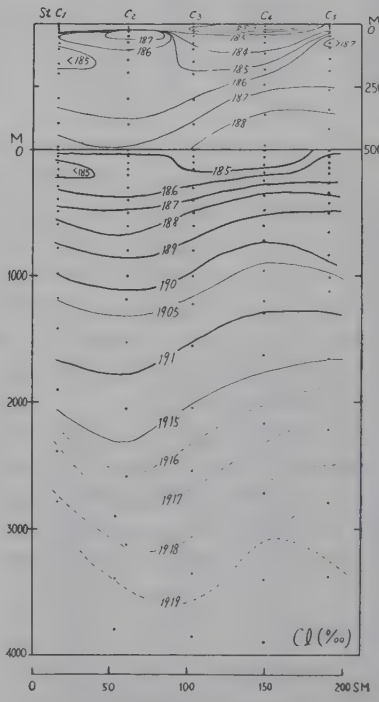


(b). Section of chlorinity.

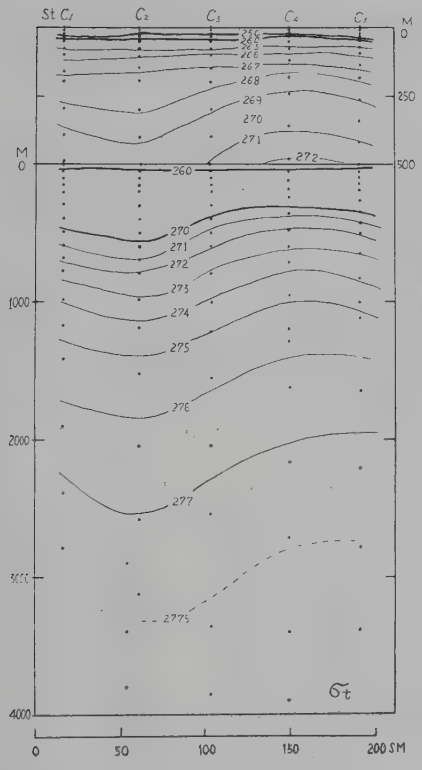


Fig. 2 (c). Section of $\sigma_t$.

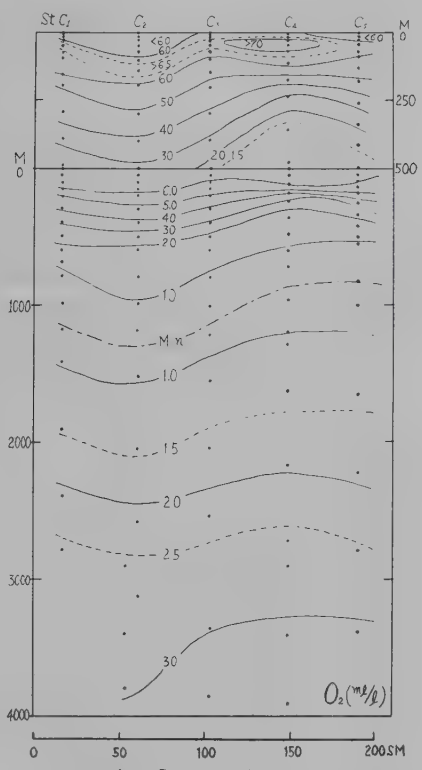


(d). Section of oxygen.

tion in the deep depths below 1000 m is similar to the temperature distribution.

(3) *Density* ($\sigma_t$)

In all depths between 200 m and 4000 m, the density at St. $C_2$ is the lowest and the one St. $C_4$ or $C_5$ is the highest. In other words, isosteric lines higher than $\sigma_t$=27.0 are almost parallel to the bottom topography across the trench.

(4) *Oxygen*

The distribution of oxygen has a feature similar to ones of temperature and salinity etc. For example, the center of oxygen-poor layer at St. $C_4$ or $C_5$ is by four or five hundred meters more shallow than the one at St. $C_2$. In the deepest depths below 2500 m, however, the horizontal gradient of oxygen

is very small, being almost constant at each level. This implies that the oxygen-poor layer is thinner at St. $C_2$, at the center of trench, than at St. $C_4$ or $C_5$, at the outer side of trench. The significance of this fact has not been clarified yet.

(5) *Geostrophic velocity*

Unfortunately, we could not measure directly current velocities to which are referred in the dymical calculation, because the neutral-buoy apparatus was not ready for this expedition. Therefore, the dynamical calculation was forced to be referred to some assumed motionless layers, for example the oxygen-minimum layer or the 3000 m depth (Table 2).

Table 2. Geostrophic current-velocity (cm/sec) in the Section C, referred to the oxygen-minimum depth (A) and 3000 db depth (B), respectively. Positive: northeastward.

| | A | | | | B | | | |
|---|---|---|---|---|---|---|---|---|
| Sec. / Dep. | $C_1$-$C_2$ | $C_2$-$C_3$ | $C_3$-$C_4$ | $C_4$-$C_5$ | $C_1$-$C_2$ | $C_2$-$C_3$ | $C_3$-$C_4$ | $C_4$-$C_5$ |
| 0 | 4.4 | −15.6 | −9.4 | 7.4 | 9.6 | −23.5 | −17.1 | 5.6 |
| 10 | 4.6 | −15.5 | −9.7 | 7.3 | 9.8 | −23.4 | −17.4 | 5.5 |
| 20 | 4.9 | −15.2 | −10.0 | 7.2 | 10.1 | −23.1 | −17.8 | 5.4 |
| 30 | 5.7 | −14.9 | −10.1 | 6.2 | 10.9 | −22.8 | −17.8 | 4.4 |
| 50 | 7.1 | −14.8 | −9.7 | 4.3 | 12.3 | −22.7 | −17.4 | 2.5 |
| 75 | 7.1 | −15.1 | −9.0 | 4.2 | 12.3 | −23.0 | −16.8 | 2.4 |
| 100 | 6.9 | −15.3 | −8.6 | 4.1 | 12.1 | −23.2 | −16.3 | 2.3 |
| 150 | 6.6 | −14.9 | −8.5 | 3.8 | 11.8 | −22.8 | −16.2 | 2.0 |
| 200 | 6.6 | −14.6 | −8.1 | 3.3 | 11.8 | −22.6 | −15.8 | 1.5 |
| 300 | 6.4 | −13.8 | −6.9 | 2.4 | 11.6 | −21.7 | −14.6 | 0.6 |
| 400 | 5.9 | −12.3 | −5.7 | 1.4 | 11.1 | −20.3 | −13.4 | −0.4 |
| 500 | 5.2 | −10.4 | −4.8 | 0.2 | 10.4 | −18.4 | −12.5 | −1.6 |
| 600 | 4.5 | −8.4 | −4.0 | 0.7 | 9.7 | −16.4 | −11.7 | −1.1 |
| 800 | 3.0 | −4.8 | −2.1 | 0 | 8.2 | −12.7 | −9.8 | −1.8 |
| 1000 | 1.4 | −2.0 | 0 | −0.7 | 6.6 | −9.9 | −7.7 | −2.6 |
| 1200 | 0 | 0 | 1.9 | −1.1 | 5.2 | −7.9 | −5.8 | −2.9 |
| 1500 | −1.1 | 2.1 | 3.9 | −0.8 | 4.1 | −5.8 | −3.8 | −2.6 |
| 2000 | −2.1 | 5.2 | 5.3 | 0.7 | 3.1 | −2.7 | −2.4 | −1.1 |
| 2500 | −3.9 | 7.4 | 6.4 | 1.6 | 1.3 | −0.5 | −1.3 | −0.2 |
| 3000 | −5.2 | 7.9 | 7.7 | 1.8 | 0 | 0 | 0 | 0 |
| 3500 | | 7.8 | 8.8 | 1.6 | — | −0.1 | 1.1 | −1.2 |

In the upper layer, northeastward currents are found at Section $C_1$—$C_2$ and $C_4$—$C_5$, while there exists southwestward currents at Section $C_2$—$C_4$ correspondent to the eastern slope of the trench. On the contrary, in the deeper layer current directions are inverse in two cases when the motionless layer is assumed to be the oxygen-minimum layer or the 3000 m depth. H. Stommel (1958) anticipates that there will be a southwestward current in the deep

layer in this area. If it is true, the current at section $C_2$—$C_4$ will be southwestward in all depths from the sea surface to the deep depths. This will be discussed in details in another place by MASUZAWA (1960).

*Acknowledgement*: These authors wish to express their thanks to Messrs. T. SAWARA, T. NAKAI, S. HASEGAWA, H. YOSHIMURA and M. HANZAWA for their assistances for the preparation of this manuscript.

*Reference*

MASUZAWA, J. (1960): Western boundary cnrrents and vertical motions in the Subarctic North Pacific Ocean. (to be published on *Jour. Oceanogr. Soc. Japan.*)

STOMMEL, H. (1958): The circulation of the abyss. *Scientific American*. July 1958.

The Oceanographical Magazine
Vol. 11. No. 2, March 1959

# A Note on the Ball Breaker and the Ball*

By

Yositada TAKENOUTI
*Meteorological Research Institute*
Masashi YASUI
*Iapan Meteorological Agency*

## 1. *Introduction*

A ball breaker and a glass ball as a device to ascertain the attainment of an instrument to the bottom in an oceanographic observation had been improved and reported by J. ISAACS and A.E. MAXWELL (1952). ZOBELL (1954) had also studied about a glass ball immersed in deep water and a sound of clashing a ball. The present authors have also constructed a several ball breakers and found some problems which are not clear yet in order to design a ball breaker and a glass ball. This is a short note to report the results of some experiments they had made. One of the ball breakers, which is used in the present studies is illustrated in (Fig. 1). A glass ball, thickness of the shell is some milimeters, is tied to the breaker. A working weight of several kilograms is dropped at the moment when the pilot weight reaches the bottom, and a point on the weight collides the glass ball and clashes the ball.

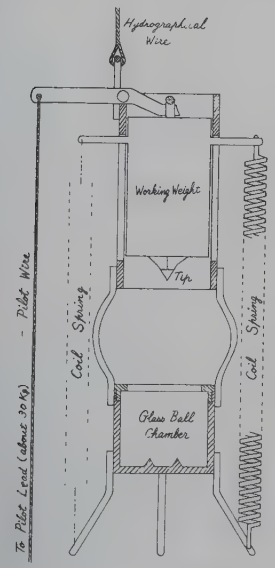


Fig. 1. Schema of the JMA-type ball-breaker.

## 2. *Thickness of glass ball*

A glass ball made of soda-calcium glass of density 2.3 gr/cm$^3$, with a diameter of about 65 mm was used for the present studies. A ball is anneald for 12 hours in ash after it is moulded. One trouble the authors had met during the experiments is, sometimes a glass ball is not completely sealed and has a very small, almost invisible, hole. A ball with a hole is, of

* JEDS Contribution No 3.

course, not useful. And also, the shell of ball is very thin; it may be sometimes clashed with static pressure. The authors made a test for these obstacles.

A glass ball is put in a cylinder and hydrostatic pressure is applied with a pump till the ball is clashed. The clashing is noticeable by a clear sound through the wall of the cylinder. The relation between the weight of ball and the depth at which it is clashed is shown in (Fig. 2). Between the

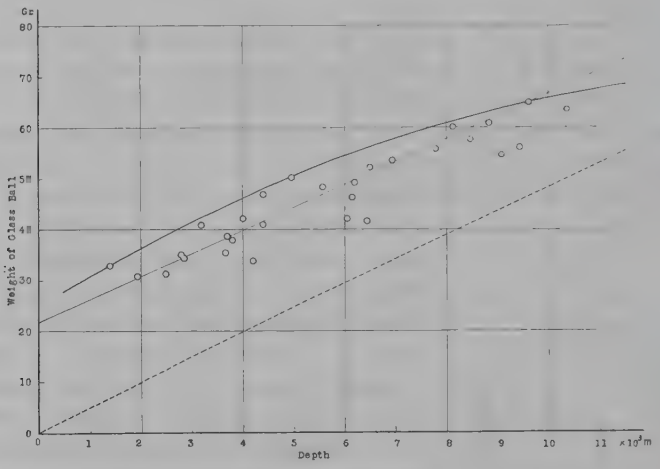


Fig. 2. Reration between the weight of glass ball and the depth at which it is naturally clashed.
Dashed line: From the theoretical formula.
Thin full line: From the same formula taking the thickness of ball 0.7 mm less than mean.
Thick full line: Reration between the weight of ball and the depth to which the ball is probably submerged without collapse.

pressure and the outer diameter $R$, the thickness of spherical shell, we have the following relation from the theory of strength of materials;

$$D=RT/2T_c$$

where $Tc$ is the tensile strength of material constructing the ball. Put $Tc=10^7 g/cm^2$, $R=3.25cm$ we have a linear relation between $P$ and the weight

of ball computed with $D$ as shown with a dashed line in the figure. There is an appreciable discrepancy between the experimental and computed relations. The thickness of shell may not be uniform and the ball may be clashed from the most thin part of the shell. Three balls having weights of 48, 77 and 101 grams are destroyed in pieces and the thickness of shell are measured. It was found that the most thin part is 0.6 to 0.8 mm thinner than the mean thickness. Taking the thickness in the above formula 0.7 mm less than mean, we have a relation shown with a thin full line in the figure, it shows fairly good agreement with the experiments. The thick full line in figure is drawn in connecting the points showing the largest weight for each depth. It illustrates the limit to that depth; a glass ball stands to the hydrostatic pressure, considering the effect of irregularities in heat treatment, shape, thickness of shell etc. The figure shows even in the deepest bottom of the ocean, a glass ball having the weight of 65 grams (the thickness is ca. 2mm) is good for the ball breaker.

The authors had also made some experiments aboard the R/V Ryōfū Maru. Three different types of ball breakers were tested. One series of experiments is to test the working of ball breakers of different types at the same depth and with a ball of almost same weight; and the other is to study the effect of weight of the ball for the same ball breaker at the same depth. The results of experiments are able to classify in three categories as regards to the breaking of the ball:

(a) A glass ball does not break, sometimes the needle of working weight is penetrated the wall with small hole.
(b) A glass ball is destroyed into a few pieces.
(c) A glass ball is clashed into fine powder.

The sound is only clearly audible for (c), therefore, the combination of ball breaker and ball should be chosen as the ball is clashed as (c). When a glass ball is under high pressure and is struck with a working weight with a small momentum or with a sharp needle, the results are generally (a). While, when a glass ball of thick shell is under moderate pressure and is struck with a working weight with a large momentum, the result is generally (b). Therefore in order that a ball breaker and a ball work satisfactory the thickness of the shell must be in a definite range according to the design of the ball breaker.

Fig. 3 illustrates the results of these experiments. In the figure a solid mark is showing the lightest ball which does not make sound and a blank

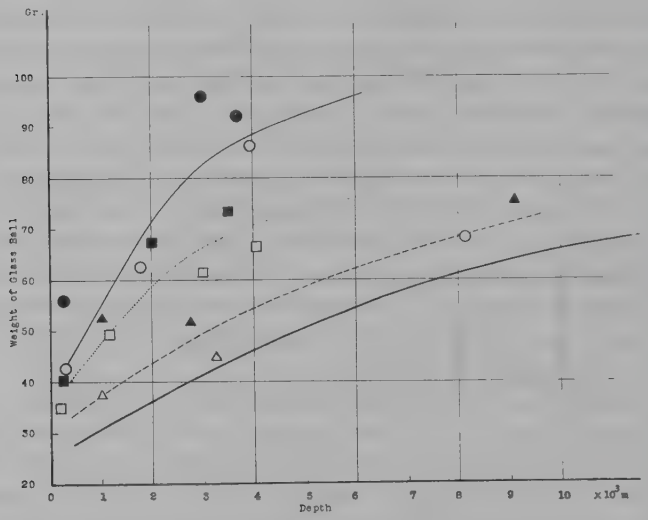


Fig. 3. Illustration of effect of ball-breakers of several types for the weight of glass balls.

| | |
|---|---|
| ○ J.M.A.-type | Solid; not make sound |
| □ Kawamoto's M-type | |
| △ Original type of Issacs & Maxwell | Blank; make sound |

mark is showing the heaviest ball which makes clear sound at the same depth for the respective breakers. The boundaries between the solid and blank marks are drawn in the figure. The curves are, therefore, showing the most thick glass ball which may make clear sound. We can see from the figure that the ball breaker of JMA type works satisfactory for the most wide range of the weight among them, which is designed to have a large momentum to strike the ball. The curve is seemed to be consisted of two straight lines crossing at the depth of about 3,000 meters. ISAACS and MAXWELL (1952) had also already reported that the effect of pressure upon a glass ball was different above and below 300 kg/cm². The results of present experiments accord with their results. As it is mentioned in the following para-

graph, the authors have found that the character of sound emitted from the clashing ball changed at the depth of about 3,000 meters. This seems to support the above consideration.

### 3. *Sound emitted from a ball clashed in deep water*

The authors have made some studies on the sound of clashing ball in deep water aboard the R/V Ryōfū Maru in occasion of the Japanese Expedition for Deep Sea I and II, 1959. The sound was recorded on a magnetic tape and it was played back in the laboratory for further studies.

Fig. 4 is showing examples of pictures of sound wave from clashing

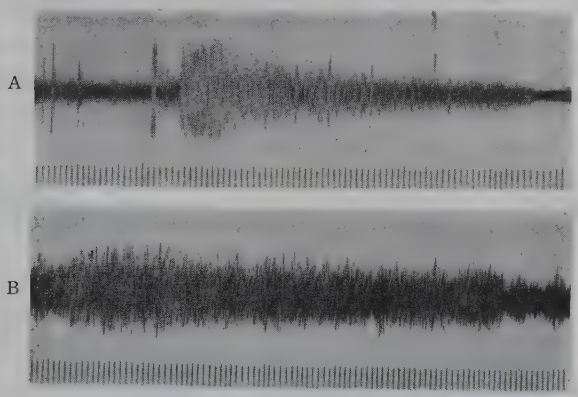


Fig. 4. Illustrating the pictures of sound wave from the ball clased under deep water. Interval of time mark is 0.005 sec.
A: The ball is clashed at 4,000 m, the weight of ball is 69.5 g.
B: The ball is clashed at 2,400 m, the weight of ball is 64.0 g.

balls at the depth of 2,400 and 4,000 m. It is noticeable from the figure that the sound is quite different in character between them. At 4,000 m, at the beginning of the sound it has very short duration and then there is a pause and next a sound of long duration follows. From the interval between the two sounds and the depth of the hydrophone it is concluded that the second one is an reflected at the surface and the initial sound of short duration is

the clashing sound of the ball. But at 2,400 meters, the clashing sound of the short duration is not found.

In Table 1, the results of the experiments are summarized, and it is noticeable from the table that the sound has the short duration for the ball clashed at great depth (3,850, 4,000 and 8,000 m) and not for the ball clashed at shallow depth (from 500 to 2,400 m). The boundary between the two types of sound seems to be at about 3,000 meters. Considering the results of ISAACS and MAXWELL (1952) as well as our experiments mentioned in the preceeding paragraph, this difference may come from the change of mechanical properties of glass at the depth of 3,000 meters.

Table 1. Results of the experiments aboard the R/V Ryōfū Maru. July and September, 1959.

| Weight of Ball | Depth at Ball Clashed | Depth to the Bottom | Type of Sound | Remarks |
|---|---|---|---|---|
| 30.0 g | 500 m | 8,600 m | One long sound | |
| 31.0 | 2,000 | 8,600 | do | |
| 41.0 | 2,300 | 8,780 | do | Clashed by pressure |
| 60.5 | 8,000 | 8,005 | Click and echo | |
| 64.0 | 2,400 | 7,300 | One long sound | |
| 68.5 | 3,850 | 5,625 | Click and echo | |
| 69.5 | 4,000 | 8,300 | Click and echo | |

Table 2. Energy of the sound.

| Depth at Ball Clashed (m) | 3,850 | 4,000 | 8,000 |
|---|---|---|---|
| Noise Level (volt) | 32 | 29 | 36 |
| Signal-Noise Ratio (db) | 13 | 12 | 10 |
| Sound Pressure of Signal (db) | 43 | 41 | 41 |
| ($\mu$bar) | 140 | 110 | 110 |
| Total Attenuation (db) | 79 | 80 | 94 |
| Sound Pressure at 1 m from the Source (db) | 122 | 121 | 135 |
| (bar) | 1.2 | 1.1 | 5.6 |
| Energy of Sound ($10^9$ erg) | 0.3 | 0.5 | 2.7 |
| Total Energy of Ball ($10^9$ erg) | 13.9 | 14.4 | 32.0 |
| Ratio of Energy (%) | 2 | 3 | 8 |

The signal-noise ratio for the clashing sound can be estimated from the record, they are shown in Table 2. The S-N ratio is smaller than that of

Isaacs and Maxwell (1952), and due to the R/V Ryōfū Maru it is more noisy than the ship where they had made the experiments. The hydrophone has a sensitivity of 110 decibels. As the noise level was measured during recording the sound, we can roughly estimate the sound pressure at the surface, as in the table. Estimating an attenuation due to absorption be 2 decibels per kilometer, the total attenuation are estimated as shown in the table, then we have a rough value of sound pressure at 1 meter from the ball. The duration of the sound is estimated from the picture of sound wave, thus we can estimate the total sound energy by the formula $E=4\pi r^2(P^2/\rho_0 c)\Delta t$, where $P$ is the sound pressure, $c$ the sound velocity in sea water, $\rho_0$ the density of sea water, $\Delta t$ the duration of sound and $r$ is the distance between the source and the point of measurement. As we are now trying to make rough estimate, we put $\rho_0=1$, $c=1.5\times10^5$, and the value of $E$ is shown in the table.

A ball under the pressure of $P$ has an energy of $(4\pi/3)Pa^3$, the total energy of ball in deep water is calculated by the above formula and is shown in the table. From the table we can see among the total energy of ball a few per cent is converted into the sound energy when it is clashed in water. The efficiency is not so good, but as the total energy is very great, the sound

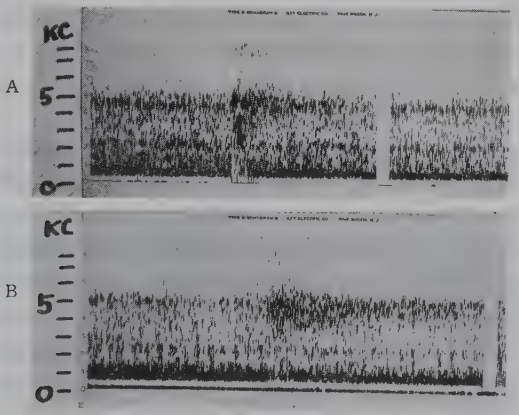


Fig. 5. Illustrating the records of frequency analyser.
A: The ball is clashed at 8,000 m, the weight of ball is 60.5 g.
B: The ball is clashed at 2,400 m, the weight of ball is 64.0 g.

energy also becomes very large.

The frequency of the sound is also measured with a frequency analyser; some example of the results are illustrated in (Fig. 5). Owing to the deffi-ciency of instruments, the results of analysis are not satisfactory, but we can make following conclusions. In the figure, we find that the sound from the ball at 2,400 m has a remarkable band at the frequency of 4 to 5 kilo-cycles per second, and at 8,000 m, the frequency band is higher than 7 kc/sec.

An air buble having a radius of $a$ cm has a characteristic frequency of $f_0=1/2\pi a\sqrt{3\gamma/\rho_1}$, where $\gamma$ is $Cp/Cv$, $P$ the pressure and $\rho_1$ is the density of water. Two types of oscillation of air buble are assumed;

Case (1) : at the moment a ball is clashed, the air in the glass ball vi-brate, so the diameter of vibrating air buble is $R_1$. Case (2) : the air in a glass is at first compressed and then vibrates, so the diameter of vibrating air buble is $R_1(P_0/P)1/2$, where $P_0$ is the air pressure in the ball and $R_1$ is the inner radius of the ball.

Put $\gamma=1.4$ and $P_0=1$ bar, we get the following value for $f_0$.

| Depth of ball | Case (1) | Case (2) |
|---|---|---|
| 2,400 m | 1.4 kc/sec | 5.0 kc/sec |
| 8,000 | 7.1 | 20.0 |

Comparing the results with the experiment, the frequency for case (1) is too small, so to estimate the frequency of sound, the radius of air buble should be considered that the air in the ball is compressed by the water pres-sure when it vibrate.

*Acknowledgement*: The authors wish to express best thanks to Mr. Shin KUWABARA, the Director of the Marine Electric Instrument Co., Ltd., for his kind cooperation to the present studies and also to Mr. H. NITANI of the Hy-drographic Office, Mr. H. AKAMATSU and the other members of the Oceano-graphical Section, J.M.A. for their kind assistance for the experiments aboard the ship. They also indebted to Mr. A. WATANABE of the Meteorological Re-search Institute who constructed the instruments in the laboratory.

*References*

ISAACS, J. D. and A. E. MAXWELL (1952): The ball-breaker, a deep water bottom signal-ing device. *J. Mar. Res.*, **11**, 1952.

ZOBELL, C. E (1954): Some effects of high hydrostatic pressure on apparatus observed on the Danish Galathea Deep-Sea Expedition. *Deep-Sea Research*, **2**, 1954.

The Oceanographical Magazine
Vol. 11. No. 2, March 1960

# Chemistry in the Japanese Expedition of Deep Sea (JEDS-2)*

By

Yasuo Miyake, Hiroshi Hamaguchi, Masumi Osawa and Naoki Onuma
*Tokyo University of Education*

Ken Sugawara, Satoru Kanamori and Sadayuki Omori
*Nagoya University*

Toshio Shimada and Kiyoshi Kawamura
*Meteorological Research Institute*

Hirozo Yoshimura
*Meteorological Agency*

Takeshi Sagi
*Kobe Marine Observatory*

## General Observation

Chlorinity, dissolved oxygen, silicate-Si, phosphate-P and total P were determined by the collaboration of Oceanographic Section of the Meteorological Agency, Nagoya University, Tokyo University of Education and Kobe Marine Observatory.

For chemical analysis the following methods were used.

Chlorinity was determined by Mohr-Knudsen method where as indicator a mixed solution of 5 ml of 0.1% uranine solution and 100 ml of 1% starch solution was used.

Dissolved oxygen was determined by Winkler method.

Silicate-Si was determined by Diénert-Wandenbulcke method where the standard solution was prepared with $Na_2SiF_6$. Measurement was made by using a photometer with a filter.

Phosphate-P was determined by Denigès-Atkins method. The measurement was made aboard by using a photometer with a filter. The used solution of stannous chloride dissolved into 2.4 N hydrochloric acid had previously been sealed in an ampoule.

* JEDS Contribution No. 4.

Total P: Unfiltered samples were subjected to the method of Hansen-Robinson. The absorbancy measurement was made by using a photometer with a filter.

The preliminary report of the results is as follows.

From the analysis of the T-Cl diagrams, the following facts were found along C-line.

(1) Oyashio water with the maximum temperature 15°C at the surface was found to contribute greatly to form the surface layers water mass with the greatest contribution at the depth of 100 m (1.5-3.0° C, 18.5 Cl‰). Oxygen maximun existed in 30-50 m layers.

(2) Beneath these surface layers and above the deep water of the North Pacific, intermediate layers of warmer water were present. (at the center, 2.8-3.8°C, 18.8-18.9 Cl‰.) where an oxygen and pH minimum were observed.

(3) Apart from this general distribution above, the 30-50 m surface layers at station $C_2$ were found to be constituted of Oyashio water which was considerably diluted with the warmer water. The 50-400 m layers at station $C_5$ were also found to have been affected by the warmer water.

(4) These circumstances reflected on the vertical distribution of other chemical elements. Thus, at sation $C_2$ the isometric lines for smaller phosphate-P and silicate-Si were found to bend downward while at station $C_5$ phosphate-P value was found in surface layers.

(5) The comparions of these results with those recently obtained by the Russian ship, Vityaz' is of interest. Both observations are in accordance at the point that the phosphate maximum lies in the layers of 500-1200 m with 3.2 $\mu$g-atoms/l, the very depth where dissolved oxygen reaches minimum. The silicate-Si maximum is at the depth of 1400-2000 m with 145-155 $\mu$g-atoms/l. In addition, the phosphate and silicate values in deeper layers tend respectively to 2.7-2.8 $\mu$g-atoms P/l and 135-145 $\mu$g-atoms Si/l.

However, as to the surface layers our results did not always agree with the Russian results. Our values were usually 50-70% of the Russian values. The difference may have been at least partly caused by that the time of observations was different.

The detail of the result will be reported later.

## Special Investigations

### *1. Arsenic**.

The present investigation was initiated: To determine arsenic separately in two different states, arsenite and arsenate. To determine the distribution of arsenic between suspended particulate and water. To determine the vertical distribution of two different states of arsenic to know whether there exists any regularity about the distribution and to make clear what factors are effective on such a distribution.

The used method of arsenic analysis was established by the investigators, the detail of which will be published soon.

The result so far obtained shows that portion less than 10% of total arsenic is associated with particulate and filtered off by Millipore Filter when the sample water is filtered immediately after the sample collected. The ratio of arsenite to arsenate is variable from one sample to another. The detail of the results and dsicussion will be published later. Here is only referred to the result from the previous test operations (Table 1).

Table 1

| Station | Date | Time | Location | | Temp. (°C) | pH | Cl(‰) |
|---|---|---|---|---|---|---|---|
| 1 | June 25, 1959 | 08.00 | 33°12.0′N | 139°53.0′E | 22.0 | 8.30 | 19.24 |
| 2 | 〃 | 12.00 | 32°42.5′N | 140°17.2′E | 21.9 | 8.16 | 19.19 |
| 3 | 〃 | 16.00 | 32°17.0′N | 140°46.0′E | 22.0 | 8.26 | 19.17 |
| 4 | 〃 | 20.00 | 31°51.0′N | 141°15.0′E | 22.0 | 8.24 | 19.37 |
| 5 | 27 | 12.00 | 30°11.0′N | 142°16.5′E | 22.6 | 8.25 | 19.05 |
| 6 | 〃 | 16.00 | 30°29.9′N | 142°29.0′E | 22.8 | 8.25 | 19.06 |

| Station | Date | Phosphate-P (μg-atoms/l) | Silicate-Si (μg-atoms/l) | $As^{V}$ (μg/l) | $As^{III}$ (μg/l) | $As^{V}+As^{III}$ (μg/l) | $As^{III}/As^{V}$ |
|---|---|---|---|---|---|---|---|
| 1 | June 25, 1959 | 0.18 | 8.2 | 1.0 | 0.5 | 1.5 | 0.5 |
| 2 | 〃 | 0.17 | 9.2 | 1.2 | 0.2 | 1.4 | 0.2 |
| 3 | 〃 | 0.15 | 8.7 | 1.1 | 0.3 | 1.4 | 0.3 |
| 4 | 〃 | 0.15 | 8.1 | 0.7 | 0.8 | 1.5 | 1.1 |
| 5 | 27 | 0.02 | 10.7 | 1.0 | 0.2 | 1.2 | 0.2 |
| 6 | 〃 | 0.10 | 7.0 | 1.1 | 0.3 | 1.4 | 0.3 |

* By Ken SUGAWARA and Satoru KANAMORI; Chemical Institute, Faculty of Science, Nagoya University.

*2. Rare earth elements**

A study of neutron activation analysis of some of the rare earth elements is being undertaken in our laboratory. Most recent abundance values of rare earth elements in geologic materials of marine environment are the following:

in sea water (mg/l) : Y 0.0003, La 0.0003, Ce 0.0004
(GOLDBERG, 1957)

in sediments (%) : Y 0.015, La 0.014, Yb 0.0021
(GOLDBERG, ARRHENIUS, 1958)

The purpose of the present study is to give check on the previous data and offer the reliable figure for the rare earths content of oceanic water, thus making a contribution to oceanic geochemistry.

When determining trace amounts of rare earths by neutrn activation analysis, it is possible to avoid various difficulties encountered with other methods, as the nuclear properties of these elements are rather favourable.

It has already been found by us that among the rare earth elements, lanthanum, samarium and europium were determinable simultaneously by counting and tracing the decay of the activity of neutron irradiated natural mixture of rare earth elements. Therefore, we made a program as follows:

(1) Collect the rare earth elements in sea water on iron hydroxide precipitate.

(2) Irradiate the iron hydroxide sample with neutrons in JRR-I reactor.

(3) After irradiation, isolate the rare earth mixture in radiochemically pure state, whereby $La^{+++}$ carrier is used to give chemical yield, and decontamination chemistry is carried out.

(4) Measure the $\gamma$ activity of the isolated sample with $\gamma$-scintillation spectrometer, and determine each element by comparing the activity of the sample with those of the monitor. The specific nuclides used for the determination are:

$^{140}La$ ($T^1/_2$ 40 h., 0.54 Mev) for lanthanum,
$^{153}Sm$ ($T^1/_2$ 47 h., 0.09 Mev) for samarium,
$^{152}Eu$ ($T^1/_2$ 9.3 h., 0.05 Mev**) for europium.

* By H. HAMAGUCHI, M. OSAWA and N ONUMA; Department of Chemistry, Faculty of Science, Tokyo University. of Education

** This is the compound peak of ($^{140}La+^{153}Sm+^{152}Eu$). By analyzing the decay curve at this peak, however, the activity of $^{152}Eu$ can be determined.

### *3. Tritium**

In 1946 LIBBY postulated the production of carbon-14 and tritium by cosmic ray. Natural tritum was detected in water by VON GROSSE.

KAUFMAN and LIBBY and VON BUTTLAR and LIBBY measured the tritium content of a number of sea-water samples. They reported the content from 0.19 to $1.6\times10^{-18}$ T/H during 1953.

BROWN and GRUMMITT reported the tritium concentrations in the range $3.0-4.2\times10^{-18}$ T/H, in the latter half of 1954 and early 1955. Subsurface samples collected at one station near Nova Scotia in mid-1955 showed a T/H value of $32.4\times1.0^{-18}$.

Samples for a study of tritium content of sea-water were collected during this operation. The tritium in 20—50 litre of samples will be concentrated 20,000 to 25,000 times by electrolysis and measured as hydrogen gas in a Geiger counter.

The electrolytic concentration of tritutium is in progress.

* By Y. MIYAKE, T. SHIMADA and K. KAWAMURA; Meteorological Research Institute.

The Oceanographical Magazine
Vol. 11. No. 2, March 1960

# Notes on the Sampling Gears and the Animals Collected on the Second Cruise of the Japanese Expedition of Deep Seas (JEDS-2)*

By

*Biological Section of the Committee of the Japanese Expedition of Deep Seas*

| | |
|---|---|
| Yasuo SUYEHIRO | *University of Tokyo* |
| Yoshiyuki MATSUE | *University of Tokyo* |
| Yaichiro OKADA | *Prefectural University of Miye* |
| Takeharu KUMAGORI | *Tokyo University of Fisheries* |
| Sigene TAKAYAMA | *Tokai Regional Fisheries Research Laboratory* |
| Ryuzo MARUMO | *Japan Meteorological Agency* |
| Osamu ASAOKA | *Japan Meteorological Agency* |
| Makoto ISHINO | *Tokyo University of Fisheries* |
| Eiji IWAI | *University of Tokyo* |
| Yuzo KOMAKI | *University of Tokyo* |
| Masuoki HORIKOSHI | *Ochanomizu University* |

On the second cruise of the Japanese Expedition of the Deep Seas, the benthic and mid-water animals were collected with several gears, a beam trawl, two sorts of dredges and two sorts of plankton nets. The collecting stations were as follows:

St. S Off Onagawa near Sendai City, 37°55′N, 143°25′E, 2,350–2,230 m, rectangular dredge and beam trawl.

St. $A_2$ 40°25′N, 144°36′E, 6,790 m, triangular mid-water plankton net.

St. $A_3$ 40°59′N, 147°26′E, 5,290 m, triangular mid-water plankton net and 130-cm conical net.

St. B Off Kushiro City, 42°40′N, 144°30′E, 490 m, Niino dredge.

St. $C_2$ 42°46′N, 148°10′E, 8,677 m, triangular mid-water plankton net.

The trawl and the dredges were operated by M. ISHINO, E. IWAI and M. HORIKOSHI, and the plankton nets were towed by Y. KOMAKI and O. ASAOKA.

Thanks are due to Dr. J. C. DAN of the Ochanomizu University for her help in preparing the manuscript in English.

* JEDS Contribution No. 5.

*1. Benthic animals**

On this cruise (JEDS-2) two sorts of collecting gear, a beam trawl and a dredge, were employed to collect the benthic animals. They were towed at St. S, which was selected in the vicinity of a Bathyscaph station of the previous summer. Good catches were obtained with both nets. At. St. B, a number of bottom-dwellers were sifted out of muddy sediment taken by a Niino dredge operated by geologists. The details of the towing data are shown in Table 1.

**Beam trawl**: The beam trawl is a modified Agassiz type (Table 2 and Figs. 1 and 2). Two plumbs of 15 kg each were fixed on the tail end to

Table 1. Towing data of the trawl and the dredges.

| Station<br>Location | S<br>37°55′N, 143°25′E | S<br>37°55′N, 143°25′E | B<br>42°40′N, 144°30′E |
|---|---|---|---|
| Sampling gear | Rectangular dredge | Beam trawl | Niino dredge |
| Date | IX 11,1959 | IX 11,1959 | IX 17,1959 |
| Depth | 2,350 m | 2,230 m | 490 m |
| Pay out | 3,153 m | 2,778 m | 945 m |
| Time: | | | |
| Shooting | 08.11 | 15.17 | 08.30 |
| Towing | 10.30 | 17.00 | 09.23 |
| Hauling | 11.00 | 18.00 | — |
| Stop hauling | 13.30 | 19.30 | 10.00 |

Table 2. The details of the beam trawl, refer to Fig. 1.
(Notations are those which are given in Fig. 1.)

| | | |
|---|---|---|
| A | towing wire | steel: diameter 6 mm, length 40 m. |
| B | chain | iron: diameter 6 mm, length 2 m. |
| C | bobbin | iron: diameter 30 cm. |
| D | bridle | steel: diameter 6 mm, length 4 m. |
| E | beam | oak: diameter 10 cm, length 2 m. |
| F | trawl head | iron: height 50 cm, length 80 cm. |
| G | sinker | china. |
| H | man rope | cremona: diameter 7 mm. |
| I | whole net | salan: knotles: ply 300 D2: mesh 45 mm. |
| J | inside net | cotton: ply 20 s/9: mesh 10.5 mm. |
| K | plumb | lead: weight 15 kg. |

* Y. SUYEHIRO, E. IWAI, M. ISHINO and M. HORIKOSHI.

Fig. 1. Beam trawl, refer to Table 1.

Fig. 2. Beam trawl coming to the surface.

prevent entaglement of the trawl bag with the tapered wire, although the Salan (synthesis fiber) net is fairly heavy, its specific gravity being 1.70, and the bag is long enough to settle in the water. A fine meshed inside net set in the bottom of the bag worked very well in bringing aboad numerous smaller forms together with soft sediments. A chain between the bridle and the towing wire works as a weight to settle the trawl mouth on the bottom. The "bobbin" is a hollow iron sphere moving freely on the chain, which fills a double role as a sinker and a means of preventing the chain and a bridle from sinking into a very soft ooze. Although the Salan net was sufficiently strong to raise the weight of a large quantity of sediment, some of the

animals were more or less crushed among the large stones and gravel in the trawl. It would be desirable to devise means for segregating the large solid materials from the organisms.

**Dredge**: The dredge is rectangular type (Fig. 3), about the size of the large Niino dredge, while, it weights a little less (70 *kg*) than the latter

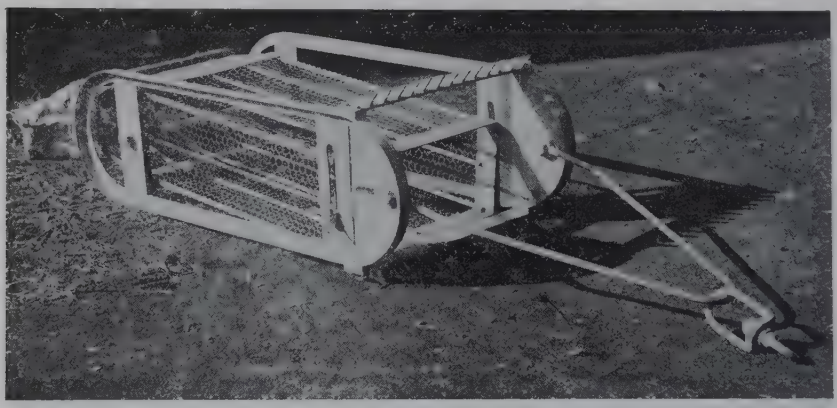

Fig. 3 Large sized rectangular dredge.

(80 *kg*). The dredge consists of two parts: a sledge-shaped outside frame, provided with 13 teeth on each front edge, and an inside frame with wire-netting and a canvas bag. The front part of the inside frame slides up and down, so that its mouth will be settled on the bottom whichever side up the dredge is towed. The mesh of the wire-netting covering the back end of the

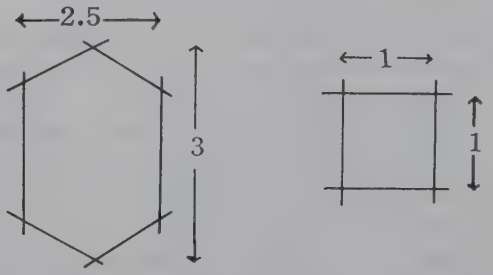


Fig. 4. Meshes of the wire-netting covering the inside frame of the rectangular dredge.

frame is finer than that of the front part, and the shape of the aperture is also different (Fig. 4). It would be convenient to replace the canvas bag with a net when the collection of sediments and minute organisms is not desired.

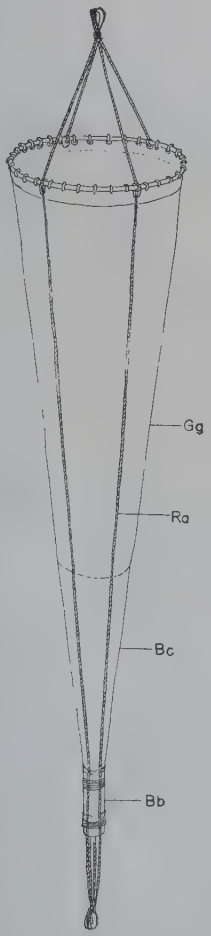


Fig. 5. 130-cm conical net. Abbreviation Bb; bottom backet, Bc; bolting cloth, Gg; grit gauze, Ra; additional rope.

**Animals Collected**: The animals were separated from coarser materials which failed to pass through a 1 mm standard mesh, and were fixed with neutral formation or 70% alcohol. Some interesting forms were photographed or sketched in colour before fixation.

The metazoan animals obtained are classified provisionally into 119 forms, and they amount to 770 in total number. The details of systematical grouping and number of species are shown in Tables 3 and 4. All the materials are awaiting further morphological and taxonomical study by specialists.

At St. S, the largest specimen was a 15 cm asteroid, *Solaster*. A few others were around 10 cm in length, including actiniarians, holothurians, macrurans and pyncnogonids. Besides bottom creepers and burrowers, sedentary forms such as sponges, alcyonarians, polychaets and chitons were also found, some of which were still attached to stones. In thick mud taken at St. B, nemertians were most conspicuous, being large sized and highly coloured.

*2. Mid-water animals**

Deep water plankton collections on this cruise (JEDS-2) were carried out with two sorts of nets. One of them is a conical net, which is known in Japan as "maru-chi" and is generally used for horizontal surface towing by Japanese fisheries survey ships. It has a mouth ring of 130 cm

*R. MARUMO, Y. KOMAKI and O. ASAOKA.

Table 3. Animals collected by the trawl at Station S.
(Off Onagawa: 2,250 m)

| Phylum | Species | Number | Group | Species | Number |
|---|---|---|---|---|---|
| Protozoa | 7 | 1,939 | Foraminifera* | | |
| Rotifera | 13 | 40 | | | |
| Coelenterata | 9 | 37 | Hydrozoa | 2 | 2 |
| | | | Alcyonaria | 2 | 23 |
| | | | Actiniaria | 5 | 12 |
| Annelida | 10 | 26 | Polychaeta | | |
| Mollusca | 32 | 351 | Loricata | 1 | 24 |
| | | | Gastropoda | 19(2)** | 65(3)** |
| | | | Scaphopoda | 2(1)** | 23(1)** |
| | | | Pelecypoda | 9 | 238 |
| | | | Cephalopoda | 1 | 1 |
| Arthropoda | 18 | 67 | Isopoda | 3 | 10 |
| | | | Amphipoda | 5 | 17 |
| | | | Cumacea | 1 | 2 |
| | | | Anomura | 1 | 7 |
| | | | Macrura | 4 | 26 |
| | | | Pantopoda | 4 | 5 |
| Molluscoidea | 3 | 21 | Brachiopoda | 1 | 1 |
| | | | Bryozoa | 2 | 20 |
| Echinodermata | 10 | 161 | Holothurioidea | 4 | 24 |
| | | | Asteroidea | 2 | 2 |
| | | | Ophiuroidea | 4 | 135 |
| Vertebrata | 2 | 3 | Pisces | | |

Total 7 (Protozoa) + 97 (Metazoa) = 104, 1,939 (Prot.) + 706 (Met.) = 2,645

* Minute forms are omitted.

** Additional numerals with asterisks indicate the animals collected by the rectangular dredge at the same locality.

Table 4. Animals collected by Niino dredge at Station B1.
(Off Kushiro: 480 m)

| Phylum | Species | Number | Group | Species | Number |
|---|---|---|---|---|---|
| Porifera | 1 | 2 | | | |
| Annelida | 7 | 18 | Polychaete | | |
| Nemertini | 3 | 8 | | | |
| Mollusoa | 6 | 16 | Aplacophora | 1 | 1 |
| | | | Pelecypoda | 5 | 15 |
| Arthropoda | 4 | 15 | Cumacea | 1 | 1 |
| | | | Amphipodo | 3 | 14 |
| Echinodermata | 1 | 5 | Irreguralia | | |
| Total | 22 | 64 | | | |

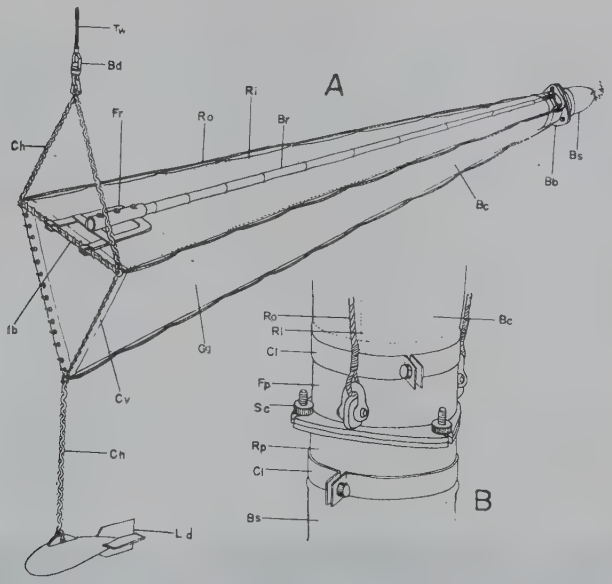


Fig. 6. Triangular mid-water plankton net, A; whole net, B; bottom backet. Abbreviation Bb; bottom backet, Bc; bolting cloth, Bd; bridle, Br; bamboo rod, Bs; bottom sack, Ch; chain, Cl; clip ring, Cv; canvas, Fp; front piece, Gg; grit gauze, Ib; iron bar, Ld; lead, Ri; inner reinforcing rope, Ro; outer reinforcing rope, Rp; rear piece, Sc; screw, Tw: tapered wire.

diameter and a fitering part which is made of rough cotton grit gauze with about 3 mm apertures and fine bolting silk (GG-54) with about 0.3 mm apertures. Since it was planned to use this net making *vertical* hauls, four additiosal ropes bearing lead weights were attached outside the net (Fig. 5).

The other net, a new type with a triangular mouth, the "triangular midwater plankton net" (Fig. 6) was designed and named by Dr. S. Motoda (Hokkaido University). Some alterations from the original size were made for convenience in handling it during the expedition.

To form the triangle of the mouth, a chain 300 cm in length is connected with shackles to eyes at the ends of an iron bar 150 cm in length and 30 mm in sectional diameter, and a fish-shaped 50 kg lead is suspended from the middle of the chain by a second chain. A third chain 300 cm in length is connected by its two ends to the eyes of the iron bar, and a tapered wire is

connected at the middle of the chain to tow the whole net. The filtering part consists of rough and fine nylon nets, the mesh size of each being the same as those of the conical net described above. The length of the whole filtering part is 600 cm. The bottom backet (Fig. 6, B) is made of cast brass and is separable into two parts, front and rear, loosening three screws. At the end of the rear piece, a sack made of GG-54 nylon bolting cloth is clipped by a brass ring. To reinforce the net, ropes are sewn to the net from both inside and outside along its whole length. The filtering part is bound to the front piece of the backet with a brass ring and the ends of three outer reinforcing ropes are also connected to the backet with shackles. A bamboo rod is stretched from the iron bar to the backet to prevent the net from winding around the tapered wire, while descending or ascending in the water. The rod is held at the middle of the iron bar of the mouth by an iron frame. In the hope of avoiding contamination with shallower plankton during the descent and ascent, the mouth of the net is kept vertical by means of the

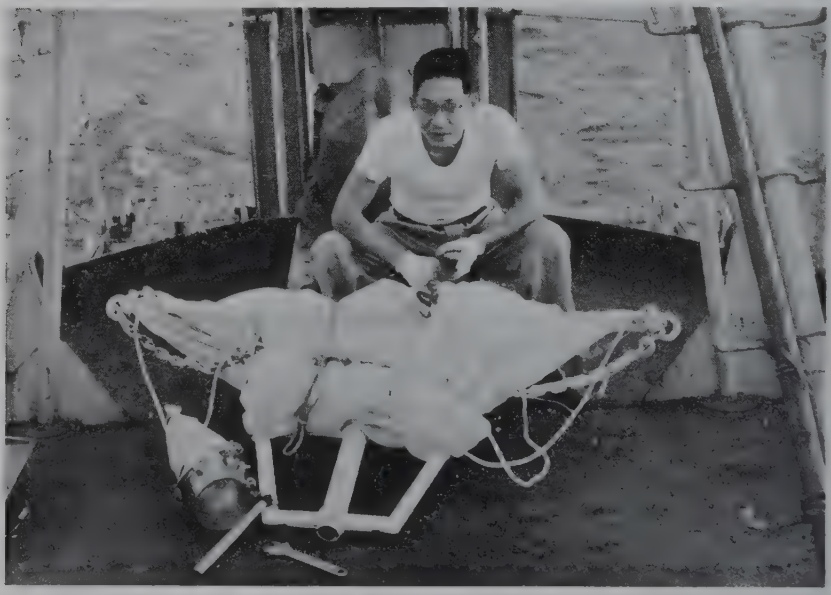

Fig. 7. Triangular mid-water plankton net folded for storing.

Table 5. Data on net haulings at each station.

| Station No. | | $A_2$ | $A_3$ | | $C_2$ |
|---|---|---|---|---|---|
| Ship positions: at the begining of, and at the end of collection | | 40°25′ N, 144°36′ E<br>40°22′ N, 144°32′ E | 40°59′ N, 147°26′ E<br>40°48′ N, 147°19′ E | 40°38′ N, 147°19′ E<br>40°36′ N, 147°19′ E | 42°35′ N, 148°23′ E<br>42°26′ N, 148°28′ E |
| Net type | | TMWN | TMWN | CN | TMWN |
| Date | | IX 12, '59 | IX 15, '59 | IX 16, '59 | IX 22–23, '59 |
| Time | Shot | 12–40 | 14–36 | 10–07 | 20–58 |
| | Towing began | 17–10 | 17–00 | 11–18 | 23–35 |
| | Towing ended | 18–30 | 21–40 | – | 00–55 |
| | Finished | 21–51 | 23–40 | 12–27 | 02–20 |
| Wire length (m) | | 6,000 | 3,764 | 2,500 | 2,335 |
| Max. W.A. at the surface | | 43° | 50° | 29° | 39° |
| Wind | Direction | WNW | N | ENE | NNW |
| | Speed (m/sec) | 3.5 | 9.2 | 4.0 | 7.0 |
| Sail or drift | | sail | drift | (vertical haul) | drift |

Abbreviations: TMWN Triangular mid-water plankton net,
CN 130-cm conical net,
W.A. Wire angle.

weight. For this purpose, the triangular shape of the mouth is mechanically more reasonable than a circular one to the suspension of the lead. It is also convenient for storing because the mouth part can be folded (Fig. 7).

The 130-cm conical net was paid out on 2,500m of tapered wire only at St. $A_3$, while the triangular net was towed horizontally in still deeper water at three stations, St. $A_2$, $A_3$ and $C_2$. Data on net haulings at each station are shown in Table 5. Because it was calm at St. $A_2$, the horizontal towing of the triangular net was carried out by proceeding a speed of 1.0–1.5kt; but there was wind of 9.2 m/sec at St. $A_3$ and 7.0 m/sec at St. $C_2$, and the ship was allowed to drift during the collection. Drifting speed was calculated to be from 0.5 to 1.0kt from the positions of the ship at the be beginning and end of the collections. Considering the fact that these nets were used for the first time in deep sea collection, we can say that the results were all very satisfactory. However, the following points are suggested for improve-

Table 6. Approximate amounts of wet weights (g), settling volumes (cc) and individual numbers of each plankton group.

| Station No. | $A_2$ | | | $A_3$ | | | $A_3$ | | | $C_2$ | | |
|---|---|---|---|---|---|---|---|---|---|---|---|---|
| Date | IX 12, '59 | | | IX 15, '59 | | | IX 16, '59 | | | IX 22-23, '59 | | |
| Net type | TMWN | | | TMWN | | | CN | | | TMWN | | |
| | Wet weight | Settling volume | Indi-viduals | Wet weight | Settling volume | Indi-viduals | Wet weight | Settling volume | Indi-viduals | Wet weight | Settling volume | Indi-diduals |
| Radiolaria | | 9.6 | | | 31.9 | | | 18.1 | | | 3.6 | |
| Coelenterata | | | numerous | | | numerous | | | numerous | | | numerous |
| Chaetognatha | | 22.8 | 632 | | 163.2 | 3,989 | | 69.0 | 1,928 | | 141.8 | 2,119 |
| Nemertini | | | 3 | | | 6 | | | 7 | | | 17 |
| Polychaeta | | | — | | | 29 | | | 32 | | | 44 |
| Copepoda | 22.4 | 132.4 | 9,440 | 176.7 | 9.32 | 44,780 | 57.7 | 274.5 | 11,520 | 81.0 | 471.4 | 12,664 |
| Ostracoda | 0.1 | | 55 | 0.4 | | 105 | 0.5 | | 157 | 0.4 | | 76 |
| Mysidacea | | | 4 | | | 48 | | | 50 | | | 31 |
| Euphausiacea | | | 88 | | | 255 | | | 236 | | | 147 |
| Amphipoda | 1.7 | | 119 | 5.9 | | 398 | 4.2 | | 239 | 3.3 | | 299 |
| Decapoda (Crustacea) | | | 15 | | | 42 | | | 20 | | | 9 |
| Pteropoda | — | — | — | — | — | — | | | 3 | | | 3 |
| Cephalopoda | — | — | — | | | 1 | — | — | — | | | 1 |
| Thaliacea | | | 12 | — | — | — | — | — | — | — | — | — |
| Pisces | | | 1 | | | 16 | | | 18 | | | 14 |
| Pisces scale | — | — | — | — | — | — | — | — | — | | | 85 |
| Egg | | | 3 | | | 37 | | | 31 | — | — | — |

TMWN: Triangular mid-water plankton net.
CN: 130-cm conical net.
—: absent.

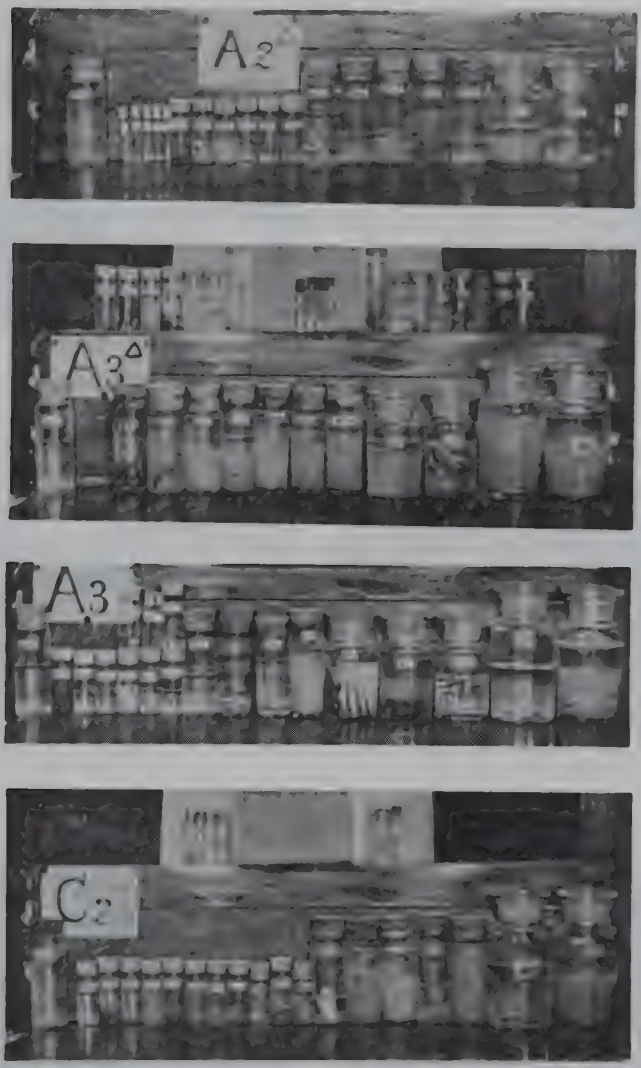


Fig. 8. Animals collected at each station; $A_2\triangle$ etc. indicates animals collected by triangular mid-water plankton net at St. $A_2$ etc. and $A_8\bigcirc$ indicates animals collected by 130-cm conical net at St. $A_8$.

ment of the nets.

(1) For the 130-cm conical net, the mouth ring and ropes for suspending the lead must be made stronger.

(2) As to the triangular mid-water plankton net:

a) heavier lead is desired for keeping the mouth as vertical as possible, and

b) the frame to hold bomboo rod must be simpler and lighter.

(3) For more detailed collections, the nets must be equipped with

a) a depth recorder which can record the depth and the distance of the net hauling, and

b) a double release to open and close the mouth, in order to collect organisms in a definite depth, and this is desirable even for the triangular net.

An outline of quantitative data on each animal group collected at each haul is given in Table 6, and their photographs are shown in Fig. 8. More detailed studies by specialists of each animal group are expected in the near future. Comparing the results of each haul, we could not recognize much difference in the composition of the plankton, except for several larger forms caught in small numbers, such as cephalopod, anglar-fish, myctophid or gonostomid fishes and several crustaceans. This would imply a zoogeographical uniformity of the great depths in the areas investigated.

We are greatly indebted to Dr. S. Motoda who was kind enough to suggest the plan of the triangular net and gave us very helpful advice.

Plate I. Photo-figures of the deep-sea animals selected from the specimens caught—I.

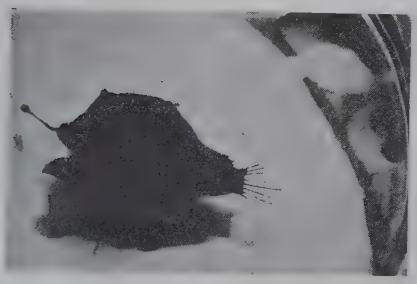

1. Lantern fish.

2. Gonostomatid fish.

3. Cottid fish.

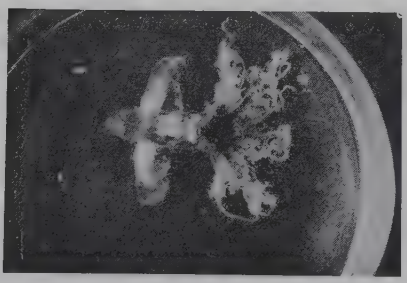

4. *Cirrothauma* sp.

5. Elpiid horothurian.

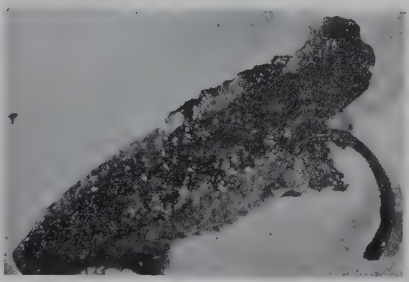

6. Synallactid horothurian.

Plate II. Photo-figures of the deep-sea animals selected from the specimens caught—II.

7. Pycnogonid.

8. Mid-water animals.

9. Polychaete worm.

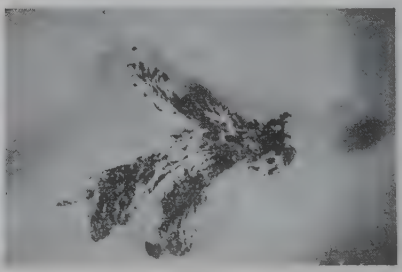

10. Sponge

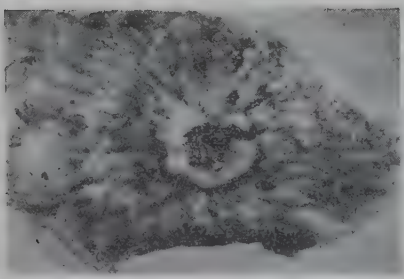

11. Actiniarian.

12. Alcyonarian.

The Oceanographical Magazine
Vol. 11 No. 2, March 1960

# Geological Results in the Japanese Deep Sea Expedition in 1959*
## —Exploration of the Ramapo Deep in the Japan Trench and the— Southernmost Part of the Kurile Trench by the Ryofu Maru

By

Noriyuki Nasu, Azuma Iijima and Hideo Kagami
*Geological Institute, University of Tokyo*

## *1. Introduction*

Preliminary survey of the Japan and Kurile Trenches has been initiated by the R/V Ryofu Maru (1200t) since the middle of 1959. The Ramapo Deep in the Japan Trench was investigated on the last week of June, and the northern part of the Japan Trench as well as the southern extreme of the Kurile Trench were crossed at several sections through the whole month of September.

The former survey is defined as the Japanese Deep Sea Expedition, the First (JEDS-1), and the latter cruise is named here as the Japanese Deep Sea Expedition, the Second (JEDS-2)

Although the main purpose of those two expeditions were to make the tests of instruments, several bottom samples were obtained successfully in the vicinity of the very bottom of the Trenches.

This series of expedition are expected to be continued in coming years. The preparation was started in the beginning of 1957 and sdince then the Japan Meteorological Agency has made efforts to reinforce the weather ship Ryofu Maru with the aid of the Committee of Deep Sea Research, Science Council of Japan.

Among eighteen scientists on the board of the First Expedition, geologists were as follows (JEDS-1) :

| | |
|---|---|
| Hiroshi Niino | Tokyo University of Fisheries |
| Noriyuki Nasu | University of Tokyo |
| Azuma Iijima | University of Tokyo |
| Hideo Kagami | University of Tokyo |
| Kazuo Kobayashi | Tokyo University of Education |

* JEDS Contribution No. 6.

The geologists among 26 scientists in the Second Expedition (JEDS-2) were

| | |
|---|---|
| Azuma IIJIMA | University of Tokyo |
| Hideo KAGAMI | University of Tokyo |
| Tadahiro SATO | Hydrographic Office |
| Kazuo KOBAYASHI | Tokyo University of Education |
| Naoki ONUMA | Tokyo University of Education |

The courses of the expeditions are shown in Fig. 1.

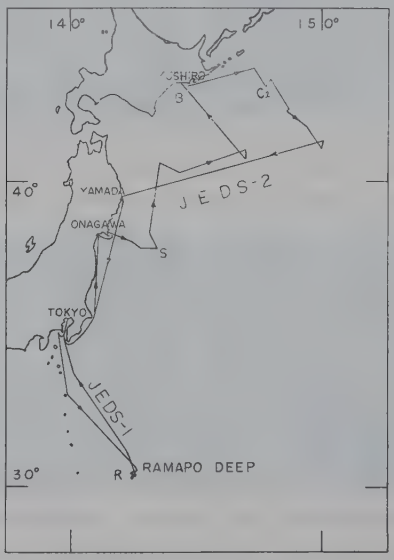


Fig. 1. Courses of the Japanese Deep Sea Expedition 1 & 2 in 1959.

The bottom sediment were collected in the following localities.

| | Loc. No. | Long. | Lat. | Depth (Corrected) | Date | Sampling Device |
|---|---|---|---|---|---|---|
| (1) | JEDS-1-R | 142°18.7′E | 30°24.6′N | 8450 meters | '59-6-26 | Tripod piston core |
| (2) | JEDS-2-$S_1$ | 143°12.1′E | 38°11.4′N | 2350 | '59-9-11 | Dredge |
| (3) | JEDS-2-$S_2$ | 143°11.8′E | 38°16.2′N | 2330 | '59-9-11 | Beam trawl |
| (4) | JEDS-2-B | 144°30′E | 42°40′N | 4ε0 | '59-9-17 | Niino type dredge |
| (5) | JEDS-2-$C_2$ | 147°00′E | 42°48′N | ε005 | '59-9-23 | Piston core |

The deepest finding of these two expeditions was recorded in the depth of 9695 meters at 142°9.5′E, 31°4.ε′N, where is a little north from the Ramapo

Deep. This newly found Deep may form another different basin from that of the Ramapo Deep.

## 2. *Sampling Devices*

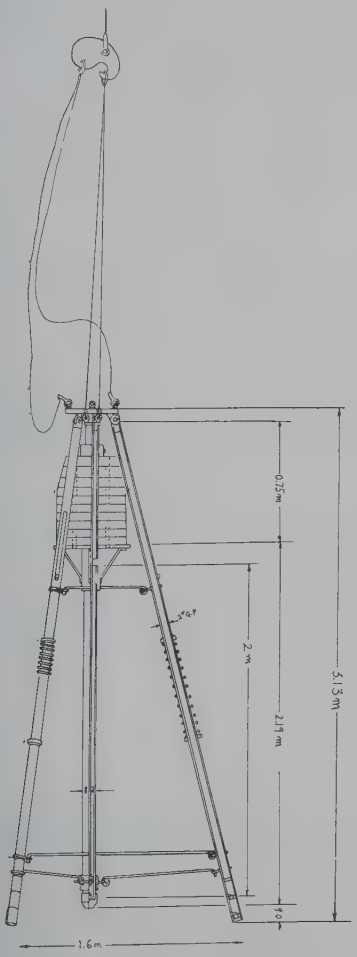


Fig. 2. Piston core with tripod side legs.

**A. Tapered Wire**

This is a newly prepared wire, of which length is 13,000 meters. The diameter at the tip is 9mm and that at the root is close to 17 mm.

**B. Piston Cores**

Two piston cores were made. Both of them are ten meters long. The one of them has a little longer diameter than 10cm, and the other has a little smaller in diameter.

The smaller one in diameter was used at JEDS-2-$C_2$, and the length of the core tube was shortened to 3 meters on that case.

The other has never been tested yet.

**C. Piston core with tripod side legs (T.S.-N.S type piston core)**

Nasu, one of the writers, invented a new type piston core with help of the Tsurumi Seiki Co. It is shown in Fig. 2.

The length of the core is 3 meters.

The piston in a main tube is fixed with an iron bar which connects with the round table on the top of three side legs. These three legs are also gravity cores.

The diameter of the main tube is approximately 8cm and holds the inner plastic tube. That of the side leg is about 5cm.

Total weight is about 800 kg.

The function of this tripod piston core is as follows. When it hits the bottom, three side legs will hold the main part of the core on the bottom after they penetrate the surface sediment slightly. Then, the wire above the lever on the top will be loosen, thus the lever will turns around. So that the wire being hooked on the lever to hold the main tube with the weights will be released. Consequently, the main tube will be push down into the sediment by its own weight. However, the piston is fixed on a stationary position relative to the side legs. As the result, the function of the piston will be, perhaps, a little better than the former type of piston cores, because the piston of the previous type must be hold and controled to keep right on the bottom directly from the boat, which has caused a lot of troubles and difficulties.

This new type piston core was used at the Ramapo Deep (JEDS-1-R) and could get the sediment from the depth of 8450 meters.

**D. Dredges**

Two large dredges with a small one were loaded on the ship. Two of them are Niino type dredges.

A small dredge was used at S station off Onagawa (JEDS-2-S) and the large Niino type dredge was used at $B_1$ station off Kushiro (JEDS-2-$B_1$).

**E. Ball Breakers**

Ball breakers were attached to the above mentioned piston cores during the operation. In case of JEDS-1-R, the result was not successful because of the stiffness of ball; incidently, the ball was not broken when the core hit the bottom. However, this was improved later and satisfied result was obtained at $C_2$ station of JEDS-2.

The diameter of those balls are about 8cm of witch weight is 60.8g.

*3. Trench Topography*

The depth was recorded continuously by a deep sea type echo-sounder. Trench topography even down to 10,000 meters could be traced very clearly by this instrument.

The positions of the ship were measured by Loran and by the astronomical methods in every another hour in general.

The depths shown in Figs. 3a and 4a are uncorrected records directly read from the echograms. The correction will be reported before long.

A. The Hachijo Island to the Ramapo Deep (JEDS-1)

The course from the Hachijo Island to the Ramapo Deep in Japan Trench is fairly straight as shown in Fig. 3a. The profiles are shown in Fig. 3b. The distances between each 1,000 meters interval in the depth are as follows along the profile a-a'.

As seen in the Figure, there is a very wide flat area in the depth of

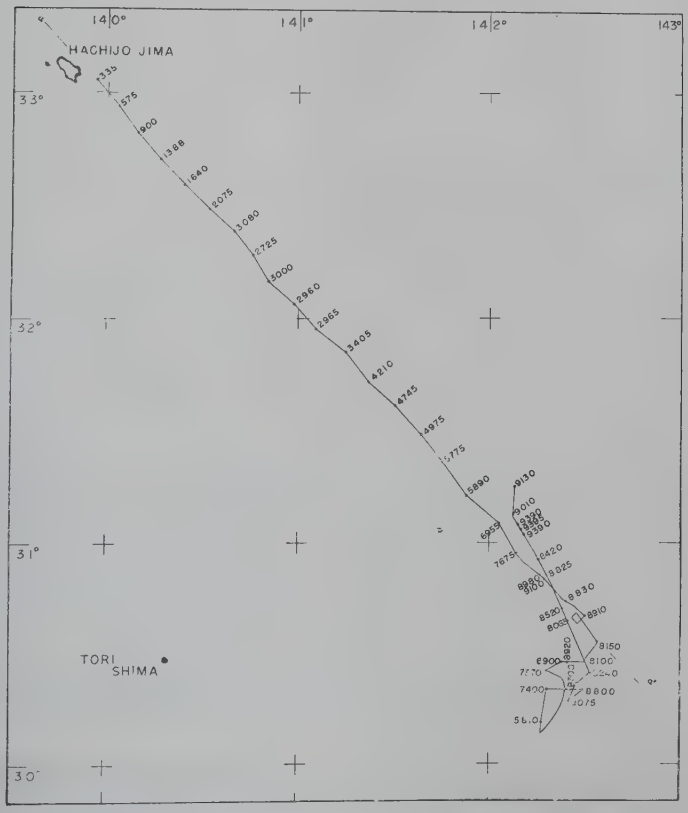


Fig. 3a. Course of the JEDS-1 and uncorrected depths by echo-sounding.. (Depth in meters)

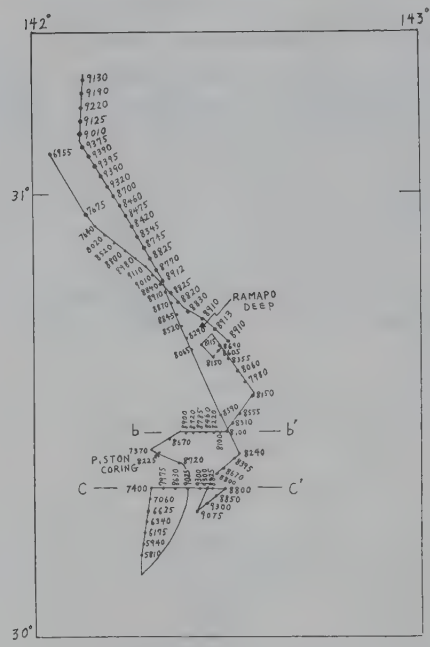


Fig. 3a.

| Depth | Distance | Depth | Distance |
|---|---|---|---|
| 0—1000 m | 45 km | 4000—5000 m | 40 km |
| 1000—2000 | 42 | 5000—6000 | 38 |
| 2000—3000 | 19 | 6000—7000 | 22 |
| 3000± | 64 | 7000—8000 | 21 |
| 3000—4000 | 30 | 8000—9000 | 14 |

3000 meters or a little shallower, while the slope between 2000 to 3000 meters deep is steeper than the sorrundings.

From 6000 meters to 8000 meters, the slope becomes also steeper, but that between 8000 to 9000 meters is the steepest.

The trench bottoms in the vicinity of the Ramapo Deep is fairly flat. Those are seen on the profiles b-b′ and c-c′. Along the profile b-b′ the depth of

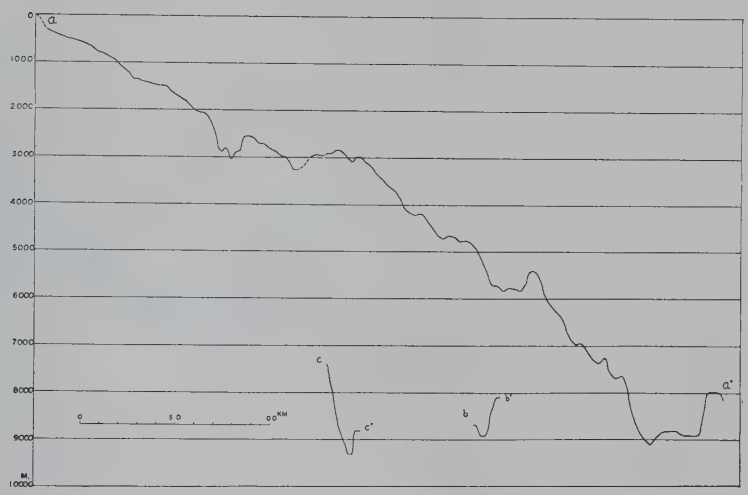


Fig. 3b. Profiles of the Ramapo Deep.

the flat bottom is 8920 meters, and the width is approximately 2.5km, while the width of the flat bottom along the profile c-c′ is about 1.6km and the depth is 9300 meters. The bottom sample was collected from the depth of 8225 meters (8450 meters with correction) along the west slope between those two profiles b-b′ and c-c′.

The deepest spot in the eastward extension of this sampling locality is 8720 meters and the bottom looks also flat so that the difference between the very bottom near-by and the sampling spot is about 500 meters.

The deepest spot during the expedition was found in a deep, several tens of kilometers north from the Ramapo Deep. The depth was 9695 meters after the correction.

Generally speaking, the slope along the west wall of the trench, incidently continental side is steeper than that of the eastern ocean side in each profile.

## B. Kushiro to Yamada (JEDS-2)

Only a course between Kushiro in Hokkaido Island and Yamada in north-eastern Honshu was presented here, and the depths are shown in Fig. 4a.

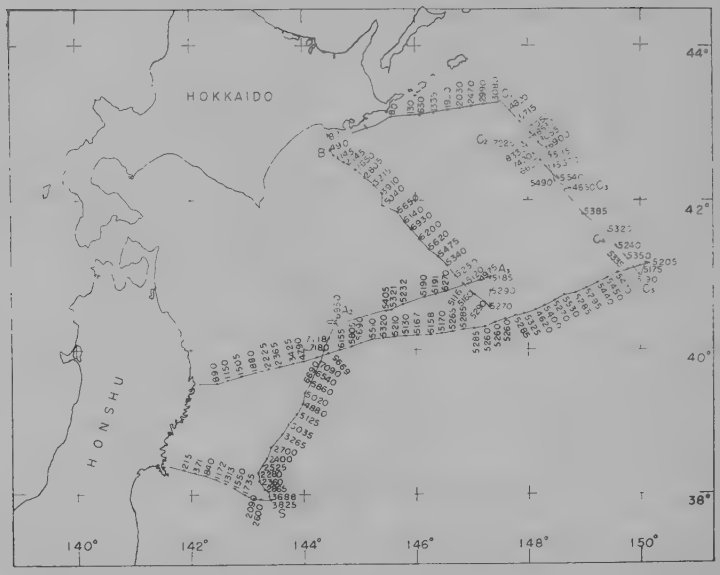


Fig. 4a. Course of the JEDS-2 and uncorrected depths by echo-sounding. (Depth in meters)

| Depth | Distance | Depth | Distance |
|---|---|---|---|
| 0—1000 m | 43 km | 4000—5000 m | 8 km |
| 1000—2000 | 8 | 5000—6000 | 5 |
| 2000—3000 | 27 | 6000± | 15 |
| 3000± | 5 | 6000—7000 | 10 |
| 3000—4000 | 10 | 7000—8000 | 16 |

The bottom profiles are drawn in Fig. 4b.

The distances between each 1000 meters interval in the depth are as follows along the profile $c_1$-$c_5'$ :

There is a flat area in 3000 meters, also a hilly configuration can be seen in 5700 meters deep along the west wall.

The deepest spot is about 8420 meters deep and is approximately 150km away from the Shikotan Island in the Kurile Arc.

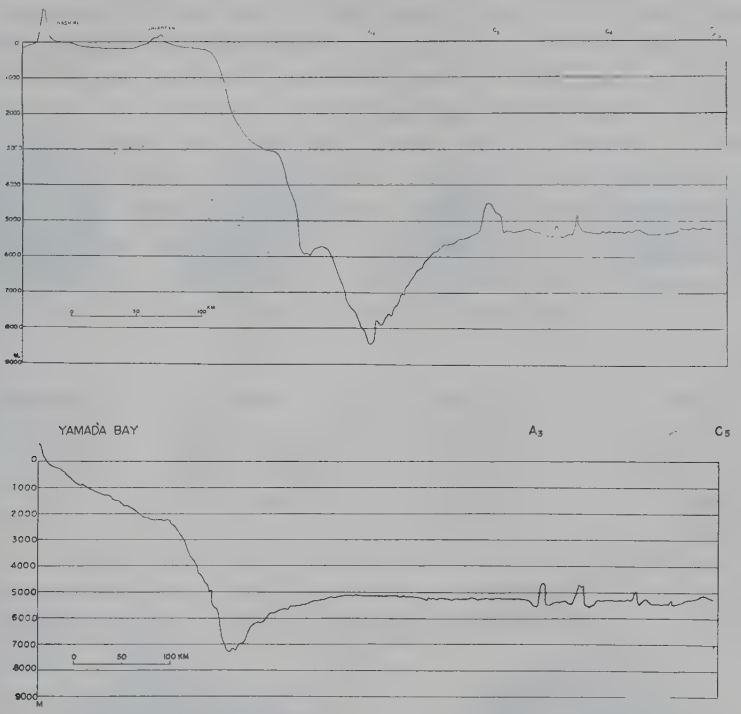


Fig. 4b. Profiles of the JEDS-2.
(The profile between B and $A_8$ is shown in KAGAMI and IIJIMA's paper in the following section.)

The slope goes up steeply along the east wall up to the depth of 6000 meters being accompanied with hilly features. The slope becomes much gentler between 6000 meters and 5000 meters and is extended into the wide, flat area of the Pacific Ocean floor, of which depth is 5300 meters along this line.

However, there are several hills or sea mounts. The westernmost one is situated right on the eastern edge of the Trench and is 800 meters higher than the sorroundings.

The other two are situated east; one is 300 meters high and the other is about 500 meters high.

Along the course between Yamada and $C_5$, these mountains are also seen in several spots on the flat area of the Ocean floor. The heights of those mountains are 1000, 800, 200 meters successively from the west to the east. The depth of the flat floor, circling these mountains, of the east of the Trench is approximately 5200 meters. The slope along the east wall of the Trench is gentle down to 6000 meter, then goes down to the bottom steeply with hilly configurations just as like that of the $C_1$–$C_5$ profile.

The deepest spot is 7280 meters. There is also a flat area at the depth of 2300 meters, 20 kilometers wide along the west wall.

The distance between each 1000 meters interval in depth along the west wall is as follows:

| Depth | Distance | Depth | Distance |
|---|---|---|---|
| 0—1000 m | 42 km | 4000—5000 m | 15 km |
| 1000—2000 | 50 | 5000—6000 | 9 |
| 2000—3000 | 46 | 6000—7000 | 5 |
| 3000—4000 | 10 | | |

There are no significant flat bottoms in the Trench along these two profiles. Minor up-and-down topography is characteristic along the walls of the Trench here.

*4. Sediment*

A. Ramapo Deep (JEDS-1-R)

The bottom sample was collected from the down slope of the west wall of the Deep. The depth was 8225 meters by echo sounder reading. The corrected depth is read as 8450 meters.

Sediment column of 22cm was collected in the main tube. The first side leg was empty; and there were fifty centimeters of mud in the second side leg. Several subangular granules of few millimeters were found in the third side leg, but there was no mud or sand in this tube (Fig. 5a). Also, one subangular basalt gravel of approximately three centimeters was found at the bottom of the main tube caught by core catcher (Fig. 5b).

The sediment was mostly reddish brown mud including abundant volcanic sand. Mineral grains in the second leg was briefly examined and reported

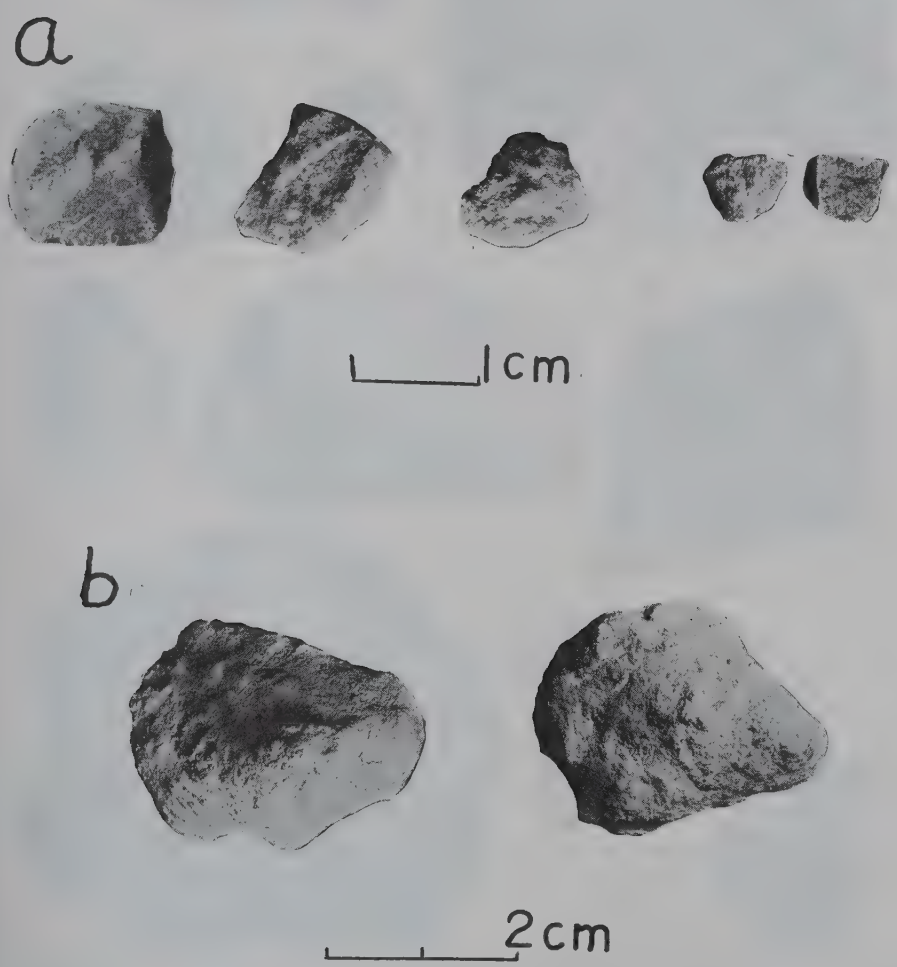


Eig. 5. Rock fragments collected from the depth of 8450m in the Ramapo Deep. (Photo. by C. Ueki.)

a. Fragments caught in a side leg of the tripod pistone core.

b. Fragment in a main tube of the core (altered basalt).

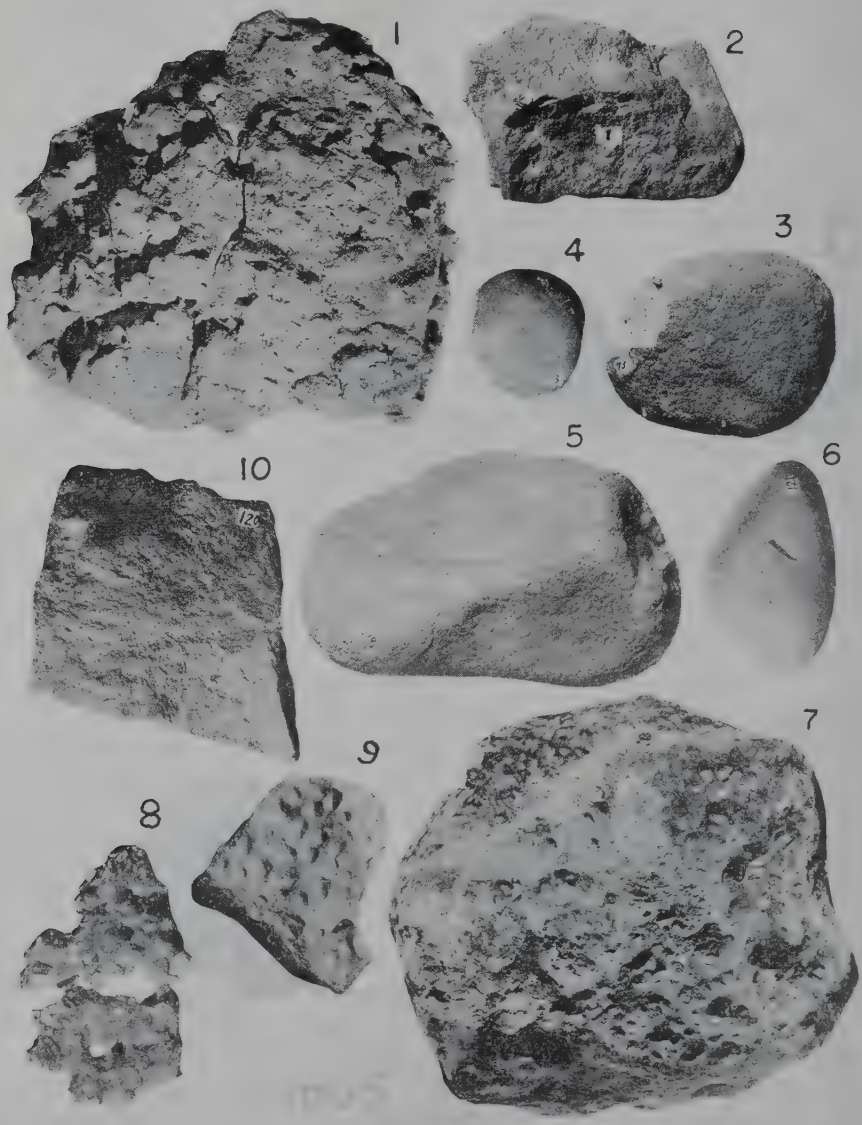


Fig. 6. Gravels dredged at S point (2300m) off Onagawa. (Photo. by C. Ueki.)

1. pumice bomb (173mm).
2. limestone (140mm).
3. granite with manganese coating (121mm).
4. chert (66mm).
5. andesite (241mm).
6. basaltic andesite (104mm).
7. yellowish brown tuffaceous sandy siltstone (160mm).
8. tuffaceous siltstone (92mm).
9. tuffaceous siltstone (82mm).
10. andesite (160mm).

by IIJIMA, one of the writers of this paper, in the following report in this issue. The sand-size grains can be considered as volcanic origin.

The heavy minerals are olivine, pyroxenes, hornblende, spinel, apatite, magnetite, hematite, and ilmenite. There are also altered basalt, chlorite and peridotite. The light minerals are glass, pumice, plagioclase, chalcedony.

The clay minerals are illite, chlorite and montmorillonite as examined by KOBAYASHI, OINUMA and SUDO of which report is also in the followning section of this issue.

There are also abundant amount of Diatoms and Radioralias. Foraminiferas are less, and the corroding effect is observed on the surface of some Foraminiferas.

B. Southernmost Kurile Trench (JEDS-2-$C_2$)

Another trench sediment was collected also from the down slope of the west wall of the southernmost Kurile Trench (8005 m after the correction).

Sediment core of 85 centimeters was obtained in a single tube of an usual type of piston core, of which length was 3 meters.

Sediment is bluish gray mud with some amount of sandy fractions. Heavy minerals are augite, hypersthene, hornblende, zircon, hematite, limonite and pyrite. The detail is described in the IIJIMA's report. There are a lot of rounded sand grains.

The clay minerals are illite, montmorillonite and chlorite according to the examination by OINUMA, KOBAYASHI and SUDO.

C. Gravels off the coast of Onagawa (JEDS-2-$S_1$ and $S_2$)

More than five hundreds of gravels were collceted with a dredge and a beam trawl on the flat area off Onagawa in the northeastern Honshu. The depth is approximately 2200 meters. Gravels are all kinds of rocks consisted of pultonic, volcanic and sedimentary types as well as the metamorphic. The maximum size is 46 centimeters (Fig. 6).

The remain of organic attachment can be seen on the surface of those gravels. KAGAMI and IIJIMA describe the detail in the following report of this issue.

D. Sediment off Kushiro, Hokkaido Island (JEDS-2-$B_1$)

Bluish sandy mud was collected in the vicinity of the Kushiro Submarine

Canyon at the depth of 430 meters. This is an ordinary type slope sediment. The detail is also described by KAGAMI and IIJIMA.

*Acknowledgment*: The writers are deeply indebted to the Japan Meteorological Agency, especially to Drs. Kiyoo WADATI, Kazuhiko TERADA, Yasuo MIYAKE, Yositada TAKENOUTI, Hidetaka FUTI, Jotaro MASUZAWA and Masashi YASUI of the Agency, and to the scientific and crew members of the Ryofu Maru.

The writers are also grateful to the Committee of Deep Sea Research, Science Council of Japan for their helps and co-operation, as NASU belongs to the Committee.

Professor Takao SAKAMOTO of the University of Tokyo has given the guidance and encouragement continuously as he is the closely related person to the writers. Deep appreciation is dedicated here to Professor SAKAMOTO.

Professor Hiroshi NIINO of the Tokyo University of Fisheries, senior marine geologist, had shown his skilful helps and experienced suggestions to the writers on the cruise. This report, perhaps, would be more procriate if written by him. However, as he is in the sea again by the time when this paper is prepared, the writers want to express their sincere thanks to him.

## *References Cited*

IIJIMA Azuma: "A report on the bottom sediments of the Japan and Kuril trenches collected by the Ryofu Maru during the Japanese Deep Sea Expeditions in 1959", in this issue.

KAGAMI Hideo and IIJIMA Azuma: "On the bottom sediments off Onagawa and Kushiro, the adjacent continental slope of Japan Trench", in this issue.

KOBAYASHI Kazuo, OINUMA Kaoru and SUDO Toshio: "Clay mineralogical study on Recent marine sediments I, II., in this issue.

## *Addendum*

Since this manuscript went to the press, a well-rounded pebble of approximately two centimeters has been found in the core at $C_2$ station in the Kurile Trench. It is found fifty-five centimeters below the bottom surface, and is a hard sandstone pebble. Also, an angular pumice fragment of the same size is found eleven centimeters below the surface in the same core.

The Oceanographical Magazine
Vol. 11. No. 2, March 1960

# Clay Mineralogical Study on Recent Marine Sediments (I)*

## —Samples JEDS-1-R′, JEDS-1-R″—

By

Kazuo Kobayashi, Kaoru Oinuma and Toshio Sudo

*Geological and Mineralogical Institute, Faculty of Science, Tokyo University of Education*

**Abstract:** Clay mineralogical study was carried on the core samples (JEDS-1-R′~R″), which were obtained from the ocean floor of 8450 m water depth, at the station JEDS-1-R, at the time of Japanese Expedition of Deep Sea, in June, 1959. The result of investigation by means of X-ray, thermal, and electron optical methods shows that the crystalline material in the minus-two-micron fraction of the samples is composed of illite, chlorite, and montmorillonite. The structural attitudes of the first two minerals unlike to those of standard materials were briefly mentioned. The cation-exchage capacity of the sample was obtained as 32 me/100 g.

### *1. Specimens*

The core samples, JEDS-1-R′ and JEDS-1-R″, were obtained by two side-legs of the core sampler designed by Dr. Nasu, University of Tokyo, from the ocean floor of 8450 m water depth, at the station of JEDS-1-R, at the time of Japanese Expedition of Deep Sea in June, 1959. Each of them is about a few cm in length and obtained from the surface of this station. They show yellowish brown colour and are composed of clay materials associated with sand grains; the latter consists of fragments of basic volcanic rocks and serpentine.

### *2. Methods*

In the present study, we did not prepare test samples by cutting off the core samples in parts, because the total amount of the these core samples was not sufficient for detailed clay mineral analyses. The minus-two-micron fraction was obtained by the usual sedimentation technique from the samples

* JEDS Contribution No. 7.

JEDS-1-R′~R″ and used for clay mineral analyses using oriented aggregates chiefly.

The steps in the preparation and examination of materials for indentification of clay minerals are summarized in Table 1.

X-ray analyses of untreated samples were carried both with orientated aggregates and randomly oriented powders.

Silica-glass slide was used in the case of heat treatments. Oriented aggregates on this slide were heated stepwise at every temperature for one hour as noticed in Table 1, air quenched, and X-ray diffraction effects were examined immediately.

Treatment with ethylene glycol or glycerol for detection of expanding lattices (WALKER, 1957, 1958) : Oriented aggregated were saturated with drops of these reagents and radiated by X-ray. Usually preferred orientation is partly disturbed by this treatment.

Treatment with ammonium nitrate solution for detection of Mg-vermiculite

Table 1. Procedure of clay mineral analyses.

Raw specimens

(Disaggregation, sieving, dispersion)

(Centrigfugation, decantation)

| Sand and silt | Clay ($<2\mu$) |
|---|---|

Sand grains:

(1) Microscopic observations of coarse grains; polished surface of opaque grains; and thin sections.

(2) X-ray, chemical, and differential thermal analyses.

Clay fraction:

(1) X-ray analysis of specimens:
  (a) untreated.
  (b) heated at every temrerature as 100° C, 200° C...1000° C.
  (c) treated by ethylene glycol or glycerol.
  (d) treated with ammonium nitrate solution (1 N).
  (e) treated with hydrochloric acid (6 N).
  (f) treated with magnesium acetate solution (1 N).
  (g) treated with sodium citrate, calcium chloride, and glycerol.

(2) Differential thermal analysis of specimens:
  (a) untreated.
  (b) treated with piperidine

(3) Chemical analysis.

(4) Electron micrographic observation.

(5) Staining test.

(WALKER 1949): Oriented aggregates were made with the sample boiled for ten minutes in 1 N solution and washed with distilled water.

Treatment with magnesium acetate solution to know the degree of weathering of illite (ROLFE and JEFFRIES, 1952): Oriented aggregates were made with the sample boiled in 1 N solution for one hour on a water-bath and washed with distilled water.

Treatment with sodium citrate, calcium chloride, and glycerol: This method is followed by TAMURA (1958) for the purpose of identification of dioctahedral vermiculite.

Treatment with hydrochloric acid to decompose most of chlorite: Oriented aggregates were made with the sample warmed in 6 N hydrochloric acid on a water-bath for one hour.

Treatment with piperidine for detection of montmorillonite (ALLAWAY, 1948): The procedure adopted in our laboratory is as follows: the sample is immersed in piperidine for about 30 minutes and dried completely on a water-bath.

### 3. *Results*

X-ray analysis:

X-ray diffraction data are shown in Fig. 1 and Table 2.

The treatment with ethylene glycol or glycerol caused the 15.2 Å reflection to be replaced partly by the 17.3 Å reflection, and the 14.5 Å reflection was confirmed. From this the presence of montrillonite can be suggested. Heat treatments caused the 15.2 Å reflection to be slightly weakened, and its spacing slightly decreased, whereas the 10 Å reflection became slightly stronger after heating at 200°–450° C. This fact suggests the presence of montmorillonite, which dehydrated to the 9–10 Å lattice. After heating at 600° C, the spacing of the 15.2 Å reflection further decreased to 13.6 Å, and the 7.4 Å reflection became just visible. After heating at 750°C, the 10 Å reflection was only remained. These facts clearly show the presence of chlorite. The temperature at which diffraction effects are lost is slightly lower in this chlorite comparing with well-crystallized sorts of hydrothermal origin; it was shown in earlier data that some chlorites in marine sediments lost their diffraction effects even after heating at 450° C (JOHNS, GRIM and BRADLEY, 1954). The diffraction behaviour of the chlorite now in question after heating

Table 2. X-ray diffraction data (JEDS-1-R′∼R″).

| Untreated | | 200° C | | 450° C | | 600° C | | 750° C | | Ammonium nitrate | | Hydrochloric acid | | Ethylene glycol | | Glycerol | | Magnesium acetate | |
|---|---|---|---|---|---|---|---|---|---|---|---|---|---|---|---|---|---|---|---|
| d(Å) | I | d(Å) | I | d(Å) | I | d(Å) | I | d(Å) | I | d(Å) | I | d(Å) | I | d(Å) | I | d(Å) | I | d(Å) | I |
| | | | | | | | | | | | | | | 17.3 | 4 | 18.0 | 6 | | |
| 15.2 | 24 | 14.5 | 15 | 14.0 | 10 | 13.6 | | | | 14.3 | 20 | 14.5 | 5 | 14.5 | 3 | 14.0 | 3 | 14.7 | 22 |
| | | | | | | 12.6 | 7b | | | 13.0 | 20 | | | | | | | | |
| 10.0 | 16 | 10.2 | 22 | 9.9 | 31 | 10.0 | 30 | 10.0 | 30 | 10.0 | 20 | 9.9 | 13 | 10.7 | 3 | 10.0 | 5 | 10.0 | 9 |
| | | | | | | | | | | | | 9.2 | 4 | 9.9 | 4 | | | | |
| | | | | | | | | | | | | | | 8.1 | 5 | | | | |
| 7.1 | 12 | 7.2 | 16 | 7.1 | 14 | 7.4 | 3 | | | 7.14 | 21 | 7.14 | 4 | 7.56 | 6 | 7.20 | 7 | 7.2 | 14 |
| 5.01 | 5 | 5.01 | 6 | 5.01 | 7 | 5.01 | 10 | 5.01 | 8 | | | 6.46 | 3 | | | | | | |
| 4.75 | 3 | 4.75 | 5 | 4.75 | 3 | 4.77 | 4 | | | 5.01 | 8 | 5.00 | 5 | | | | | 4.98 | 5 |
| | | 4.65 | 5 | | | | | | | 4.77 | 4 | | | | | | | | |
| | | 4.53 | 3 | | | 4.55 | 5 | | | | | | | | | | | | |
| | | 4.30 | 3 | 4.25 | 4 | 4.25 | 3 | | | 4.50 | 4 | 4.51 | 3 | | | | | 4.51 | 6 |
| 4.04 | 3 | 4.00 | 3b | 4.02 | 3 | | | | | 4.27 | 3 | 4.25 | 3 | | | | | 4.29 | 6 |
| | | | | 3.77 | 2 | | | | | 4.04 | 3b | 4.04 | 3 | | | | | | |
| 3.56 | 4b | 3.55 | 6 | 3.68 | 2 | | | | | | | 3.72 | 3 | | | | | 3.66 | 6 |
| | | | | 3.56 | 2 | | | | | 3.54 | 11 | 3.56 | 2 | | | | | 3.55 | 11 |
| 3.34 | 13 | 3.35 | 16 | 3.34 | 14 | 3.36 | 13 | 3.34 | 27 | | | | | | | | | | |
| 3.19 | 5 | 3.22 | 5 | 3.20 | 5 | 3.22 | 6 | | | 3.35 | 26 | 3.34 | 18 | | | | | 3.35 | 83 |
| 3.93 | 4 | 2.91 | 2 | | | | | | | 3.21 | 10 | 3.19 | 5 | | | | | 3.20 | 9 |

b: broad.

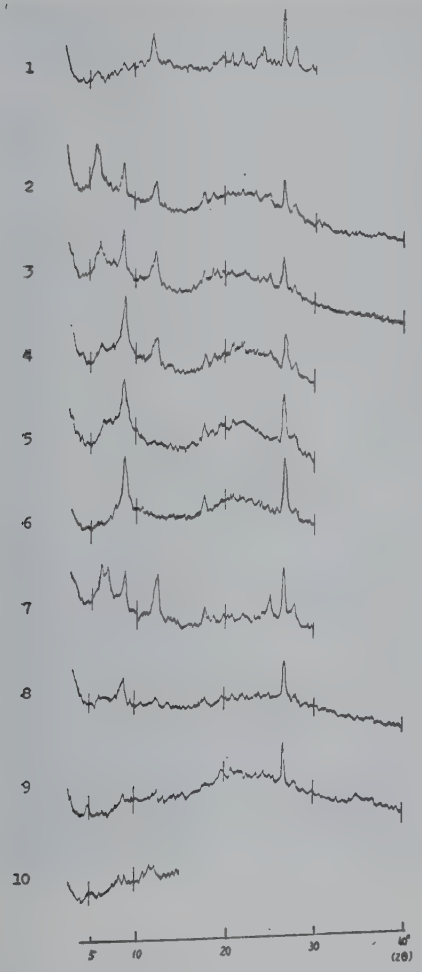


← Fig. 1. X-ray diffractometer curves (JEDS-1-R′∼R″).
(1) Raw sample. Randomly oriented powders. Air dry state.
(2)-(10) Clay fraction less than two microns (e.s.d.). Oriented aggregate.
(2) Untreated.
(3) Heated to 200° C.
(4) Heated to 450° C.
(5) Heated to 600° C.
(6) Heated to 750° C.
(7) Treated with ammonium nitrate.
(8) Treated with hydrochloric acid.
(9) Treated with glycerol.
(10) Treated with ethylene glycol.

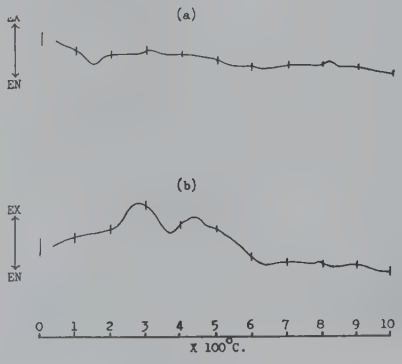


Fig. 2. Differential thermal analysis curves of clay fraction less than two microns (e.s.d.) (JEDS-1-R′∼R″).
(a) Untreated sample.
(b) Treated with piperidine.

at 600° C closely resembles the behaviour of pseudochlorite (Stephen and MacEwan 1951). The existence of the broad 12.6 Å reflection along with the 13.6 Å one may be attributed to a partial alteration of the brucite layer of the chlorite, which may have a vermiculitic nature.

Treatment with ammonium nitrate solution caused the 15.2 Å reflection to be replaced by the doublet of 14.3 Å and 13.0 Å reflection. This treatment was recommended by WALKER (1949) for confirmation of vermiculite. But we have confirmed in Japanese clay minerals that pure montmorillonites and pure Mg vermiculites frequently show a partial contraction by this procedure. Such facts may be attributed to effects of particle sizes, or times for treatments. Further the presence of interlayer contaminants as Al prevents lattice contraction (BROWN 1953, TAMURA 1958), and, generally speaking, the presence of dioctahedral analogues of vermiculite or chlorite can be anticipated in marine sediments. Future further studies are needed to solve whether vermiculite is present or not in the present sample.

It was suggested that treatment with magnesium acetate solution caused the 10 Å reflection to be replaced partly by the 15 Å one. This fact implies that the illite has the property of "degraded illite".

Treatment with hydrochloric acid caused the 7 Å reflection to be just visible. This fact leads to a conclusion that kaolinite is absent in this specimen.

Differential thermal analysis: The differential thermal analysis curve (Fig. 2) of the specimen shows an endothermic peak at about 150° C caused by dehydration of absorbed water, and a very broad endothermic peak between 500° and 700° C, due to dehydroxylation of illite, chlorite, and montmorillonite. A small exothermic peak at about 800° C can be recognized. The present specimen failed to show an exothermic peak (600°–700° C) after treatment with piperidine, where the usual montmorillonite and vermiculite do (ALLAWAY, 1948). It is needful to carry further study in future.

Electron micrographic observation: Electron micrographs of the samples are as shown in Fig. 3. Clay minerals show flakes having irregular but well-defined outlines. It is worthy of notice that elongated and fibrous particles are rarely found. Such particles may be of serpentine mineral because sand grains of serpentine are also rarely included in this sample. It is considered that we could not confirm the presence of serpentine mineral by X-ray because of its small amount, and overlapping effects of serpentine and chlorite reflections.

Cation-exchange capacity: The cation-exchange capacity of the original sample was obtained as 32.31 me/100 g by the ammonium acetate method (by

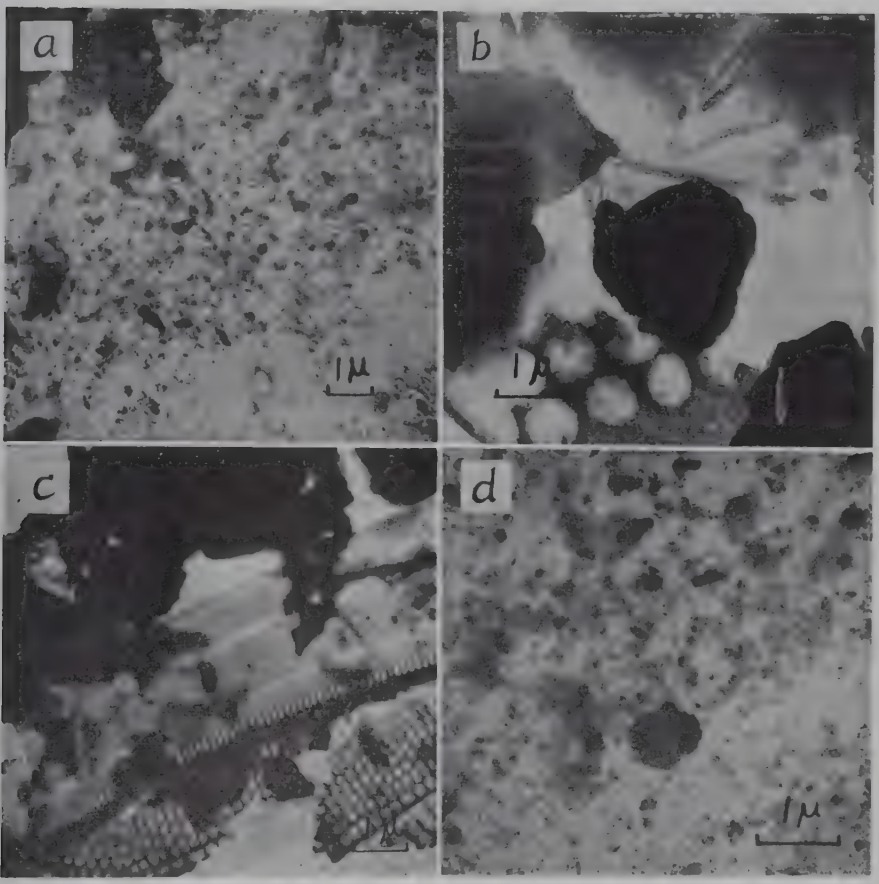


Fig. 3 Electron micrographs (JEDS-1-R′∼R″).
(a) Irregular plates of clay minerals.
(b) Irregular plates of clay minerals, fragments of diatom, and elongated crystals probably of serpentine minerals.
(c) Fragments of diatom.
(d) Irregular plates of clay minerals.

T. Matsui and K. Kuwano).

*Conclusion*: The clay minerals in the clay fraction of the sample now under consideration can be identified to be montmorillonite, illite and chlorite

by following the criteria having hitherto been accepted. Recent advance of clay mineralogy, however, has revealed subtle variations of properties even in each clay mineral species, and intermediate minerals have been found frequently particularly in Recent marine sediments. So our attention is drawn to the urgent need for further careful scrutiny on the properties of each mineral component.

*Acknowledgements*: We wish to thank Dr. N. Nasu, University of Tokyo, for the material used in this investigation, and to T. Matsui and K. Kuwano for determination of the base-exchange capacity.

*References*

Allaway, W. H. (1948): *Soli Sci. America, Proceeding*, **13**, 183-188.
Brown, G. (1953): *Clay Miner. Bull.*, **2**, 64-69.
Johns, W. D., Grim. R. S., and Bradley, W. F. (1954): *Journ. Sed. Petrol.*, **24**, 242-251.
Rolfe, B. N. and Jeffries, C. D. (1952): *Science*, **116**, 599-600.
Stephen, I. and MacEwan, D. M. C. (1951): *Clay Miner. Bull.*, **1**, 157-161.
Tamura, T. (1458): *Journ. Soil. Sci.*, **9**, 141-147.
Walker, G. F. (1949): *Nature*, **164**, 577.
Walker, G. F. (1957): *Clay Miner. Bull.*, **3**, 154-163.
Walker, G. F. (1958): *Clay Miner. Bull.*, **3**, 302-313.

# Clay Mineralogical Study on Recent Marine Sediments (II)
## —Sample "JEDS-2-$C_2$"—

Kaoru Oinuma, Kazuo Kobayashi and Toshio Sudo

*Geological and Mineralogical Institute, Faculty of Science, Tokyo University of Education*

**Abstract:** Core sample —JEDS-2-$C_2$— was obtained from the station, 42° 48′ N. 147° 59′ E., water depth 8005 m, at the time of Japanese Expedition of Deep Sea in August, 1959. Clay mineral analyses were carried by X-ray, means of thermal, and electron micrographic methods on each test sample cutting off every 4 cm from the top of core sample downward The crystalline clay material in the minus-two-micron fraction of each test sample is composed of complex mixtures of the following clay minerals: illite, montmorillonite and chlorite. The wide latitude of variations in the clay-mineral composition was not noticed from the top of the core sample downward. Subtle variations of properties of each mineral component were made clear by more careful scrutiny.

The Oceanographical Magazine
Vol. 11. No. 2, March 1960

# The Bottom Sediments of the Japan and Kuril Trenches Collected by the Ryofu Maru during the Japanese Deep Sea Expeditions in 1959*

By

Azuma Iijima

*Geological Institute in University of Tokyo, Dr. Sci.*

Fortunately the writer had the chance of a lifetime to joint the 1st and 2nd Japanese Deep Sea Expeditions (JEDS) for the Japan and Kuril Trenches by the Ryofu Maru, a meteorological ship of the Japan Meteorological Agency, in June and September, 1959. In the 1st preliminary cruise were we successful in collecting a short but significant sediment column from the bottom of the Ramapo Deep in the southern Japan Trench, down to 8,450 m in depth: in the 2nd, more than 500 gravels from the continental slope east off Shiogama at a depth of 2,230 m(1); and farther, a column from 8,005 m in the depth of the southern Kuril Trench off the Habomai Islands.

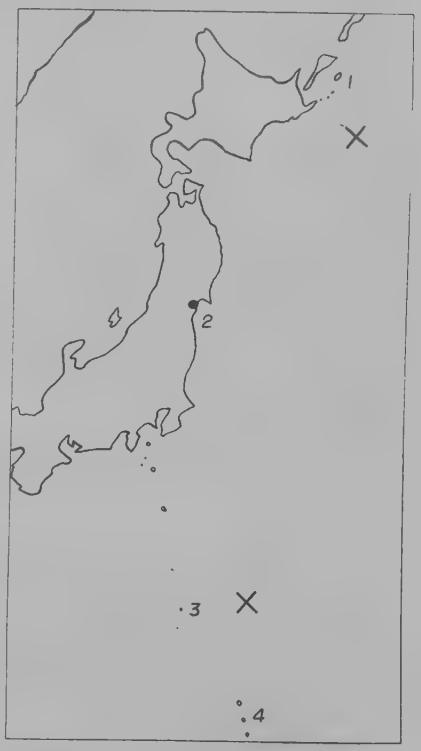


Fig. 1. ×: Sampling localities, 1: Shikotan Is., 2: Shiogama, 3: Tori-shima, 4: the Bonin Is.

* JEDS Contribution No. 8.

(1) The largest boulder, a Younger Tertiary diatomaceous marl, has a diameter of 46 cm, the surface of which is ornamented by *Lebensspuren* of *Arenic la.* Various kinds of rounded gravels, such as andesite, granite, gneiss, gabbro, amphibolite, chert, slate etc. are found. It is expected that detail description will be reported in near future.

He has been investigating these sediments viewing from their petrographic natures. This paper briefly reports the results now obtained, which suggest important and interesting facts about the origin and the process of deposition of the trench-filled sediments.

The general geological results of the Expeditions are described in the preceding paper by NASU, IIJIMA and KAGAMI in this issue.

*1. Bottom sediment of the Ramapo Deep*

A small quantity of the bottom sediment caught by a pod of the TS–NS–type tripodal piston-core sampler was used for this study.

Sample No.: JEDS–1–R″ (2nd side leg)

Situation: 30°24.6′N, 142°18.7′E. Landward slope of the Ramapo Deep in the southern Japan Trench east off Tori-shima, a vulcanic island of the Izu Islands.

Date: June 26, 1959.

Depth: About several centimeters beneath the deep sea floor, down to 8,450 m in depth.

The sediment is a reddish brown, ill-sorted, silty sand with clay as well as a little amount of granule-size rock fragments and pumice grains. The grain-size and heavy-residue distribution is given in Table 1. All rock fragments and also sand grains are very angular, and have a maximum diameter of 6.6 mm. They make up largely of vulcanic materials and decomposition products as follows;

white, gray to pale brownish gray pumice,
clear, colorless to pale pink, vesicular vulcanic glass,
Pele's hair,
white, gray, pale brownisn to greenish gray, fibrous aggregates of glass,
various shades of glass fragments, obsidian and devitrified glass, dark gray to reddish brown scoria,
basic vulcanic rock fragments with various color,
green alteration product of basaltic rock with chlorite,
serpentinized peridotite (Plate),
chalcedony,
plagioclase (anorthite to andesine),
heavy minerals, such as olivine, monoclinic and rhombic pyroxenes,

Table 1. Grain-size and heavy-residue distribution of the Ramapo Deep sediment.

| Fraction | Grain size distribution | Heavy residue | Parameters |
|---|---|---|---|
| $-0.5\phi <$ | 3.9 wt. % | 0.53 wt. % | $Md\phi=2.98$ |
| $-0.5-1\phi$ | 5.9 | 0.47 | $\sigma\phi=2.78$ |
| 1 — 2 | 8.4 | 0.36 | $\alpha\phi=0.41$ |
| 2 — 3 | 23.2 | 1.03 | |
| 3 — 4 | 16 6 | 1.21 | |
| 4 — 5 | 11.1 | | |
| 5 — 6 | 7.8 | | |
| 6 — 7 | 7.8 | | |
| 7 — 8 | 5.6 | | |
| 8 > | 9.7 | | |
| Total | 100.0 | | |

Table 2. Specific gravity distribution and grain component of the Ramapo Deep sediment.

| Fraction | Specific gravity distribution | Grain component |
|---|---|---|
| 2.89< | 10.3 wt. % | Heavy minerals and rock fragments |
| 2.89—2.78 | 10.3 | Vulcanic rock fragments and obsidian |
| 2.78—2.69 | 10.3 | Scoria, vulcanic rock fragments, glass fragments and basic plagioclase |
| 2.69—2.61 | 18.1 | Scoria, glass, pumice and plagioclase |
| 2.61—2.52 | 42.0 | Glass fragments, devitrified glass, pumice, scoria and chalcedony |
| 2.52—2.41 | 1.3 | |
| 2.41—2.33 | 4.5 | Pumice, vesicular glass fragments and scoria |
| 2.33—2.24 | 1.3 | |
| 2.24> | 1.9 | Pumice, fibrous aggregates of glass, Pele's hair, radiolaria, diatom etc. |
| Total | 100.0 | |

$Mds=S_{50}=2.50$

$\sigma_s=\frac{1}{2}(S_{84}-S_{16})=0.14$

$\alpha_s=\{\frac{1}{2}(S_{84}-S_{16})-Mds\}/\sigma_s=1.29$

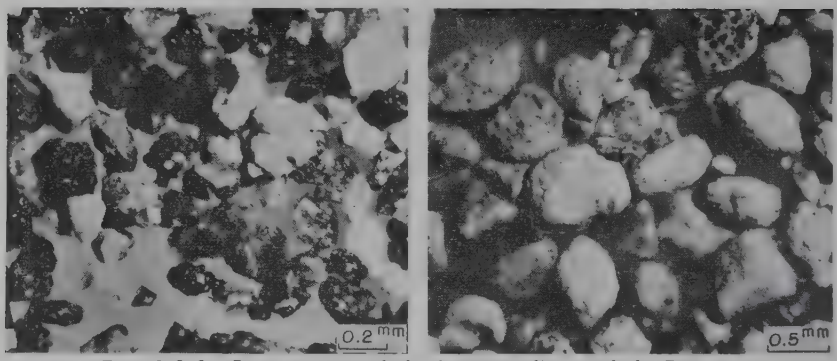


Figs. 2 & 3. Coarse grains of the bottom sediment of the Ramapo Deep; Left: vulcanic rock fragments, scoria (dark) and glass fragments (light); Right: pumice grains.

greenish brown to bluish green hornblende, chromite, apatite, magnetite, hematite, ilmenite, etc. (Plate).

Table 2 is a tabulation of specific gravity distribution in per cent and grain component. Each heavy mineral assemblage of grain size fractions is represented in Table 3.

Associated with them are often found organic matters, consisting largely of the skeletons of siliceous radiolaria and diatom, together with a smaller proportion of other organisms, such as the tests of arenaceous foraminifera, *Trochammina*, *Haplophragmoides* and *Reophax*, and chitinous dendritic substance.

Table 3. Heavy mineral assemblages of each fraction.

| Heavy mineral | 1φ—2φ | 2φ—3φ | 3φ—4φ |
|---|---|---|---|
| Nonopaques | 29% | 49% | 72% |
| Opaques | 71 | 51 | 28 |
| | **100** | **100** | **100** |
| Olivine | 12.0% | 7.4% | 10.5% |
| Monoclinic pyroxene | 37.0 | 48.8 | 54.0 |
| Rhombic pyroxene | 19.4 | 17.0 | 10.8 |
| Hornblende | 19.6 | 14.6 | 13.0 |
| Greenish mineral | 12.0 | 12.2 | 7.7 |
| Chromite | — | — | 3.4 |
| Apatite | — | — | 0.6 |
| | **100.0** | **100.0** | **100.0** |

*2. Bottom sediment of the Kuril Trench*

A very small quantity of a sandy sediment adhered to the cut-edge of the normal piston-core sampler is used for this investigation.

Sample No.: JEDS-2-$C_2$ (Sample was organized by Hideo KAGAMI).

Situation: 42°48′N, 147°00′E. Landward slope of the southern Kuril Trench off Shikotan Island.

Date: September 23, 1959.

Depth: Bottom of the trench, down to 8,005 m.

The sediment is bluish gray, silty sand, the heavy mineral association of which is mainly composed of green augite, hypersthene, brownish green hornblende and iron opaques, together with a smaller proportion of brown augite, reddish brown hornblende and a well-rounded grain of purple zircon.

Table 4. Heavy mineral association of a bottom sediment of the Kuril Trench and a beach sand of Southeastern Hokkaido.

| Heavy minerals* | | Kuril Trench | Beach sand |
|---|---|---|---|
| Olivine | | | 1.5% |
| Augite (green) | embedded in glass | 3.3% | 1.5 |
| | angular fragment | 12.0 | 8.5 |
| | hackly-etched | 6.0 | 6.5 |
| | abraded | 12.0 | 15.0 |
| Augite (brown) | angular fragment | 1.3 | 0.5 |
| | abraded | 0.7 | |
| Hypersthene | embedded in glass | 4.7 | 6.0 |
| | angular fragment | 13.2 | 15.0 |
| | hackly-etched | 4.7 | 5.5 |
| | abraded | 7.4 | 16.5 |
| Hornblende (brownish green) | embedded in glass | 2.0 | 0.5 |
| | angular fragment | 8.0 | 6.5 |
| | abraded | | 2.0 |
| Hornblende (reddish brown) | angular fragment | 0.7 | 0.5 |
| Biotite | angular fragment | | 0.5 |
| Garnet | angular and etched | | 0.5 |
| Zircon (purple) | well-rounded | 0.7 | |
| Magnetite | embedded in glass | 9.3 | 2.0 |
| Iron opaques | angular and abraded | 14.0 | 11.0 |

* Except hematite, limonite and pyrite grains.

Hematite, limonite and pyrite grains are found as secondary materials.

Emphasis is on the present of abraded sand grains (ca. 20% in counted grains number) among the residue composed largely of angular and euhedral to partly-broken grains; the latter are often enclosed by vulcanic glass (ca. 20% in counted grains number). Table 4 is a tabulation in per cent of about 200 observations of the heavy mineral residues of the trench-filled sediment with that of a recent beach sand of Southeastern Hokkaido for comparison.

It is significant to collect very angular, coarser sediment from the bottom of the Ramapo Deep, down to 8,450 m in depth; furthermore, to discover some serpentinized peridotite fragments and many bluish green hornblende grains which are not yet found on the islands near the Deep[1]. Older amphibolite and schist basement crops out of Miocene formations in the Yap group. The presence of basement series —may be the origin of the serpentinite fragments and hornblende grains in the Deep sediment —are reasonably expected in the submarine ridge on which the Bonin Islands stand, composed of Older Tertiary, Nummulites beds and altered vulcanic rocks. The majority of the sediment are derived from the adjacent volcanoes, Tori-shima etc., both directly by eruptions and after drift on the sea.

It is interesting to find a considerable proportion of abraded, terrigenous grains in the bottom sediment of the Kuril Trench, as opposed to that of the Ramapo Deep. They are undoubtedly derived from the adjacent land by submarine slides and/or drift with icebergs.

*Acknowledgements*: May here be made to Captain T. SUENAGA and all crewmen of the Ryofu Maru, who presented a united front against the research fellow throughout the expeditions. The writer is greatly indebted to the Committee of Japanese Deep Sea Expedition for allowance to joint the expeditions. He expresses his thanks to the research fellow for help in collecting the samples at sea. He is also indebted to Dr. H. KUNO, Professor of University of Tokyo who rendered valuable suggestions in the identification of some thin sections. Thanks are also to Dr. S. ARAMAKI, Dr. F. SHIDO, Dr. K. KANEHIRA, Dr. T.

[1] H. H. HESS (1948) stated that "On Ototojima of the Hahajima group, Suzuki (1885) reported serpentinized peridotite, a significant discovery." However, he referred to YOSHIWARA (1902) who inadequately translated SUZUKI's original in Japanese. The rock in question is altered basalt or andesite judging from SUZUKI's original.

MATSUDA and Mr. S. YUI of University of Tokyo for many helpful suggestions in the preparation of this manuscript.

*References*

CORWIN, G. and FOSTER, H. L.: The 1957 explosive eruption on Iwo Jima, Volcano Islands, *Amer. Jour. Sci.*, **257**, pp. 161-171, 1959.

HESS, H. H.: Major Structural features of the Western North Pacific, an interpretation of H. O. 5485, Bathymetric Chart, Korea to New Guinea, *Bull. Geol. Soc. Amer.*, **59**, pp. 417-446, 1948.

ISSHIKI, N.: Explanatory Text of the Geological Map of Japan. "Hachijo-jima-5", *Geol. Survey of Japan*, pp. 1-58, 1959.

KUNO, H.: Volcanoes and volcanic Rocks, *Iwanami-zensho*, **196**, pp. 1-255, 1955.

MORIMOTO, R.: The 1952-1953 eruption of Myojin Reef with special reference to the volcanic rock fragments embedded into the wreckage of "No. 5 Kaiyo-maru", *Studies Geol. & Min. Inst., Tokyo Univ. Educatin*, No. 3. pp. 5-14, 1954.

—— and OSSAKA, J.: The 1952-1953 submarine eruption of the Myojin Reef near the Bayonnaise Rocks, Japan, *Bull. Earthq. Res. Inst., Tokyo Univ.* **33**, pp. 221-250, 1955.

—— and ——: On the Mihara-yama lavas, *Jour. Geogr.*, **60**, pp. 36-39, 1951.

NASU, N., IIJIMA, A. and KAGAMI, H.: Geological results in the Japanese Deep Sea Expedition in 1959, *Oceanogr. Mag.*, **11**, pp. 201-214, 1960.

SUZUKI, B.: Petrography of the Chichijima Group of the Bonin Islands, *Bull. Geol. Soc. Japan*, pt. A, **1**, pp. 23-29, 1885.

TAKABATAKE, A.: Volcano Torishima, Izu Archipelago, *Bull. Geol. Survey Japan*, **2**, pp. 547-552, 1951.

TSUYA, H.: The eruption of Miyake-sima, one of the Seven Izu Islands, in 1940, *Bull. Earthq Res. Inst., Tokyo Univ.*, **19**, pp. 265-522 and 492-294, 1941.

——: The eruption of Miyake-sima, in 1940, *Earthquake*, **12**, pp. 474-478, 1940.

——: On the Volcanism of the Huji Volcanic Zone, with special reference to the geology and petrology of Idu and the Southern Islands, *Bull. Earthq. Res. Inst., Tokyo Univ.*, **15**, pp. 215-257, 1937.

——: On the Volcano Islands, Sulphur Island, *Volcano*, **3**, pp. 28-52, 1936.

YOSHIWARA, S.: Geological age of the Ogasawara Group (Bonin Islands) as indicated by the occurrence of Nummulites, *Geol. Mag.*, No. 457, New Series, Decade IV, **9**, pp. 296-302, 1902.

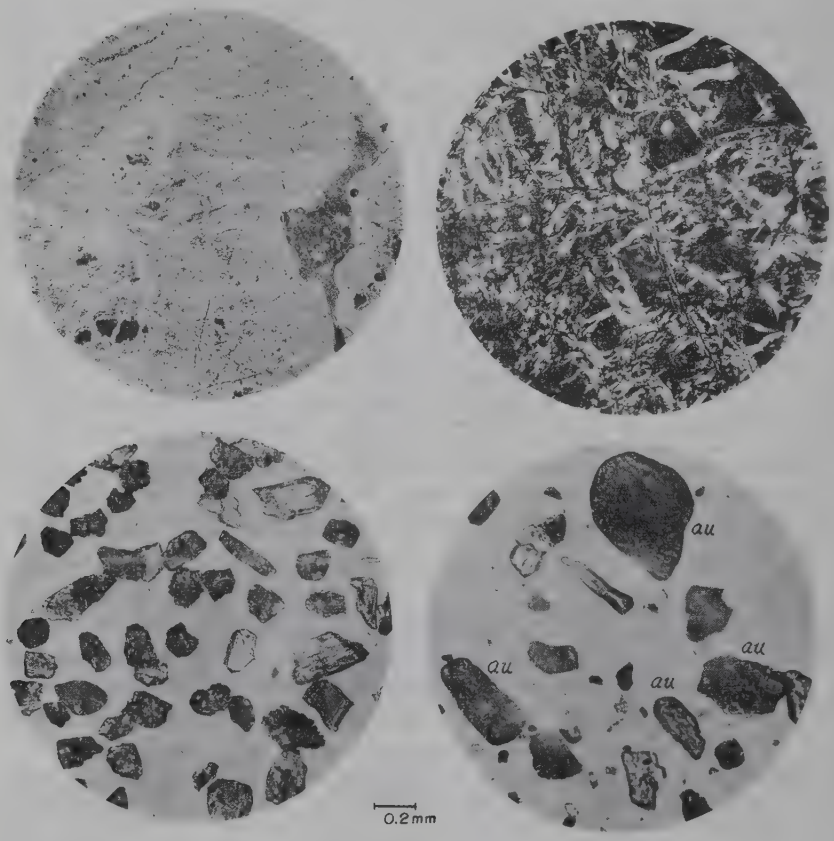


Upper left: Serpentinized peridotite composed of chromite (black), celadonite and chlorite (dark gray) in the "mesh structure" with much secondary minute grains of magnetite; a fragment with a diameter of 3.3 mm, from the bottom of the Ramapo Deep, down to 8.450 m.

Upper right: Ditto, +Nicol.

Lower left: Heavy residue of the bottom sediment of the Ramapo Deep, composed of olivine, pyroxenes, hornblende and opaques.

Lower right: Heavy residue of the bottom sediment of the southern Kuril Trench, composed of green augite (au), hypersthene (others), hornblende (not seen) and opaques. It is very important to discover abraded grains.

The Oceanographical Magazine
Vol. 11. No. 2, March 1960

# On the Bottom Sediments off Onagawa and Kushiro, the Adjacent Continental Slope of Japan Trench*

By

Hideo KAGAMI and Azuma IIJIMA

*Geological Institute, Faculty of Science, University of Tokyo*

## 1. *Introduction*

Two bottom samples were obtained on September 11, 1959 from the continental slope off Onagawa in a course of the Deep Sea Expedition of Japan by Ryofu Maru, the observation ship of Japan Meteorological Agency.

One of them (JEDS-2-$S_1$) was obtained at 38°11.4′ N. and 143°12.1′ E. in the depth of 2360 meters by a small biological dredge by means of the tapered wire of which length was marked on 3153 meters long. The other (JEDS-2-$S_2$) was obtained at 38°16.2′ N. and 143°11.8′ E. in the depth of 2250 meters by a beam trawl, then the length of the tapered wire was 2709 meters long.

In addition to them, bottom sediment off Kushiro (JEDS-2-$B_1$) was obtained in the depth of 480 meters at 42°40′ N. and 144°30′ E.

Depths were recorded by continuous echo sounding and the correction for temperature and salinity has not yet been completed.

## 2. *Bottom Sediments*

Bottom sediment obtained by the small biological dredge is muddy sand including pebble-size gravels. The compact bluish grey mud was stuck to the corner of the outer wall of the dredge.

Bottom sediment obtained by the beam trawl is also muddy sand including boulders, cobbles and pebbles. Presence of gravels in these two localities is the characteristic feature of the bottom sediment. Beam trawl was lifted from the bottom with over 500 pieces of gravels (Fig. 1). Appearance of gravels shows that some of them are completely buried by mud and some of them are buried in their lower half. In the later case sponges and sea-anemones are stuck to the gravels.

* JEDS Contribution No. 9.

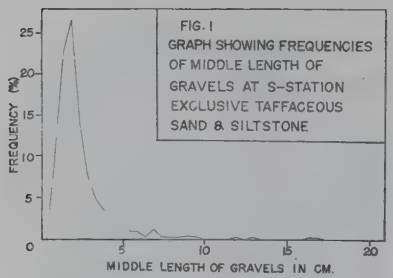


The median roundness (visual roundness identified by KRUMBEIN, 1941) of the gravels is 0.57. As the central tendency each value is concentrated to 0.6 and 0.7. They seem to be very round as a whole (Table 1).

Petrography of the gravels has not been finished at present. Rock-type of the gravels is variable. They are granodiorite, gabbro, prophyrite, rhyolite, andesite (including boulder-size), pumice (volcanic bomb), schalstein, pre-Tertiary sandstone, chert (abundant), gneiss hornfels and tuffaceous sandstone or siltstone.

One of pumice is measured about 18 cm. in maximum length. It has very fresh appearance though other gravels are coated with iron and manganese. It may be transported to this place at last.

One of the marl is measured about 46 cm. in maximum length. It is the largest of all gravels. The surface of the tuffaceous sand or siltstone is irregularly concaved. Some of them look like the features made by weathering and some of them are that of boring shells. Abundant presence of loose and breakable tuffaceous sand or siltstone contaminated with very hard rounded gravels may be considered that they are the bed rock of the slope or they outcrop not so far from the sampling location. Presence

Table 1. Roundness of the gravels obtained at JEDS-2-S.

| Roundness | Numbers | Percent |
|---|---|---|
| 0.1 | 2 | 1.5 |
| 0.2 | 8 | 5.9 |
| 0.3 | 10 | 7.3 |
| 0.4 | 13 | 9.6 |
| 0.5 | 10 | 7.3 |
| 0.6 | 44 | 32.4 |
| 0.7 | 31 | 22.8 |
| 0.8 | 18 | 13.2 |
| 0.9 | 0 | 0.0 |
| | 136 | 100.0 |

of angular cobble-size gravels indicates that it may be also one of the slope makers.

Mechanism to transport and concentrate abundant rounded gravels such as chert is explained in two ways. One of them is that they are transported from the continental shelf by landslides or slumps or density currents. The other is that they are transported by river on land when the sea level was in great lowering. Can we imagine when sea level lowered to about 2000 meters from the present level once before? If we adhere to the mass movement in the water, it is difficult to answer why gravels are deposited at the seaward shelf-edge of the broad bench. DIETZ (1952) mentioned that turbidity currents erode on steep slopes and they generally deposit when slope gradient is low. Therefore their occurrence is not suitable for the mass movement.

Grain size analysis of the bottom sediment off Onagawa was made by using shieves, Emery-tube and Pippete methods. In addition to it, bottom sediment off Kushiro obtained in the depth of 480 meters was also analysed. Results obtained are shown in Table 2.

Table 2. Data of the bottom semiments.

| Station | Depth (m.) | Situation | | $\phi 5$ | $\phi 16$ | $\phi 50$ | $\phi 84$ | $\phi 95$ | $M\phi$ | $\sigma\phi$ | $\alpha\phi$ |
|---|---|---|---|---|---|---|---|---|---|---|---|
| | | Long. | Lat. | | | | | | | | |
| JFDS-2-$S_2$ | 2250 | 38°16.2′ | 143°11.8′ | (−4) | −2.10 | 2.22 | 4.45 | ( 8.9) | 1.18 | 3.28 | −0.32 |
| JEDS-2-$B_1$ | 480 | 42°40.0′ | 144°30.0 | 2.15 | 2.72 | 3.61 | 7.05 | (10.3) | 4.89 | 2.17 | 0.59 |

Sediment off Kushiro is silty sand. Median diameter in $\phi$ scale is 3.61 $\phi$. It consists of 66.4% of sand, 24.0% of silt and 9.6% of mud. From the other sediment parameters it seems to be a uppermost slope sediment with abundant fine sand.

On the other hand, sediment off Onagawa is very different though it was obtained in the depth of 2250 meters. It is pebble silt with 2.22 $\phi$ in Md$\phi$ and it has worse sorting ($\sigma\phi$=3.28). It consists of 19.5% of gravel, 62.8% of sand, 13.9% of silt and 5.8% of mud. This sediment type is often observed in the shore sediment or the rocky bottom sediment.

Dominant heavy minerals in the bottom sediment off Onagawa are common hornblende (brown and green brown), hypersthene, iron opaques and augite

Table 3. Heavy mineral frequencies of bottom sediment and tuffaceous sandstone.

| Heavy Minerals | Characteristics | Tuff. Sandstone | | | JEDS-2-$S_2$ | | |
|---|---|---|---|---|---|---|---|
| | | % | Total | Glass | % | Total | Glass |
| Opaque | euhedral | 4.5 | 37.2 | 5.1 | 7.9 | 20.2 | 3.8 |
| | angular | 0.3 | | | 1.4 | | |
| | round | 32.4 | | | 10.9 | | |
| Limonite | | | 0.8 | | | | |
| Biotite | | | | | | 0.3 | |
| Chlorite | | | 0.3 | | | 0.3 | |
| Detrital | | | 57.2 | 3.9 | | 74.8 | 15.0 |
| Decomposed | | | 4.5 | | | 4.4 | |
| | | | 100.0 | 9.0 | | 100.0 | 18.8 |
| Augite (green) | angular | 3.6 | 18.7 | | 2.7 | 6.3 | |
| | round | 12.0 | | | 2.7 | | |
| | etched | 3.1 | | | 0.9 | | |
| Augite (brown) | euhedral | 1.0 | 21.9 | | 1 3 | 14.7 | |
| | angular | 0.5 | | | 1.8 | | |
| | round | 17.8 | | | 10.7 | | |
| | etched | 2.6 | | | 0.9 | | |
| Hornblende | dark green | 0.5 | 26.1 | | 0.9 | 48.1 | |
| | green brown | 13.1 | | | 21.8 | | |
| | brown | 12.0 | | | 24.1 | | |
| | reddish brown | 0.5 | | | 0.4 | | |
| Hypersthene | euhedral | 7.3 | 31.2 | | 11.2 | 28.7 | |
| | angular | 3.6 | | | 1.8 | | |
| | round | 10.9 | | | 8.5 | | |
| | prismatic | 4.2 | | | 5.4 | | |
| | etched | 5.2 | | | 1.8 | | |
| Others | | | 2.1 | | | 2.2 | |
| | | | 100.0 | | | 100.0 | |

in descending order (Table 3). Separation of heavy minerals from the sand between 0 and 4 $\phi$ was made by bromoform (specific gravity, 2.89). These mineral component may be derived from the pyroclastic rocks. As about

19% of heavy minerals are enclosed with volcanic glass, some of them might be deposited like pumice fall. A part of the volcanic bomb (pumice) contains iron opaque, green brown hornblende, brown green augite and hypersthene as dominant heavy minerals.

To compare with it, heavy minerals contained in tuffaceous sandstone of gravels were separated. Dominant heavy minerals are iron opaque, augite, hypersthene and common hornblende (green brown) in descending order. In this case about 11% of non-opaque minerals are etched and 9% of the minerals are enclosed with glass, while non-opaque minerals in the bottom sediment have only 4% of etched minerals. The differences may be explained partly by the concentration of common hornblende in the bottom sediment. During the transportation heavier minerals such as magnetite and ilmenite are set aside and lighter minerals such as hornblende and mica are concentrated (KAGAMI 1951). Flaky shape of hornblende is suitable for particle transportation. Then it is considered that the bottom sediment represented by heavy minerals might remove at least as long as they received sorting.

Minerals below the specific gravity of 2.89 are observed by binoculars. They are pumice, quartz including volcanic glass (black and white), feldspar, scoria and Radioralian shells.

### 3. *Continental Slope*

We obtained four sounding lines acrosss the trenches in September, 1959. They are off Onagawa, off Yamada, off Kushiro and off Shikotan Island. Profiles of bottom topography between Onagawa at 38°26′ N. and 141°27′ E. and Station "S" at 37°55′ N. and 143°25′ E., and that from Kushiro at 42°57′ N. and 144°36′ E. to seaward at 41°29.5′ N. and 146°04.0′ E. are shown in Fig. 2.

The single geomorphic unit comprising the continental shelf and the continental slope has been termed as the continental terrace (DALY, 1942). In the profile of upper part of the continental terrace off Onagawa, first prominant break is observed in the depth of 2200 meters. Above this depth gradient of the slope is generally smooth. Width of this area is about 155 kilometers. In order to make the topography of the continental slope clear, detail descriptions are made. Width of the continental shelf is about 40 kilometers. The gradient of this part trends to about 350 meters deep. It is

FIG. 2 PROFILES OF THE CONTINENTAL TERRACES REDRAWN FROM FATHOGRAM

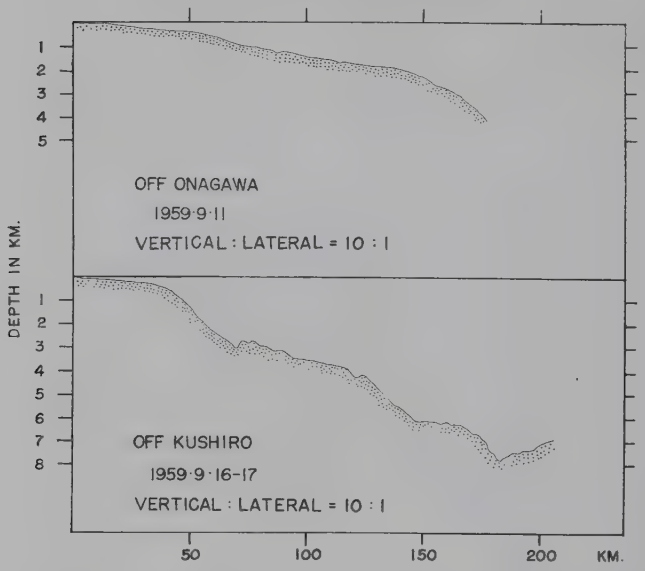


smoothly sloping at average gradient of 30′. From 350 to 1000 meters the gradient of slope varies rather steep. It has an average gradient of 1°20′. At the base of this slope a shallow trough is observed in the depth of 1170 meters and 100 meters deeper than the surroundings. Width of the trough is about 3.5 kilometers. A small scale trough is also observed in the depth of 1570 meters. It is 70 meters deeper than the surroundigs with 2 kilometers width. From here to about 1650 meters deep, the slope becomes very smooth again. It has an average gradient of 40′. Below 2170 meters gradient of the slope is very steep again with an average gradient of 3°50′. Other sounding line off Yamada shows the same features. Below 2250 meteres to the depth of 4300 meters, the continental slope is very steep with an average gradient of 3°50′. In the depths of about 4500 meters and 5600 meters, gentle slopes like a bench are observed. It has 5 to 10 km. of width.

The profile of the continental terrace off Kushiro has different features from the former. From the shore line, the shelf typically slopes out to a

depth of about 200 meters where an abrupt increase in declivity or shelf-break is present. The width of the continental shelf is about 35 kilometers. Further down slope over 2000 meters long is a very steep scarp with an average gradient of 4°10′. At the bottom of the scarp there is a trough 400 meters deeper than the surrounding with 4 kilometers of width in the depth of 2880 meters. A broad rise adjacent to the trough is observed with 10 kilometers of width and 300 meters of height. From the trough and rise to the depth of 3480 meters, gradient of the slope is smooth at an average gradient of 1°20′. Near the shelf-edge of the slope another trough is observed with 400 meters deep and 6 kilometers of width. This topographic flat plain is called bench or deep sea terrace. It has 50 kilometers of width and is 120 kilometers distance from the shore of Kushiro at the end of the bench. This distance corresponds to that of Yamada (120 km), and it is a median value between that of Onagawa (155 km) and that of Shikotan Island (85 km). From 3850 meters to 5630 meters deep, the slope becomes very steep at an average gradient of 4°40′. A very flat bench develops with 20 kilometers of width in the depth of 5650 meters adjacement to the scarp. It has an average gradient of 30′. The essential natures of the continential slope observed in the profile off Kushiro are also found in the profile off Shikotan Island.

There is a markable difference in the nature of the continental slope in these two areas above-mentioned. The characteristics of the continental slope off Hokkaido and Kurile, and north-eastern part of Honshu are here summerized.

| North-eastern part of Honshu | Hokkaido and Kurile |
|---|---|
| 1. Upper part of the continental terrace is broad and shows smooth slope. | 1. Upper slope is interrupted by a scarp between 200 and 2500 meters. |
| 2. Upper bench is broad; about 30 to 40 kilometers. | 2. Upper bench is narrow; about 15 to 25 kilometers. |
| 3. Lower bench does not well develop. | 3. Lower bench is recognized in the depth of about 5700 meters. |
| 4. Troughs and rises do not well develop at the base of the scarp. | 4. Troughs and adjacent rises are generally recognized at the base of the scarp. |

These differences may be a reflection of different bed rocks by which the

basement of the slopes is composed, of different degree of tectonic movement, and of different lapse of time since it was constructed in which different degree of sedimentation was made.

The continental slope is considered initially to be structural. Troughs and adjacent rises at the base of the scarp of the continental slope off Kushiro and Shikotan Island may in part be due to faulting as metioned by UDINTZEV (1955). As they did not suffer the dominant sedimentation, they may remain their original topography. According to DIETZ (1952) the continental terraces around most of the Pacific Ocean appears to be geomorphically youthful in his geomorphic cycle of the continental terrace; The continental shelves are narrow and the continental slopes are steep; The aprons of sediments at the base of the slope, if present, are small.

Though DIETZ's proposal seems to be suitable to the continental slopes off Hokkaido and Kurile, those of north-eastern part of Honshu are very different. In this area prominant troughs and rises at the base of the scarp and lower bench are absent. It might be resulted in part by the influence of the former deformation and sedimentation on the continental slope, so that the basement of the continental terrace in this area had been built before that of Hokkaido and Kurile was made.

As to the upper bench in the depths of 2000 and 3000 meters, the problem is rather complicated. It can be observed not only in these two areas, but also along the southern slope of Shikoku in south-western Japan (TAYAMA, 1949). The problems of the uniform existence of the upper bench will be discussed in near future, so far as our expeditions of deep sea are continued.

*4. Conclusions*

(1) Two bottom sediments obtained at JEDS-2-S have abundant gravels in which loose and breakable tuffaceous sandstone and siltstone are dominant. They may be one of the slope makers.

On the other hand, existence of gravels shows that the upper parts of the continental terrace are being burried by coarse sediment.

(2) Heavy minerals of sand-size sediment are consisted of pyroclastic minerals such as common hornblende, hypersthene, iron opaques and augite in order. Some of them are derived from pumice fall, as large volcanic bombs are present and about 19% of heavy minerals are enclosed with volcanic

glass. The other majority are thought to be derived from the loose and breakable tuffaceous siltstone and sandstone. Dominant heavy minerals of them are iron opaques, augite, hypersthene and common hornblende. In the course of derivation sorting by transportation affects the deposition of heavier minerals and concentration of lighter minerals such as hornblende in the bottom sediments. Thus the bottom sediment represented by heavy minerals is thought to have moved at least as long as they received sorting action like the continental shelf sediments.

(3) The differences in the nature of the continental slopes between the areas of Hokkaido and Kurile and those of north-eastern part of Honshu are described. These differences may be a reflection of different lapse of time since it was constructed and different degree of sedimentation. Broad and smooth slope of the upper continental terrace off Onagawa and Yamada may suggest that the Abukuma and Kitakami metamorphic and non metamorphic complex situate in the deeper portion of this upper continental terrace.

In view of the differences of the continental terraces between Hokkaido-Kurile and north-eastern part of Honshu, there is some reason to believe why UDINTZEV divides Kurile-Kamchatcha Trench from Japanese Trenches off the southern coast of Hokkaido.

*Acknowledgements*: The writers are sincerely indebted to Professor Takao SAKAMOTO of the University of Tokyo for his kind instruction and encouragement. They wish also to express their thanks to Assistant Professor Noriyuki NASU for his planning and realization of the deep sea expedition and co-operation in the laboratory work. Appreciations are also expressed to Dr. Yositada TAKENOUTI of the Meteorological Research Institute and to Dr. Jotaro MASUZAWA of the Marine Division, Japan Meteorological Agency. They are also indebted to Mr. Kazuo KOBAYASHI of the Tokyo University of Education and other copartners and the crew members of the Ryofu Maru.

## *References*

DALY, R.A. (1942): The floor of the ocean. 177 pp., *Univ. of North Carolina Press, Chapel Hill.*

DIETZ, R.S. (1952): Geomorphic evolution of continental terrace. *Bull. Amer. Assoc. Pet. Geo.*, V. **36**, pp. 1082—1819.

IIJIMA, A. "A report on the bottom sediments of the Japan and Kuril trenches collected

by the Ryofu Maru during the Japanese Deep Sea Expeditions in 1959", in this issue.
JORDAN, G.F. and H.B. Stewart, JR. (1959): Continental slope off southwest Florida. *Bull. Amer. Assoc. Pet. Geol.*, V. **43**, pp. 974—991.
KAGAMI, H. (1958): Sedimentological study of the marine sediments off Sakata, Yamagata, Japan. *Master Thesis of the Geol. Inst. of the Univ. of Tokyo (MS)*.
KOBAYASHI, K., OINUMA, K. and SUDO, T. "Clay mineralogical study on recent marine sediments I, II., in this issue.
KRUMBEIN, W.C., (1941): Measurement and geological significance of shape and roundness of sedimentary particles. *Jour. Sed. Petrol.*, V. **11**, pp. 64—72.
NASU, N., IIJIMA, A. and KAGAMI, H. "Geological results in the Japanese Deep Sea Expedition in 1959", in this issue.
TAYAMA, R., (1949): On the bottom topography off Shikoku. *Geographic Review of Japan.* V. **22**, pp. 120—121.
UDINTZEV, G.B., (1959): Relief of abyssal trenches in the Pacific Ocean. *International Oceanographic Congress Preprints*, pp. 54—55.

## *Postscript*

Dr. Taro KANAYA, in the Scripps Institution of Oceanography, sent a letter to Dr. NASU, and said diatom separated from the marl in JEDS-2-$S_2$ might be middle Miocene C-assemblage (by the presence of Cosinodiscus marginatus Ehrenberg) for his micropaleontological study in northeast Japan.

Then it is found that one of the slope makers is thought to be Miocene sedimentary rocks.

気象庁

# 欧文海洋報告

第 11 巻

# THE OCEANOGRAPHICAL MAGAZINE

Vol. 11

*Published by the Japan Meteorological Agency*

1960

# CONTENTS

**J. Sugiura**: On the currents south off Hokkaidō in the western North Pacific ..... 1

**S. Moriyasu**: Supplementary note on the dynamical property of the cold water region ..... 13

**S. Ishiguro**: A method of analysis for long-wave phenomena in the ocean, using hydraulic models and electronic and cybernetic techniques... 21

**S. Unoki**: An investigation on meteorological tides in the neighbouring seas of Japan (IV): General features of regional distribution and seasonal variation ..... 51

**T. Ichiye**: On the hydrography near Mississippi Delta..... 65

**J. Sugiura**: On the currents south off Hokkaidō in the western North Pacific (II) ..... 79

**T. Ichiye**: On the deep water in the Western North Pacific..... 99

**T. Ichiye**: On water budget in a two-layered ocean..... 111

**J. Fukuoka**: An analysis on the mechanism of the cold water mass appearance in the Enshū-nada ..... 127

**Preliminary Report of the Japanese Expedition of Deep Sea**

**K. Terada and H. Futi**: Introductory remarks of Japanese Expedition of Deep Sea ..... 145

**J. Masuzawa, M. Yasui and H. Akamatsu**: A hydrographic section across the Kurile Trench ..... 165

**Y. Takenouti and M. Yasui**: A note on the ball breaker and the ball..... 173

**Y. Miyake and others**: Chemistry in the Japanese Expedition of Deep Sea (JEDS-2) ..... 181

**Y. Suyehiro and others**: Notes on the sampling gears and the animals collected on the second cruise of the Japanese Expedition of deep seas (JEDS-2) ..... 187

**N. Nasu, A. Iijima and H. Kagami**: Geological results in the Japanese Deep Sea Expedition in 1959 ..... 201

**K. Kobayashi, K. Oinuma and T. Sudo**: Clay mineralogical study on Recent marine sediments (I), (II) ..... 215

**A. Iijima**: The bottom sediments of the Japan and Kurile Trenches collected by the Ryofu Maru during the Japanese Deep Sea Expeditions in 1959 ..... 225

**H. Kagami and A. Iijima**: On the bottom sediments off Onagawa and Kushiro, the adjacent continental slope of Japan Trench ..... 233

# ERRATA in OCEANOGRAPHICAL MAGAGINE VOL. 10 No. 1

T. ICHIYE: The response of a stratified, bounded ocean to variable wind stresses.

| Page | Line | Text | Correction |
|---|---|---|---|
| 19 | 7b | a east | an east |
| 20 | 2 | under-standing | understanding |
| | E(2.1) | $\frac{\tau_x}{H}$ | $\frac{\tau_\varpi}{H}$ |
| | 5b | blime | prime |
| 21 | 1 | vorti | vorti- |
| | E(2.11) | $p'H'_\lambda$ | $p'H'_\varpi$ |
| | E(2.13) | should read | curl $\tau)+\frac{\beta}{f^2}$(... |
| 22 | 9b | $F$ | $F$ |
| | | (This is different from $F$ in page 21) | |
| 23 | 7 | in homogene-ous | inhomogene-ous |
| | 10 | $O_bR_I=O$ | $O_bR_I=0$ |
| | | (The terms $O_fR_I=F_f$...$O_bR_{II}=F_b$ should be put in the next line.) | |
| | 15 | $F=F_0k$ | $F=F_0\Re$ |
| 24 | E(3.9) | $R_I=\frac{1}{2}k\{\ \}$ | $R_I=\frac{1}{2}\Re\{\ \}$ |
| | E(3.9a) | $R_I=k\{\ \}$ | $R_I=\Re\{\ \}$ |
| | 14b | $K_i$ | $K_s$ |
| | E(3.10) | $R_{IIi}=(B_{Ii}+B_{2i})$ | $R_{IIs}=(B_{Is}+B_{2s})$ |
| 25 | E(3.14) | $\fallingdotseq\|\tau\|I/\mu f$ curl $\tau$ | $\fallingdotseq\|\tau\|I:\mu f$ curl $\tau$ |
| 26 | T1L3C2 | 4.2 | 42 |
| | T2 | $f\sigma_e/gH$ | $f\sigma_i/gH$ |
| 27 | 4 | $af$ | $of$ |
| | 7b | Replace ", the curves ....." with ". The effect of the decrease in $\theta$ is more conspicuous than that in $\mu$ particularly in the baroclinic mode." | |
| | 5b | changed as | [as] |
| 28 | 5b | infinitive | infinite |
| 30 | 1 | infinitive | infinite |
| | 4b | such | of such |
| | 1b | differcent | different |
| | 1b | paysical | physical |
| 31 | 11 | spart | apart |
| | 13 | $a\delta_s\rangle\|$ | $a\delta_s$ is much larger than one |
| | 8b | attenuates | [s] |

| Page | Line | Text | Correction |
|---|---|---|---|
| 32 | T3 | $\nu=\mu=10^{-7}\|10^{-5}$ | $\nu=\mu=10^{-7}\|10^{-5}$ |
| 32 | T3 | | |
| | L2C3 | $0.192\pm$ | $0.192-$ |
| | L3C4 | $0.98\pm$ | $0.98+$ |
| | L4C8 | $-25i)10^{-4}$ | $-25i)\times10^{-4}$ |
| | L6C5 | $4{,}25\times10$ | $4{,}25\times10^{-4}$ |
| | L6C6 | $10{,}125\times10$ | $20{,}5\times10^{-4}$ |
| | L6C7 | $40{,}625\times10^{-5}$ | $40{,}25\times10^{-5}$ |
| | L6C8 | $200{,}5\times10^{-5}$ | $200{,}125\times10^{-5}$ |
| 33 | E(5.1a) | $n_i$ | $in$ |
| | 15 | onother | another |
| | 9b | velid | valid |
| | 3b | lock | look |
| 34 | 7 | $\beta_1a\rangle\|$ | $\beta_2a\rangle\|$ |
| | 1b | $\pi/\beta,$ | $\pi/\beta_1$ |
| | F7 | $Df$ | $D_f$ |
| 35 | 7b | Replace ", since $\kappa\rangle\lambda_i^2$, $u^2$ and $\delta_1$ is ....." by ", since $\delta_1$ is given approximately by $2\kappa/(1-ni)$ for the range $\kappa\rangle\lambda_i^2$, $\mu^2$. | |
| | 5b | Replace "the increase in $k$ .....the value of $D_f$" by "the values of $D_f$ increases as increasing $k$" | |
| 36 | 13 | $0.049_i$<br>$0.152_i$ | $0.049i$<br>$0.152i$ |
| 37 | 1 | $R_i$ | $R_I$ |
| | 2 | $\chi$ | $x$ |
| | 2 | rear | near |
| | 8b | $R_i$ | $R_I$ |
| | F10 | $\delta_1$ -waves: | $\delta_2$ -waves: |
| 38 | 1 | $-63_i$ | $-63i$ |
| | 3 | $ad_{1e}$ | $a\delta_{1l}$ |
| | 3 | $54.0_i$ | $54.0i$ |
| | 4 | $R_i$ | $R_I$ |
| | 6 | $e^{i\delta_2(\theta+x)}+$ | $e^{i\delta_1(a+x)}+$ |
| | 5,6b | eq. (6.3) | Delete |
| 39 | 1 | Then | When |
| | 8 | near | close |
| | 8 | weve | wave |
| 40 | 4 | $R_1$ | $R_I$ |
| | E(7.2) L1 | $\cos\pi/ax$<br>$\epsilon_r\sin(\nu t+\pi/ax)$ | $\cos\pi x/a$<br>$\epsilon_r\sin(\nu t+\pi x/a)$ |

| Page | Line | Text | Correction |
|---|---|---|---|
| | E(7.3) | | |
| | L1 | $\sin \pi/ax$ | $\sin \pi x/a$ |
| | | $\epsilon_l \sin(\nu t+\pi/a)$ | $\epsilon_l \sin(\nu t+\pi x/a)$ |
| 41 | 9b | 1951a | 1951b |
| | F12 | $t=t$ | $t=\pi/2\nu$ |
| 42 | 6, 7 | $29.7_t$ etc. | $29.7i$ etc. |
| | 12 | wave $\sin(\nu t+\pi x/a)$ | Delete |
| 43 | 8b | $\nu^2(\mu^2\lambda_J^2)$ | $\nu^2(\mu^2+\lambda_J^2)$ |
| | 3b | $_1\psi$ | $\psi_1$ |
| 44 | 1 | $4_1$, $4_2$ | $\psi_1$, $\psi_2$ |
| | 4 | $\tau x$ | $\tau_x$ |
| | 8 | $\frac{2\beta}{f}\frac{\partial}{\partial y}R$ term | the term $\frac{2\beta}{f}\frac{\partial}{\partial y}R$ |
| | E(7.6a) | $\{\ \}^{-1}\ \dot{d}$ | $\{\ \}^{-1}$, $\bar{d}$ |
| | | $(1+2l_i)$ | $(1+2l\dot{i})$ |
| | T4 | | |
| | C1 | $I_{\psi a}$, $I_{\psi_2}$ | IVa, IVb |
| | C10L6 | $-4_2$ | $-\psi_2$ |
| 45 | E(7.6b) | $m_t e^{i\psi_t}$ | $m_s e^{i\psi_s}$ |
| | | $=(1+p\delta_t)^{-1}$ | $=(1+p\delta_s)^{-1}$ |
| | | $m_t e^{i\psi i}$ | $m_s e^{i\psi_s}$ |
| | | $=(1-p\bar{\delta}\dot{i})^{-1}$ | $=(1-p\delta_s)^{-1}$ |
| | 12&13b | such as $v_r=\ldots$in $R_r$ | Delete |
| | 4b | $\Phi$ | $\bar{\Phi}$ |
| | 2b | or ginal relationship | equations |
| 46 | 1 | — | Delete |
| | 6 | $\psi'$ | $\psi_1'$ |
| 47 | F15 | $U_r$ and $V_r$ | $u_r$ and $v_r$ |
| 49 | E(8.4) | $f\sigma j$ | $f\sigma_J$ |
| | 6b | $(1-e^{-i\delta_1 d})$ | $(1-e^{-i\delta_1 d})$ |
| | E(8.5a) | $e^{i\delta_0(a+x)}$ | $e^{i\delta_1(a+x)}$ |
| | 1b | $F(x)-F_0$ | $F(x)=F_0$ |
| 50 | 5&4b | (*Vb*). For the | (*Vb*), because the |
| 51 | 5 | of *Va* | of (*Va*) |
| | | $P(\lambda)$ | $P(x)$ |
| | 8 | $-\frac{1}{\partial_2}\Big)$ | $-\frac{1}{\delta_2}\Big)$ |
| | 6b | belt the | belt in the |
| | 4b | only a little | slightly |
| 52 | 5 | ocean and when | ocean. When |
| | 14 | $\partial p/\partial x$ | $\partial P/\partial x=P_x$ |
| 53 | 7 | valve | value |
| | E(8 16b) | $\left(1-\frac{\delta_2}{\delta_1}\right.$ | $\left(1-\frac{\delta_2}{\delta_1}\right)$ |
| | 12&13b | and as symmetry | . Assymmetry |
| 54 | 2b | $(\delta_2-\delta_1)_e\vert$ | $\vert(\delta_2-\delta_1)_l\vert$ |
| | 2 | $Px(a)$ | $P_x(a)$ |
| | F19 | is $10>$ | is $10^7$ |
| 56 | 10 | $\vert/\nu\vert\delta_2(\delta_2-\delta_1)\vert$ | $\vert\nu\,\delta_2(\delta_2-\delta_1)\vert^{-1}$ |
| | E(8.18) | $P_2$ | $P_x$ |
| | 2b | $e^{B_2(\Delta-2x)}$ | $e^{\beta_2(\Delta-2x)}$ |
| 57 | 8 | $B_x$ | $P_x$ |
| | 9 | of course | Delete |
| | 3b | $\Delta\dot{i}$ | $4\dot{i}$ |
| 58 | 13 | $P_{xy}$ | $P_{xx}$ |
| 61 | F25 | $10^{-6}S^{-1}$ | $10^{-6}\,\mathrm{sec}^{-1}$ |
| | | $2\times10^{-6}S^{-1}$ | $2\times10^{-6}\,\mathrm{sec}^{-1}$ |

(Abbreviations for this ERRATA)

b : from the bottom
F : Caption for figure
T : Table
E : Equation
L : Line
C : Column
[ ] : Delete

T. ICHIYE: On convective circulation and density distribution in a zonally uniform ocean.

| Page | Line | Text | Correction |
|---|---|---|---|
| 101 | 14, 15, 19 | $C$ | $c$ |
| 102 | E(26) | $\sinh\sqrt{-2p\sigma_2}Z$ | $\sinh\sqrt{-2p\sigma_2}Z$ |
| 104 | 6b | menidional | meridional |
| 105 | 9 | ($B_1$ in it | ($B$) it |
| 105 | 13b | up to the square | up to the coefficient of $Y^2$ |
| | 8b | $\beta=$ | $\beta-$ |
| | 5b | equaling degree side | equating powers sides |

| Page | Line | Text | Correction |
|---|---|---|---|
| 106 | E(37) | $\tanh(qcZ/z)$ | $\tanh(qcZ/2)$ |
| | 15b | $\log\cosh(qcZ/z)$ | $\log\cosh(qcZ/2)$ |
| | | $\int_0^z \ldots dz$ | $\int_0^Z \ldots dZ$ |
| | 1b | $\psi$ | $\Psi$ |
| 107 | 9 | $1+\partial Y$ | $1+\gamma Y$ |
| | 2, 4, 9 | $\psi$ | $\Psi$ |
| 108 | 5b | descrided | described |
| | 2 | $\psi$ | $\Psi$ |
| 109 | 7b | $\psi$ | $\Psi$ |
| 111 | E(45) | $-\frac{\partial\sigma}{\partial Z}$ | $-\frac{\partial\sigma}{\partial X}$ |
| | E(47) | $\int^z$ | $\int_0^X$ |
| 112 | 14b | $a_c$ | $a_0$ |
| | E(53) | $F''$ | $\phi''$ |
| 113 | 8 | because | because it |
| 114 | 6&7 | Replace "The exact...curve" by "The agreement of the exact curve and the approximate one" | |
| | 9 | is | if |
| | 11b | the value or | Delete |
| | 7b | have | have to |
| | 4b | for example | say |
| 115 | 1 | $e^{\eta}$ | $e^{-\eta}$ |
| | 2b | Singular... | SC |
| 116 | 11 | At | at |
| | 6b | Approximate... | SC |
| 117 | 5 | Insert "where" between *Eq.* (63) and the next line | |
| | 3b | Examples... | SC |
| 118 | 4b | gives picture deviates | give pictures deviate |
| 122 | 4 | that in | the one in |
| | 5 | the in latitude | the other in latitudes |
| 125 | 2 | Change... | SC |
| | 6 | $25\times$ | $2.5\times$ |
| 125 | 7 | paragraphy | paragraph |
| | 17b | Miscellaneous... | SC |
| | 16b | $\phi_0=1.5$ | $\phi_0=-1.5$ |
| | 6b | A solution... | SC |
| 127 | 5 | An approximation... | SC |
| 128 | 8 | $\psi$ | $\Psi$ |
| 129 | 5&4b | Replace "even...toerefore", by "as assumed in" | |
| 130 | 7 | profiles A 13 | profile A equal to 13 |
| | 17 | fils | is |
| | 13b | expressob... | express ob... |
| | 12b | theregion | the region |
| | 11&10b | Replace "As aseries...up" by "We take series up" | |
| | 10b | of | of $Y$ |
| | 3b | $F_1(Z)$ | $F_1(Z)$ and |
| | 1b | Stream... | SC |
| 133 | E(68) | $\delta\varpi$ | $\delta\kappa$ |
| 134 | E(69) | $e^{wz}$, $e^{w}$ | $e^{WZ}$, $e^{W}$ |
| | 14b | changed | Delete |
| 135 | 2 | in higher | toward higher |
| | 3 | in lower | toward lower |
| | 3 | Eoth types | Each type |
| | 4 | to | Delete |
| Ref | 1 | Schtung | Schichtung |
| 117 | F8 | upper most | uppermost |
| 119 | F9 | upper most | uppermost |
| 124 | F19 | $\psi$ | $\Psi$ |

(Abbreviations for this ERRATA)

- b : from the bottom
- E : Equation
- SC : Sub-chapter, the title of which must be in italics and also be head of the line.
- Ref : References
- F : Caption to figures

昭和35年3月25日印刷
昭和35年3月31日発行

編集兼発行人　気象庁
東京都千代田区大手町一ノ七

印刷人　花崎実
東京都中央区新富町二ノ十九

印刷所　大東印刷工芸株式会社
東京都中央区新富町二ノ十九